Mineral Res. Expl. Bull., 137, 1-27, 2008

GEOLOGY OF THE TERTIARY ROCKS AROUND KEMAH-ERZİNCAN-ÇAYIRLI REGION AND THEIR SOURCE ROCK CHARACTERISTICS

Abdullah GEDİK*

ABSTRACT.- Basement of the study area is comprised of Paleozoic rocks which are overlain by rather thick Triassic-Cretaceous Munzur limestone in carbonate facies. This unit is tectonically overlain by Cretaceous ophiolitic complex. In the region, these units are unconformably overlain by Tertiary clastic and carbonaceous deposits. The basement of the Tertiary is comprised of Paleocene clastic rocks which is conformably overlain by Eocene turbiditic deposits. In Erzincan and Çayırlı region the Eocene rocks are unconformably overlain by rather thick clastic and carbonaceous Miocene sequence. The sequence in the basin ends up with Pliocene clastic deposits. In the region, in the north of the Pülk (Balıklı) village, live oil seeps are observed. In Eocene Gülandere formation and in Kömür member of the Miocene Kemah formation, and also in different levels of the Balıklı formation bitumen and asphaltic levels are observed. Results of geochemical analyses show that these rocks do not have source rock potential considering the amount of total organic matter, maturity and type of organic matter. Biomarker analyses of the oil seep indicate that the oil was derived from an early mature clastic source rock of marine origin.

Key words: Oil seep, source rock, total organic matter, biomarker

INTRODUCTION

Neftlik oil seep in Erzincan-Çayırlı basin in Eastern Anatolia has long been known (Figure-1). The first research on this local oil seep was made by Nalifkin (1919), Lucius (1926), Petunikoff (1932), Paige (1933), Roothan (1940) and Stchepinsky (1940). Later on the seep area and the surrounding region were studied in detail from petroleum geology point of view by Kurtman (1962), Arpat (1964), Akkuş (1964), Bulut (1965), Demirmen (1965) and Pisoni (1965). Following these studies Neftlik-1, Neftlik-2, Neftlik-3 and Neftlik-4 wells were opened by the MTA but these wells were abandoned dry (Bulut and Akyol,1966; Akyol and Birgili,1966; Akyol,1968; Birgili and Yurdakul,1971; Gedik,1976). The first regional geological studies in Erzincan region were conducted by Ketin (1950). In the following years Deveciler et al. (1994), Aktimur (1986) and Aktimur et al. (1995) conducted regional studies as well. Tekin (2002) studied the source rock characteristics of the sequences located in the region. During this work, from the research conducted by Aktimur et al. (1995) was highly benefited (Figure-2). In 2000, in Kemah, Erzincan and Çayırlı regions Tur-Kan oil company conducteda geological research, measured stratigraphic sections and carried out geochemical investigations.

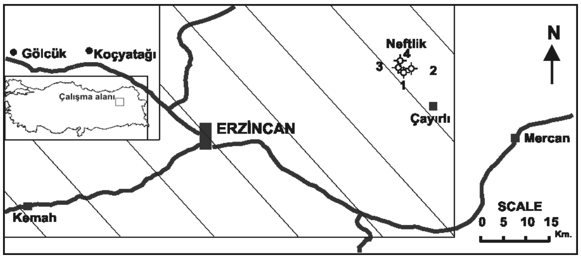

Figure-1 Study area and location map

In this study, source rock facies in the region, organic maturity, organic matter type and its maturity were investigated, also interpreted the geochemistry of the seep, seep-source rock relation and the petroleum potential of the region. Source rock analyses were made by Rock-Eva-II device. Biomarker analyses, on the other hand, were made by using GC-MS.

* Beril Sitesi 436. Sok. No: 4 Ümitköy, Ankara - Türkiye

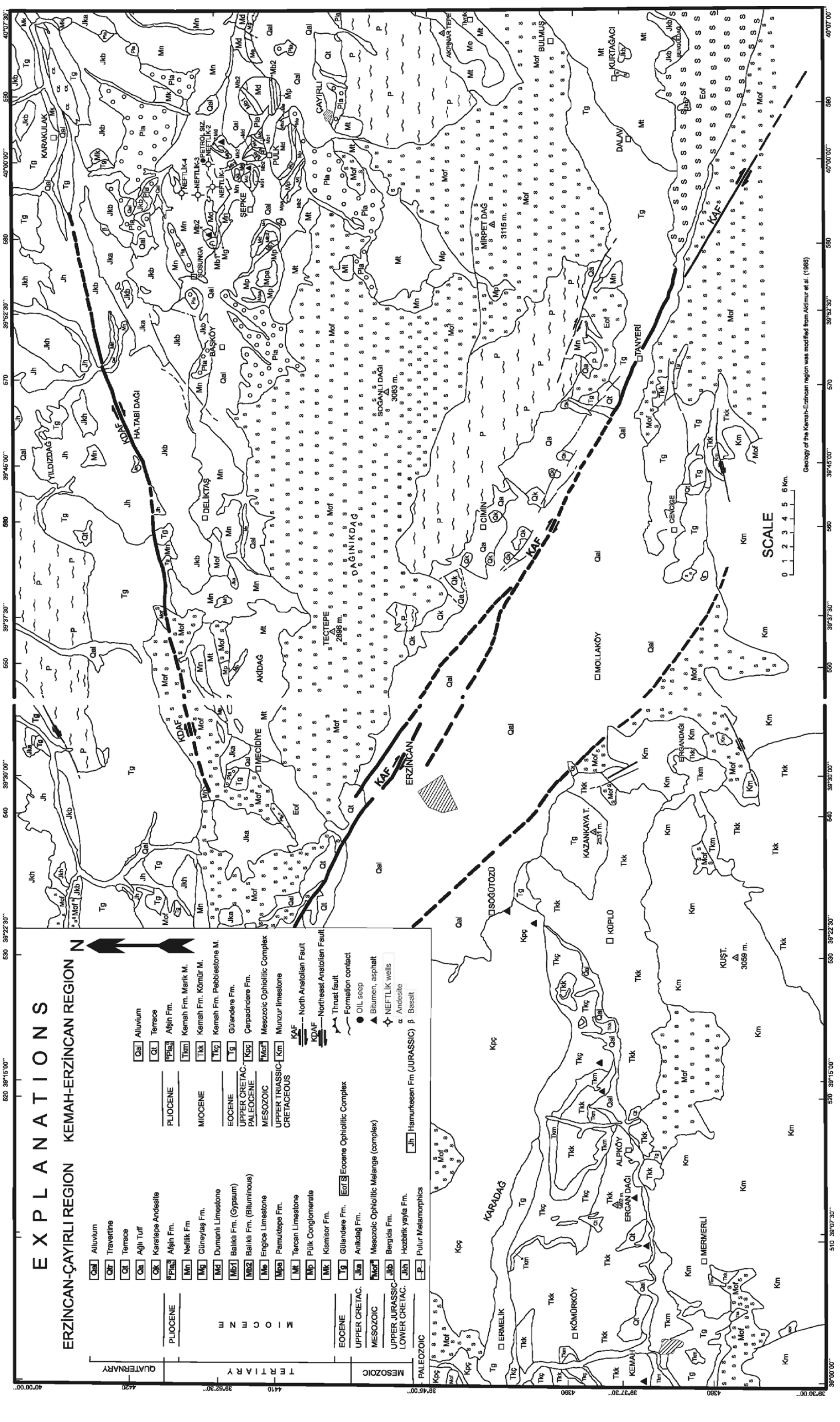

Figure-2 Geological map of the Kemah-Erzincan-Çayırlı region

GENERAL GEOLOGY

The Kemah-Erzincan-Çayırlı region which is located in the Eastern Anatolia is divided into two subbasins by the North Anatolian Fault. While Erzincan is located on the fault, Çayırlı and Kemah take place on the eastern and western sides of the fault, respectively (Figure-2).

In pre-Tertiary basement in the region there are some geological differences. The basement of the Erzincan and Kemah regions are composed of Paleozoic metamorphic rocks. This basement is overlain by rather thick Triassic-Cretaceous Munzur limestone in carbonate facies. Cretaceous ophiolitic complex is tectonically emplaced on this unit. These units are unconformably covered by Tertiary clastic deposits (Figure 3a, 3b). The basement of the Çayırlı region is comprised of Paleozoic metamorphic rocks which is tectonically overlain by Jurassic-Lower Cretaceous carbonates, Cretaceous ophiolitic melange and Upper Cretaceous clastic deposits. All these units are overlain by Tertiary clastics and carbonaceous deposits (Figure 3c). Detailed description and of the Tertiary units and the formations are given below.

Gülandere formation (Tg)

Distribution: In the north of the study area, in the north and south of the Karakulak stream, sandstones with limestone matrix and shale including *Nummulites* are observed. Besides, the formation crops out in the south of Kemah, in the east of Erzincan plain (around Çağlayan and Selepur), in Spikör, Karacaviran and Günbatur. The formation was first described by Aktimur et al. (1995).

Type Locality and Type Section: The typical section of the formation can be measured on the southern flanks of Şeyhmehmet hill in Çayırlı region. Its typical section also can be observed between Değirmendere-Bulanık which are located in the north of the Erzincan-Erzurum highway.

Lithology: The Gülandere formation is constituted of deposits having olisthostromal flysch and turbiditic flysch character. It is comprised of sandstone, claystone, conglomerate, siltstone, tuff and agglomerate succession and it includes andesitic and basaltic lavas. It also includes olisthostromal levels and blocks similar to those in an ophiolitic complex. The formation is blackish gray, brown, claret red, green in colour; it is thin-medium-thick bedded, folded, faulted and jointed. Thick conglomerates, agglomerates, andesites and basalts, thick tuff beds, intra-formational unconformities, unconformities caused by dislocational surfaces, repetitions caused by dislocations have caused the formation to have different sequences in different localities.

Contact Relations: It has gradational contact with Çerpaçindere formation in Erzincan-Kemah region and unconformably overlies Kemah formation. In Çayırlı region, the formation unconformably overlies the Anikdağ, and is unconformably overlain by Kismisor formations.

Thickness and Lateral Changes: The formation is 420 m thick around Çayırlı region. It was measured as 1020 m in Erzincan, and 1200 m in Kemah regions (Aktimur et al., 1995).

Fosil Content and Age: The formation includes *Nummulites* sp., *Discocylina* sp., *Distichoplax biserialis* Dıetrıch fossils and accordingly the age of the formation is determined as Lower-Middle Eocene.

Environmental Interpretation: The Gülandere formation was deposited in a deep marine environment which is suitable for flysch deposition. Lateral movements in form of dislocations which cause repetitions in the sequence and the andesitic-basaltic volcanism are synchronous with deposition. These lateral movements have also drifted large ophiolitic blocks into the depositional basin.

Correlation: The Gülandere formation can be correlated with the Sığırcı formation observed in Bayburt region (Aktimur et al., 1995).

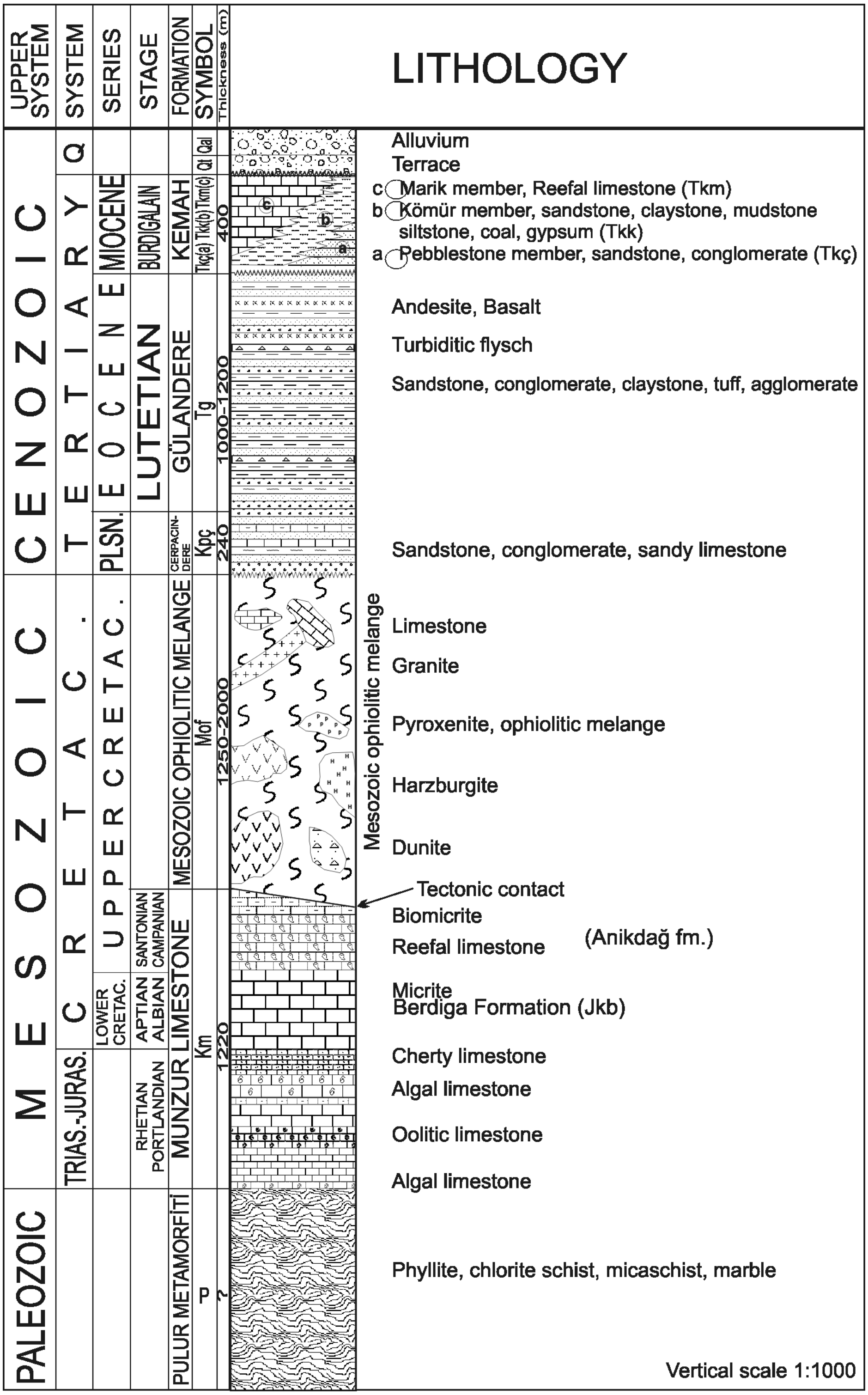

Figure-3a Generalized columnar section of the Kemah region

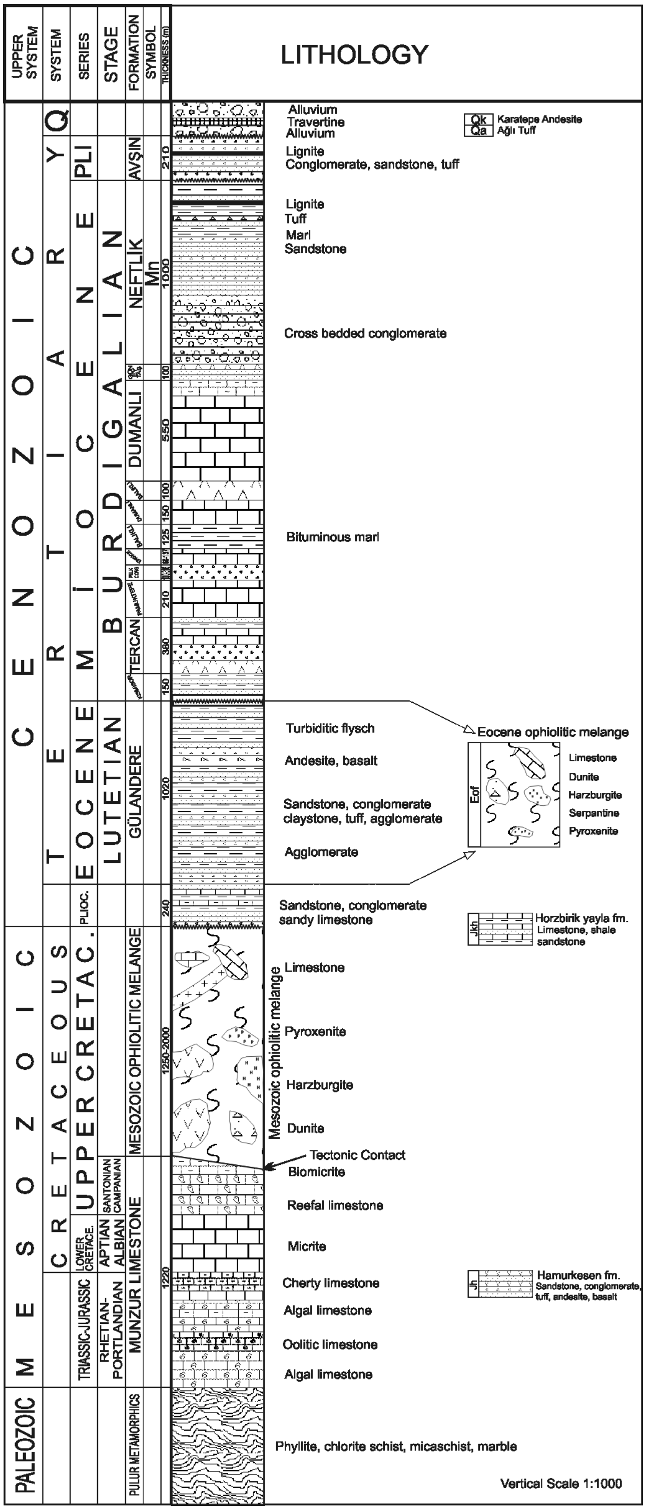

Figure-3b Generalized columnar section of the Erzincan region

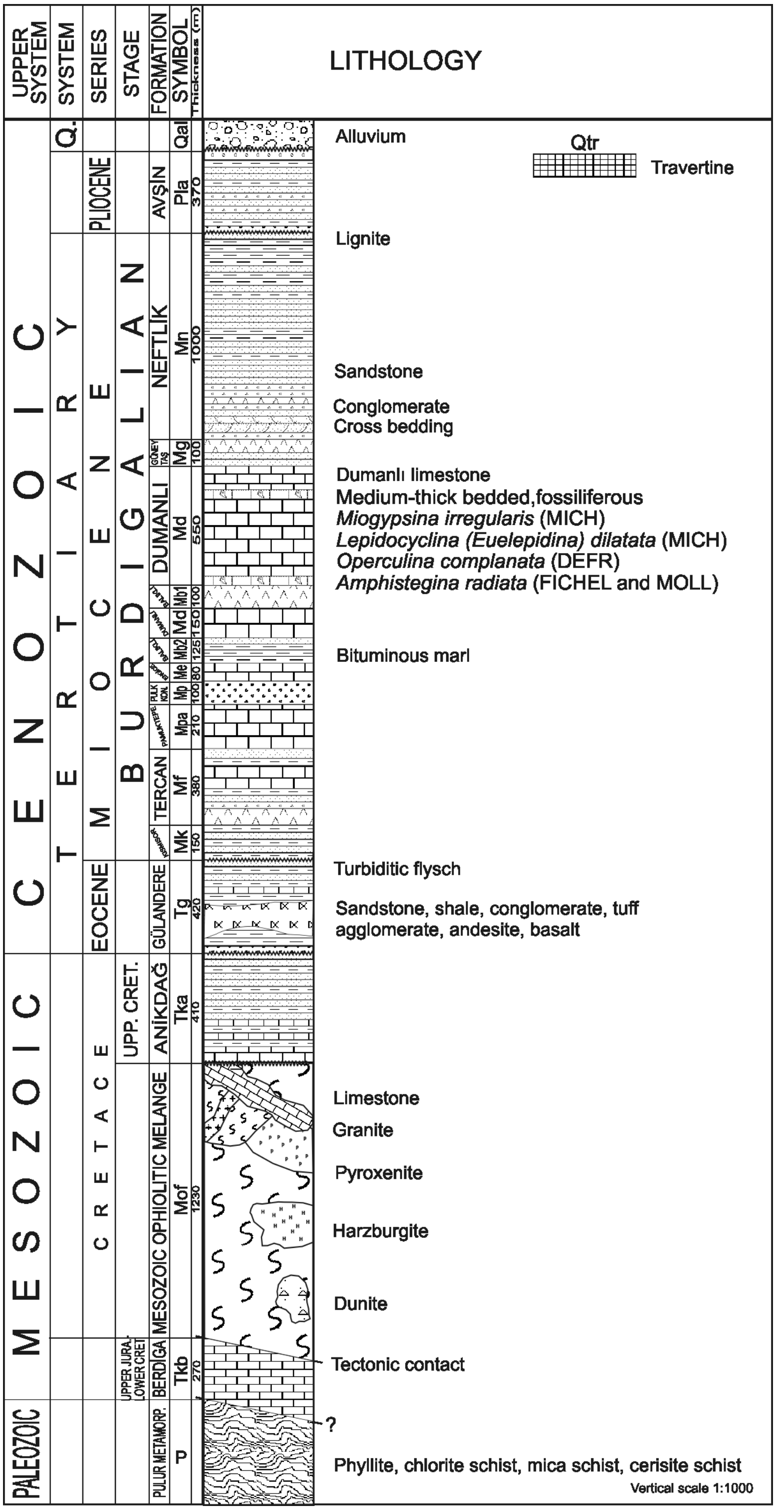

Figure-3c Generalized columnar section of the Çayırlı region

Eosen ophiolitic complex (Eof)

This complex was formed by the translation of the ophiolitic melange into the Eocene sea which crop out on the northern banks of the Fırat river and emplaced during Lower Campanian-Lower Maastrichtian interval. It displays similarities with Mesozoic ophiolitic melange. There are blocks of Çerpaçindere formation in the Eocene ophiolitic melange. The matrix of the complex is comprised of sandstone, claystone, mudstone of the Gülandere formation. According to the fossils such as Nummulites sp., Diccocyclina sp., Assilina sp. found in the matrix, the age is Eocene (Aktimur et al., 1995).

Kismisor formation (Mk)

Distribution: The formation crops out along the Karakulak stream valley, around Kismisor village, on the ridges of Söğütlü and in the west of Mirzaoğlu in the map of İ44 a1 sheet.

Lithological Features: The formation is comprised of red and purple coloured clay, marl, sandstone and conglomerates. It was named by Arpat (1964).

Contact Relations: In the west of Mirzaoğlu, the Kismisor formation overlies the Eocene units with angular unconformity. It is gradationally transitive to the Miocene units at its upper contact.

Thickness and Lateral Changes: The thickness of the formation is 150 m.

Fosil Content and Age: No fossils were collected in the unit. It was assumed to be of Miocene age since it overlies the Eocene units.

Environmental Interpretation: According to its lithological features, the Kismisor formation must have been deposited in shallow sea conditions.

Correlation: The Kismisor formation is similar to the Hürrübaba formation in Erzurum-Tekman basin. There is no bitumen in this formation. The age of the formation is Oligocene according to Arpat (1964). Pisoni (1965) defines the formation as Lakoğlu formation (Deveciler et al., 1994).

Tercan limestone (Mt)

Distribution: The colour of the formation is light yellow, grayish white. It includes foraminifera, lamellibranch, echinides, gastropoda and algae. The formation was named by Pisoni (1965). It crops out around Pülk mountain, Sırataş hills and Engice mountain.

Type Locality and Type Section: The type section of the formation was measured in Babanın Şenliği located in the south of Çayırlı (Figure-4).

Lithological Features: In the section measured in the south of Çayırlı, at the bottom limestone, marl and claystone succession, and at the top white coloured, medium bedded limestone with bioclast intercalations and at the topmost calcarenite including lamellibranches were observed.

Contact Relations: It overlies the metamorphic rocks and ophiolites with angular unconformity in Gelinpertek village located in the south of Çayırlı. It is overlain by Pülk conglomerate with gradational transition.

Thickness and Lateral Changes: The thickness of the formation was measured as 125 m in Babanın Şenliği section. The average thickness of the formation is 150 m.

Fossil Content and Age: The formation includes *Miogypsinoides* sp., *Miogypsina* sp., *Lepidocyclina* sp., *Amphistegina* sp., *Tarbellastraea reussina* (Edwards ve Haıme), *Favites neglecta* (Mıchelottı) fossils and the age of the formation is Burdigalian-Early Miocene accordingly.

Environmental Interpretation: According to the lithological and paleontological features of the

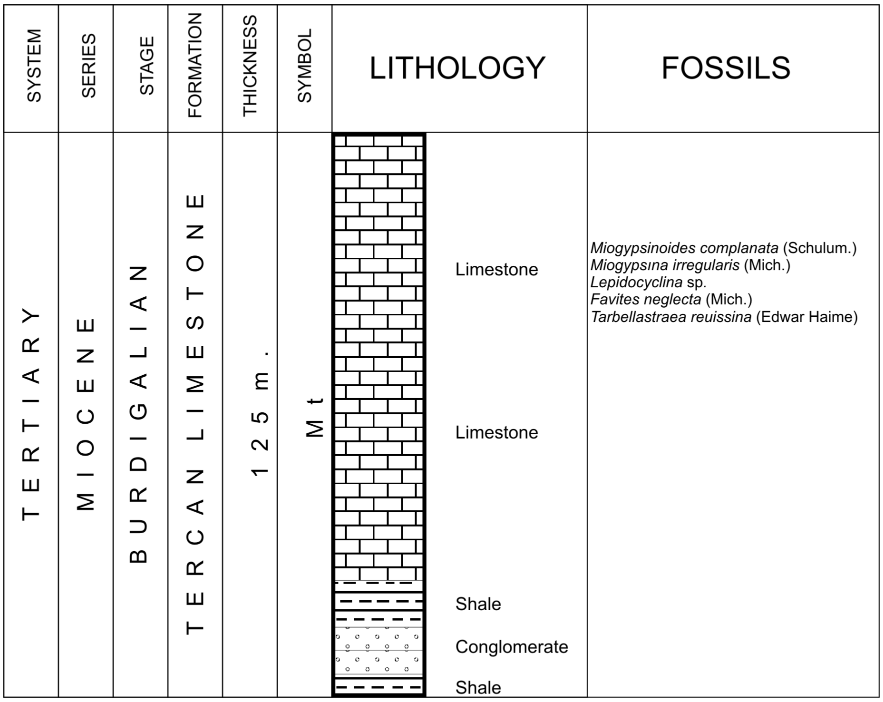

Figure-4 Measured stratigraphic section of Tercan limestone

formation, it must have been developed in an environment affected by high energy conditions. The coral reefs indicate that the environment has reefal characteristics (Deveciler et al., 1994).

Correlation: The formation can be correlated with the Haneşdüzü limestone observed in Erzurum-Pasinler, Tekman, Hınıs regions.

Pülk conglomerate (Mp)

Distribution: This unit crops out in the south of Çayırlı. In the east of the study area, the same unit was named as Lakoğlu formation. It is reddish, purplish in color and comprised of sandstones and mudstones with rounded, semi-rounded pebbles. It has conglomeratic features. The unit was defined by Arpat (1964).

Type Locality and Type Section: The typical localities of the unit are Pamuktepe, Pülkdağı and Pülkdağı hill around Çayırlı.

Lithological Features: The sequence is comprised of purplish, reddish, conglomerate with rounded, semi-rounded pebbles, reddish sandstone and mudstone. Conglomerates are thick bedded and lenticular, with erosional basements. The sandstones are medium bedded and locally display cross beddings. They have good porosity. The mudstones are brick coloured and thin bedded; they include sundry cracks and thin gypsum beds.

Contact Relations: The unit is gradually transitive on the Tercan limestone in Babanın Şenliği section. It is also gradually transitive to the Balıklı formation in Pamuktepe section and in Pülkdağı hill, and with Engice limestone in Pülkdağı and in Kızılkayalar sections. Its base is gradationally transitive on the Tercan limestone in Babanın Şenliği and Pamuktepe sections only.

Thickness and Lateral Changes: Thickness of Pülk conglomerates is 270 m at Pülk hill, 316 m in Pamuktepe hill ve 98 m at Pülkdağı (Figure 5).

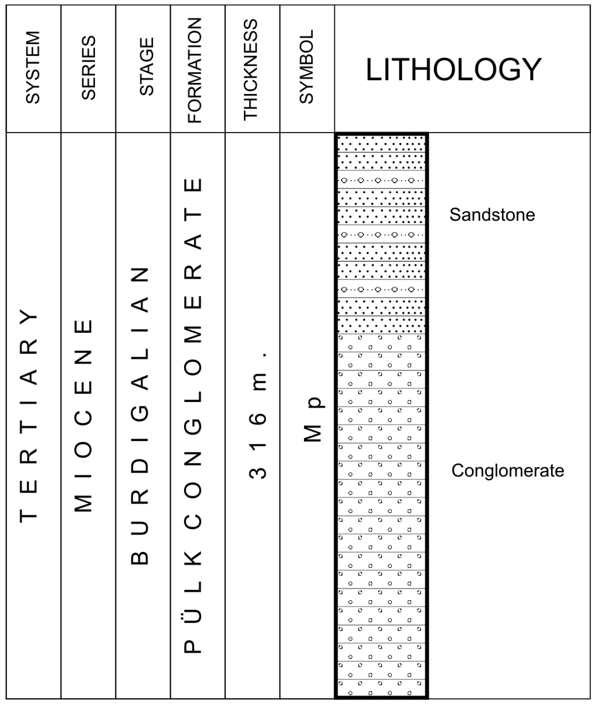

Figure-5 Measured stratigraphic section of Pülk conglomerate

Fosil Content and Age: No fossils were collected in the Pülk conglomerates. Because of its stratigraphic position, by overlaying the Tercan and underlaying the Engice limestones, the age of the unit is assigned as Early Miocene.

Environmental Interpretation: The Cross bedded sandstone lenses, and conglomerates indicate debris flows low energy and shallow stream deposits. The unit was deposited in upper-medium alluvial fan environment. Pebbles that form the conglomerate are of metamorphic and ophiolitic rock origin; this indicate that ophiolitic and metamorphic rocks are present in the source area.

Correlation: The unit can be correlated with Hürrübaba conglomerates in Erzurum-Tekman basin.

Pamuktepe limestone (Mpa)

Distribution: The unit crops out in the west of Çayırlı (İ43 b3) only. It was first defined by Arpat (1964).

Type Locality and Type Section: The type locality of the unit is Pamuktepe.

Lithological Features: The unit has light gray coloured, hard, well bedded sandy limestones in the lower levels, in the central sections it comprises white coloured, brittle, fossiliferous, sandy and clayey limestones. The unit has yellowish grey coloured, thin bedded, laminated and fossiliferous limestones in the upper levels.

Contact Relations: The unit overlies the gypsum unconformably. It is overlain by Miocene Neftlik formation.

Thickness: Pamuktepe limestone is 210 m thick (Figure-6).

Fossil Content and Age: The following fossils collected from the unit indicates Burdigalian age: *Miogypsina irregularis* (Mish), *Amphistegina radiata* (Fichtel ve Moll), *Operculina complanata* (Defr).

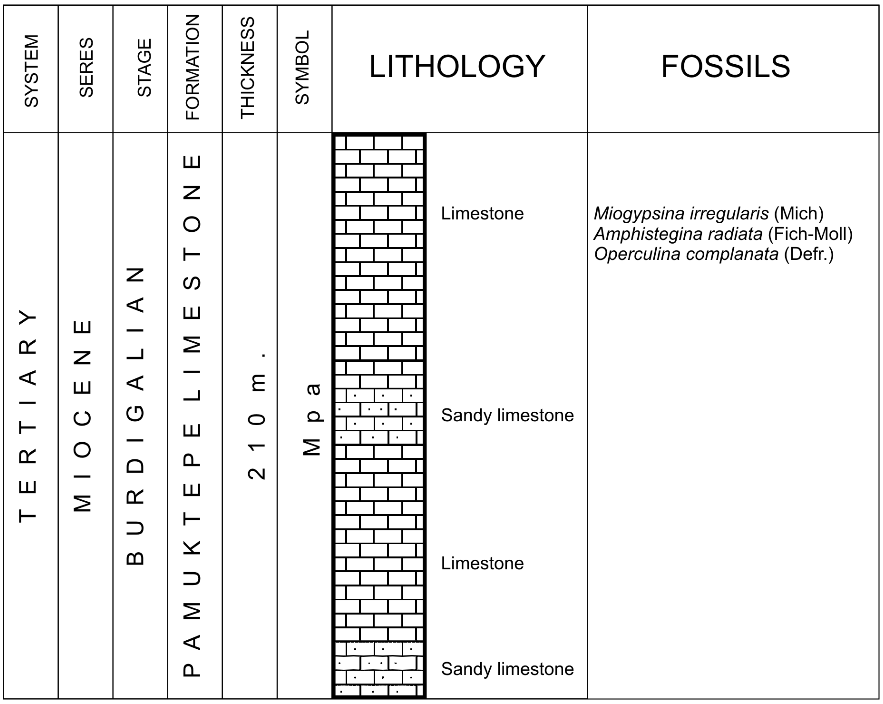

Figure-6 Measured stratigraphic section of Pamuktepe limestone

Environmental interpretation: According to lithological and paleontological features of the unit, it was deposited in a shelf environment of a warm sea.

Correlation: Pamuktepe limestone can be correlated with the Haneşdüzlü limestone observed in Erzurum-Tekman, Karayazı, Pasinler basins.

Engice limestone (Me)

Distribution: The unit crops out in the Pülk mountain, Kızılkayalar, Mırcıgataşı hill, Engice mountain and Şahinkalesi hill in the study area. Engice limestone which is comprised of light red -pink coloured, fossiliferous limestones was defined by Arpat (1964).

Type locality and type section: The type sections of the sequence were measured at Pülk mountain, Kızılkayalar and Engice mountain.

Lithological features: The Engice limestone which overlie the Pülk conglomerate in Pülk mountain is white coloured and includes large shell fragments and crinoid fragments; however, in Kızılkayalar it is a red - pink coloured, well sorted calcarenite with coarse sand and includes terrigenous clastics derived from ophiolites, lamellibranch and shell fragments. Silicium and ophiolitic pebbles are found in limestones around Şahinkalesi hill. The 1-1.5 cm sized pebbles are ill-sorted and medium-well rounded. They are thick bedded. In the south of Mırcıga village, Pülk conglomerates with large blocks (marbles of 80 cm in diameter, serpantines of 50 cm in diameter, andesite, granite blocks of 20 cm in diameter) are located below the red limestones.

Contact relations: Pülk conglomerates are located below the Engice limestone. In the upper contract, it is transitive to Balıklı formation.

Thickness and lateral changes: The average thickness of the Engice limestone is 80 m. The unit is 64 m in Pülk mountain, 125 m in Engice mountain and 137 m in Kızılkayalar. Thickness gradually decreases in the west of Pülk mountain (Figure-7).

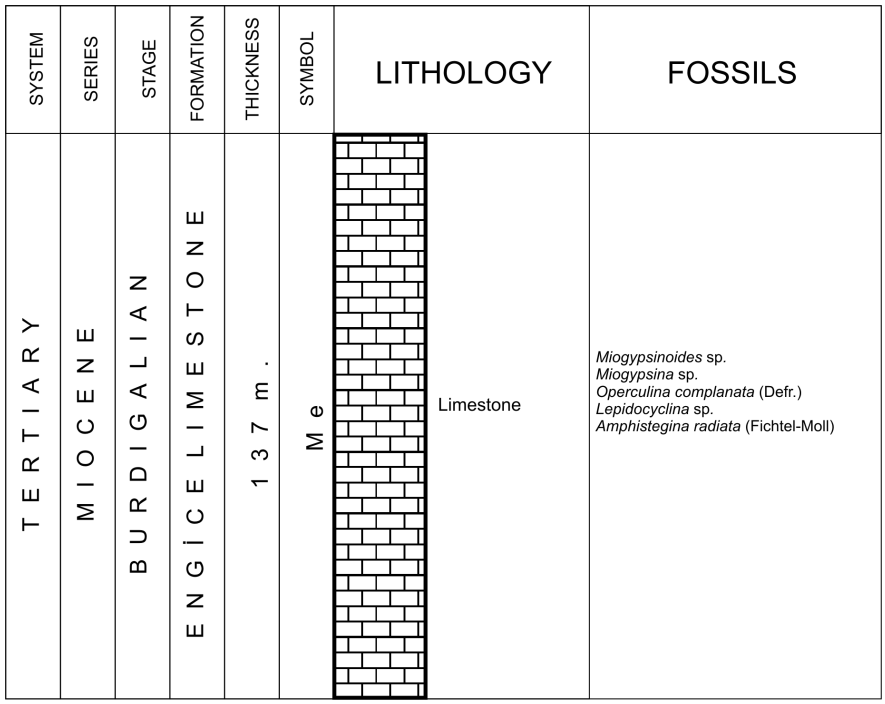

Figure-7 Measured stratigraphic section of Engice limestone

Fossil content and age: The age of the unit is Burdigalian according to the following fossil assemblage: *Miogypsinoides* sp., *Migypsina* sp., *Amphistegina* sp., *Lepidocyclina* sp., *Lithothamnium* sp., *Operculina* sp., *Elphidium* sp., Bryozoa, corals, gastropoda, echinoides.

Environmental interpretation: The fossils stated above indicate marine environment between 0-50 m and indicate that the section of the Engice limestone with coarse grains, including shell fragments, sandy, pebbly sections were formed in high energy sea shore environments. Fine grained, massive or thick bedded calcarenites indicate deposition in deeper environments by the fossils pointing the conditions below the wave base. In general, The Engice limestone is in clastic limestone facies; it was formed in clastic and carbonaceous seashore environment. It is transitive in lateral and vertical directions.

Correlation: The unit can be correlated with Haneşdüzü limestone observed in Erzurum-Pasinler-Karayazı, Tekman basins.

Balıklı formation (Mb1, Mb2)

Distribution: Balıklı formation which crops out in Çayırlı region is comprised of bituminous marl and gypsum. The gypsum is indicated on the map by Mb_1 and the bituminous marl is indicated by Mb_2. The sequence was defined by Arpat (1964). It overlies the Engice formation and is comprised of clay, marl and limestone levels with clastic elements. The limestones include bitumen.

Lithological features: The sequence is comprised of a marl, shale and claystone succession and gypsum levels gradually thickening and thinning and after a thin limestone level.

Contact relations: The unit is laterally and vertically transitive to Engice limestone in the lower contact and to Dumanlı formation in the upper contact. It is below the Neftlik formation in Neftlik-4 well.

Thickness and lateral changes: The unit is 220 m in Pülk mountain section, 121 m in Kızılkayalar, 222 m in Pamuktepe, 1050 m in Neftlik-4 well (Figure-8, 12).

Fossil content and age: The following fossils indicate that the age of the Balıklı formation is Burdigalian (Arpat, 1964): *Miogypsina* spp., *Gyroidina neosoldanii* Brotzen, *Uvigerina longistriata* Perconıg, *Nonion pompilioides* (Fıcht-Moll), *Nonion boueanum* (D'orb) and *Pyrgo depressa (D'orb).*

Environmental interpretation: Evaporites such as gypsum, anhydrite and halite were formed by the primary deposition at the bottom of the lagoon and between tidal flat environment which resemble the Holocene sabhkas.

Dumanlı limestone (Md)

Distribution: Dumanlı limestones crop out in Pülk mountain, Sırataştepe, Kırklartepe and Güneytaştepe. The general lithology is limestone. In the study area it crops out in Çayırlı region and was first defined by Arpat (1964).

Type locality and type section: The typical locality of the sequence is Pamuktepe, Pülkdağı and Kızılkayalar.

Lithological features: The lower levels of the Dumanlı limestone are comprised of conglomerates and limestones with shell fragments. This limestone is gray-white, yellowish in color, hard, with abundant fossils, and includes large shell fragments, echinides and lamellibranch fragments in some levels. It is medium to thick bedded and its upper levels include fine grained limestones. It is sandy in general.

Contact relations: The unit is gradationally transitive onto the Balıklı gypsum and Balıklı claystone. It also is gradationally transitive to Güneytaş formation in the upper contact.

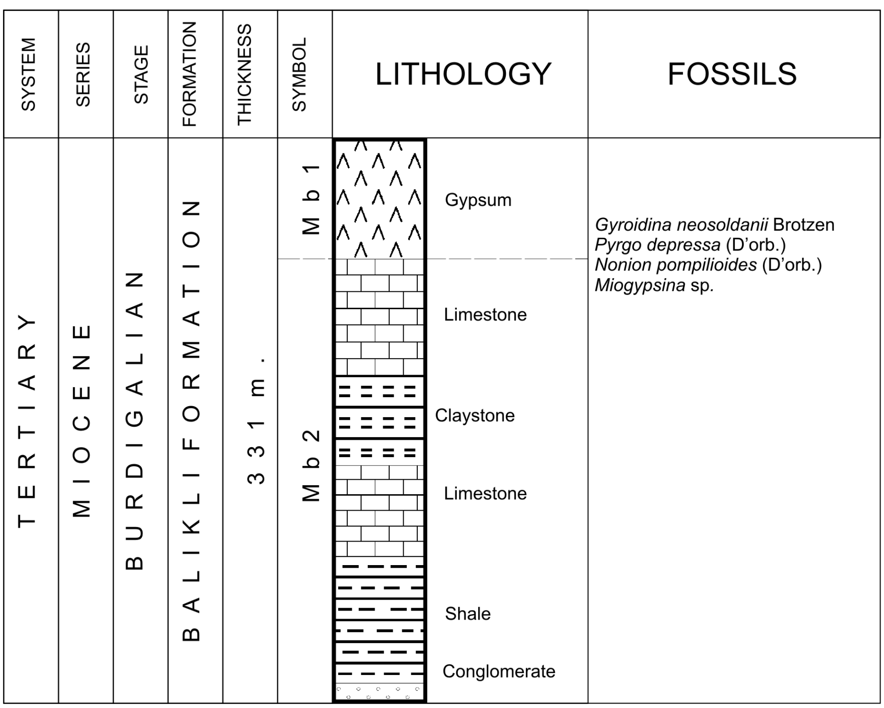

Figure-8 Measured stratigraphic section of Balıklı formation

Thickness and lateral changes: The unit is 345 m in Pülkdağ, 452 m in Kızılkayalar, 193 m in Neftlik-1 well and 550 m in the west of Çayırlı (Figure-9).

Fossil content and age: The following fossils collected in the unit indicate Burdigalian: *Miogypsina irregularis* (Mıch), *Miogypsina* sp., *Lepidocyclina* sp., *Amphistegina radiata* (Fıchtel and Moll), *Rotalia* sp., *Elphidium* sp., *Operculina complanata* (Defr.)

Environmental interpretation: Coarse grains, shell fragments, sand and pebble content of the Dumanlı formation indicate that the formation was deposited in a high energy marine condition.

Correlation: The formation can be correlated with the Lower Miocene Haneşdüzü formation in Erzurum basin.

Güneytaş formation (Mg)

Distribution: The formation crops out at Güneytaştepe and Sırataştepe hills located in the north of the Pülk village. It is comprised of white coloured marl, red sandstone, clay and gypsum. The formation was defined by Arpat (1964).

Type locality and type section: No typical sections were measured.

Lithological features: The sequence is comprised of white coloured marls, red coloured sandstones, clay and gypsum succession. It uncludes abundant ostrea

Contact relations: The lower contact of the formation is unconformable with Dumanlı limestone while the upper contact is gradationally transgressive to Neftlik formation.

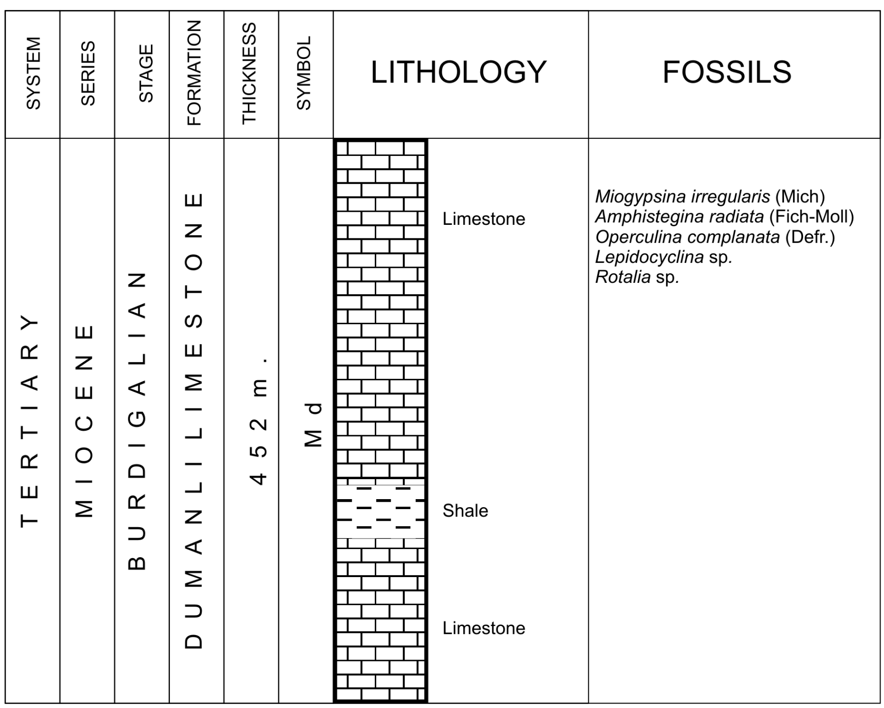

Figure-9 Measured stratigraphic section of Dumanlı limestone

Thickness and lateral changes: The thickness of the formation is 110 m.

Fossil content and age: The following fossils were determined in the formation and accordingly the age of the formation is Burdigalian: *Miogypsina* sp., *Rotalia* sp., *Elphidium* sp., *Operculina* sp., *Ostrea* sp.

Environmental interpretation: The formation was deposited in a shallow marine environment.

Neftlik formation (Mn)

Distribution: The succession of conglomerate, sandstone, claystone and sandy marl observed in the study area is named as Neftlik formation. It crops out in wide areas in İ44 a_1 and a_4 sheets. It was first described by Arpat (1964).

Type locality and type section: The typical section of the unit was measured on the roadcuts between Çayırlı-Karakulak and Neftlik mountain. Besides, it can be mesured at Kenetaşı hill in İ44 a_3 sheet.

Lithological features: The lower sections of the Neftlik formation was comprised of red coloured conglomerate with abundant magmatic pebbles. In the central parts sandstones and in the upper parts marls are dominant. Between the thick conglomerate levels white coloured tuff beds are observed. Thickness of the lower conglomerate level is 280 m. Conglomeratic levels become rare upwards and sandstones become dominant in general. Thickness of the sandstones is 420 m. The upper levels of the Neftlik formation is comprised of white-yellow, green coloured clays and marls. There are two tuffaceous levels which display clay mineralization.

Contact relations: The lower contact of the Neftlik formation is gradationally transitive with Dumanlı limestone and Güneytaş formation whle the upper contact is unconformable with Afşin formation.

Thickness and lateral changes: Thickness of the Neftlik formation is 1050 m. 986 m of the formation was cut in the Neftlik-4 well (Figure-12).

Fossil content and lateral changes: The following fossils were determined in the unit and accordingly the age of the formation is given as Burdigalian *Miogypsina* sp., *Lepidocycüna* sp., *Heterostegina* sp., *Elphidium* sp., *Operculina* sp., Miliolidae.

Environmental interpretation: The formation was deposited in underwater delta platform and was buried under the floodplain with alluviums of which deltaic ceiling is advancing. Grain size of the conglomerates, erosional bottom contacts and the cross beddings indicate that the formation was deposited in high energy flow beds (Deveciler et al., 1993).

Correlation: The formation can be correlated with Yastıktepe formation located in Horasan, Pasinler (Erzurum) region.

Kemah formation (Tkç, Tkk, Tkm)

Kemah formation crops out in the south of the North Anatolian Fault between Kemah town and Erzincan and on the north and south of the Erzincan-Kemah road. Three members were differentiated in the formation. These three members are laterally and vertically transitive to each other: Pebblestone member (Tkç), Kömür member (Tkk) and Marik limestone member (Tkm).

Pebblestone member (Tkç)

Distribution:The sequence crops out in the core of the Kömürtuzlası anticline, in Kömür village and around Tortan, Mazerik, Zikri, Arbos and Sürek regions.

Type locality and type section: No typical sections were measured.

Lithological features: The Pebblestone member is comprised of reddish, locally grayish, gren

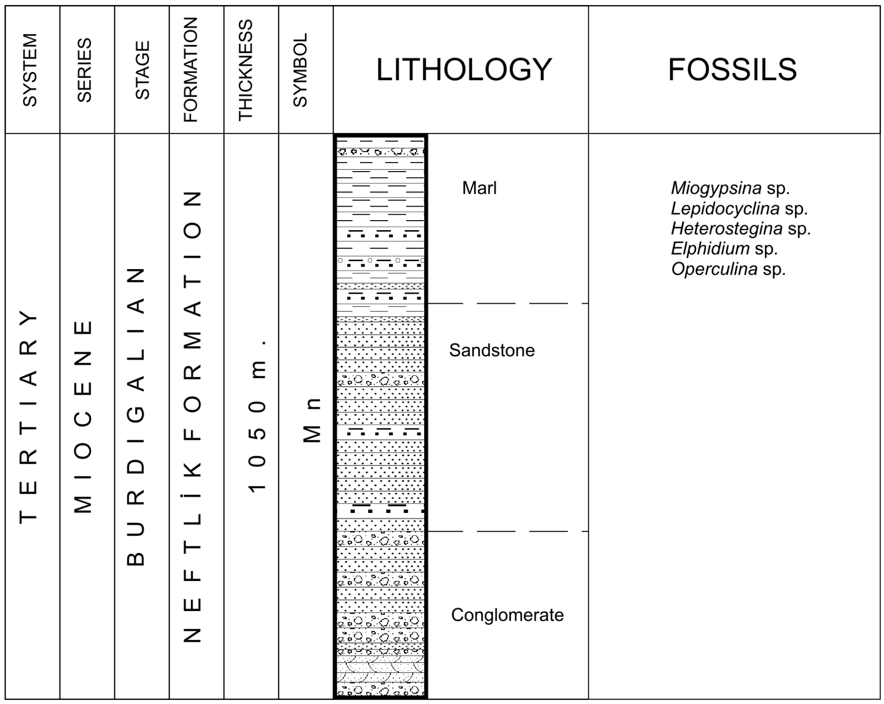

Figure-10 Measured stratigraphic section of Neftlik formation

coloured, medium to thick bedded, well sorted pebblestones and sandstones with clayey and carbonaceous matrix. It crops out in the core of the Kömürtuzlası anticline and in the north of the Kemah-Erzincan road. It can easily be differentiated from the other red coloured formations.

Thickness and lateral changes: Thickness of the Pebblestone member of the Kemah formation is 400 m. It is laterally and vertically transitive to the Kömür member.

Fossil content and age: No datable fossils were found in the red, variegated coloured conglomerates, sandstones and shales beds of the member.

Environmental interpretation: The Peblestone member of the Kemah formation, cross bedded sandstone and shale beds were deposited in underwater fan delta environment.

Correlation: The unit can be correlated with the Lakoğlu formation located between Tercan-Aşkale.

Kömür member (Tkk)

Distribution: This member crops out on the northern and southern banks of the Fırat river between Erzincan and Kemah.

Type locality and type section: No typical sections were measured.

Lithological features: The units in general is comprised of a succession of sandstone, claystone, mudstone, clayey limestone, siltstone. It includes red, yellow, white, gren coloured, thin-medium-thick bedded, folded, jointed, locally overturned levels including fine carbonates, coal and gypsum.

Contact relations: It is laterally and vertically transitive to the overlain Pebblestone member and Marik limestone. Locally the unit unconformably overlies some other older units.

Thickness and lateral changes: Thickness of the unit is 400 m, however it can observed thicker in some places. It is laterally and vertically transitive to Marik limestone.

Fossil content and age: Based on the following fossils the age of the member is determined as Burdigalian: *Cyclammina latidossata* (Born), *Singmoilina miocenica* Cushman, *Margulina* cf. *incerta* (Egger), *Discorbis* cf. *orbicularis* (Terquem).

Environmental interpretation: The Kömür member was deposited in a terrestrial, lagoonal and shallow marine environment (Aktimur et al., 1995).

Correlation: The unit can be correlated with Hürrübaba formation located in Tekman-Erzurum regions.

Marik limestone member (Tkm)

Distribution: Marik limestone member crops out in Kemah, Zoga, Marik, Tavginer and Acemsuyu regions.

Typical locality and typical sections: No typical sections were measured.

Lithological features: The unit is white, yellowish coloured in general and is medium to thick bedded with calcite veins and joints. It is sandy and in some places it is observed as clayey limestone. It includes algae, micro and macro fossils.

Contact relations: The lower contact of the sequence is transitive to Pebblestone member and in places it is transitive to Kömür member. In general the Marik limestone member is located at the topmost. It unconformably overlies the older units.

Thickness and lateral changes: Thickness of the Marik limestone member is 400 m. It is laterally and vertically transitive to Kömür and Pebblestone members.

Fossil content and age: Based on the following fossils and algae and shell fragments collected in the Marik limestone member the age of the member is determined as Burdigalian: *Miogypsina irregularis* Mich, *Miogypsina saitoi* Yabe ve Hanzawa, *Miogypsina* sp., *Lepidocyclina* sp., *Amphistegina* sp.

Environmental interpretations: Marik limestone member has abundant fossils, it was deposited in a warm and shallow marine environment.

Correlation: The unit can be correlated with Haneşdüzü formation located in Pasinler-Tekman-Hınıs regions.

Avşin formation (Pla)

Distribution: This unit which forms slightly rough, rounded hills in the region by conglomerate with hard matrix and sandstone with coarse-medium size grains. It crops out around Kirazdağ and Kazburnu hills in the map of İ44 a_1 sheet and Avşin and Aşağı Avşin in İ44 a_3 sheet. It was first described by Akkuş (1964).

Type locality and type section: Type locality of the Afşar formation is in the south of Avşin stream located between Yukarı Avşin and Aşağı Avşin villages.

Lithological features: Avşin formation is comprised of a succession of conglomerate with hard matrix and sandstone with coarse-medium size grains. Th epebbles at the upper levels are not consolidated. Thickness of the pebblestone levels is 50-75 cm. The pebbles were derived from serpentines, radiolarites, Mesozoic and Miocene limestones. Large scale cross beddings are observed. At the upper levels of the Avşin formation marl, swamp deposits with coal and tuff beds are located. The beds are horizontal or have dips varying between 10°-25°.

Contact relations: Avşin formation unconformably overlies the older units. It is unconformably overlain by the Quaternary terraces and alluviums.

Thickness and lateral changes: Thickness of Avşin formation is 370 in Çayırlı region and 210 m in Kemah region. In DSİ Pekeriç drillings the thickness of the formation is measured as 235 m.

Erzincan volcanics

The young volcanic rocks cropping out in the eastern side of the Erzincan plain have formed in two phases. These are Ağlı tuff (Qa) and Karatepe andesite (Qk).

Ağlı tuff (Qa): This is unit is comprised of tuff, perlite and pumice. The name of the unit is after Ağlı. It crops out around Üzümlü in the eastern sections of the Erzincan plain. The tuffs are white - gray coloured, thin to medium bedded, jointed, faulted. The age of the unit is Plio-Quaternary and it unconformably overlies the older units and is unconformably overlain by the alluviums and alluvial cones.

Karatepe andesite (Qk): The unit is comprised of rocks such as andesite, trachyandesite, rhyolite, rhyodacite and trachyte. It was named after Karatepe. It crops out around Üzümlü, in vicinity of Erzincan-Pülümür highway, and around Güneyli. They include andesine, augite, hornblende and biotite crystals.

Travertines

In Kismisor stream valley, along Başköy reverse fault travertines were formed. Recent travertine formations stil continue in the region. Besides, in southeast of Erzincan, travertine formations can be observed around Çağlayan and Brastik villages.

Alluviums (Qal) and alluvial terraces

Alluvial terraces cover large areas in the study area. The Mans and Pülk streams joining to Karasu river have formed their own beds on the hanging alluviums. The terraces lithologically include flat or angular pebbles, sandstones, sands, pebbles and clay successions. Pebbles are generally derived from basic and ultramafic rocks. They are partly well rounded and ill sorted. Clay levels are dark coloured (Aktimur et al., 1986). The younger alluviums are mostly found in stream beds and in valleys and can easily be differentiated from the older terraces.

STRUCTURAL GEOLOGY

Folds

In the north of the study area, there is a 1-3 km wide folded zone which extends between Pülk and Çığaloğlu bridge. In this zone, there are anticlines and synclines in Miocene sequences. These folds continue in the east of Pülk village. The largest anticlines and synclines are located in the north of Pülk mountain. The axis of the anticline which is located in the south of the Bozağa village extends in E-W direction for 10 km. Pülk mountain, Kırklar hill, Sırataş hills and Engice mountain forms the southern flank of this anticline. Pülk mountain is a double plunging syncline and its axis extends in E-W direction. Jurassic-Cretaceous, Late Cretaceous, Eocene and Oligocene formations have folded in E-W, NE-SW directions. Miocene deposits have formed wider folds and plunging anticlines and synclines. The irregularity in the folds of the gypsums are mainly for this reason.

Thrusts

In the north of the Karakulak and Başköy, it was observed that ammonites, belemnites bearing Upper Jurassic-Early Cretaceous (Jkb) Bedirga limestone is located on the Eocene Gülandere formation and the abnormal contact has very little dip and the thrust was developed from north to south. In the south of Kismisor village the Upper Jurassic-Early Cretaceous Berdiga limestone and Neftlik formation has an abnormal contact with right angle and reverse fault.

Westward the fault becomes a fault with right angle. The Neftlik fault which traverses the area where the Neftlik oil seep is observed continues westward with increaisng slip rate. This fault is the most important fault in the region since it affects the oil prospect of the area. The oil seep is located on this fault which cuts the northern flank of the anticline. The slip of this fault decreases in the west of the oil seep and disappear in İ43 b_2 sheet. The fault plane is vertical.

In Kemah region, around Cirzini and Kürkentli, the older units have thrusted onto the Early Miocene units. This thrust continues for kilometers in the east. As a result of these thrusts the northern flank of the Miocene Kemah formation was overturned and overturned synclines were formed. In Tanyeri-Bulanık region, along an E-W line of 25 km long, older units were observed to thrust onto Gülandere and Miocene Kemah formation.

Normal Faults

In the study area, the North Anatolian Fault (NAF), the Northeast Anatolian Fault (NEAF) and small scale normal faults joining these faults under certain angles are located.

North Anatolian Fault (NAF)

The North Anatolian Fault zone traverses the Erzincan region in SE-NW direction. The fault which has caused many earthquakes in historical times and recently form a 10-15 km wide zone in Erzincan basin. The right-lateral strike-slip North Anatolian Fault is comprised of two segments in the region. The first segment is located around Yarbaşı village in the south of Üzümlü and is 30 km long. The second segment begins in the west of Üzümlü and follows the line along Geçitköy and Yalnızbağ. The North Anatolian Fault which is active on the northern border of the Erzincan basin recently was active in the southern border of the basin in the past.

East Anatolian Fault (EAF)

The Northeast Anatolian Fault which joins to the North Anatolian Fault just outside the study area, traverses along the line passing 2.5 km south of Spikör, Köroğlu, north of Hatabi mountain and the region around Büyükgelenç. It is a left-lateral strike-slip fault and its length in the study area is about 30 km.

SOURCE ROCK INVESTIGATIONS

The oil seep in Çayırlı-Neftlik region and the signs of presence of oil in the shales and marls in Balıklı formation indicates that the region has importance from the oil occurrence point of view and oil was formed here (Figure 11). Organic geochemical features of the sequences in the basin and the geochemical features of the oil seep were analyzed (Table 1). Depending on these analyses, the type and amount of total organic matter and its maturity were determined and the hydrocarbon potential of the sequences were interpreted. The source of the oil seep was investigated making use of the source rock-oil analyses. The analyses were conducted in the TPAO Research Laboratories. The pyrolysis analyses are given in table 2.

Amount of Organic Matter

The Total Organic Carbon (TOC) analysis was made to determine the amount of the organic matter in the rock (Table 1). The total organic matter amount is equal to the addition of the hydrocarbons present in the rock freely and the organic carbon related to kerosene (Tissot and Welte, 1984; Barker, 1986; Jarvie, 1991). The TOC value of the sample collected from the Upper Cretaceous Anikdağ formation is zero, that means this formation does not include organic matter. The TOC value of a sample collected from the Gülandere formation is zero, however, that of another sample collected from the same formation is 0.48. According to these values, the Gülandere formation has weak

Table 1- Pyrolysis analyses of source rocks of Kemah-Erzincan-Çayırlı region and the calculated parameters

AGE	Formation Name	Sample No	TOC (weight%)	S_1 (mg HK/g rock)	S_2 (mg HK/g rock)	S_3 (mg CO_2/g rock)	T_{max} (^oC)	Genetic Potential (S_1+S_2) (mg HK/g rock)	Transformation Rate [$S_1/(S_1+S_2)$]	HI (S_2/TOK) (mg HK/g TOC)	OI (S_3/TOK) (mg CO_2/g TOC	Residual Carbon (%)
Miocene	Kemah (Kömür Mem.)	200997	0.33	0.02	0.27	0.16	436	0.29	0.070	81	48	0.31
	Kemah (Kömür Mem.)	200999	0.01	0.02	0.05	0.25	466	0.01	0.333	50	2500	0.01
	Neftlik	200995	0.02	0.02	0.02	0.77	-	0.04	0.500	100	3850	0.02
	Neftlik	200994	0.00	0.03	0.00	0.89	-	0.03	1.000	-	-	-
	Balıklı	200998	1.43	0.03	1.07	0.41	434	1.10	0.030	74	28	1.34
	Balıklı	200992	0.49	0.25	0.64	2.10	374	0.89	0.280	130	428	0.42
	Kismisor	201001	0.00	0.01	0.23	-	-	0.01	0.000	-	-	-
Eocene	Gülandere	201000	0.00	0.01	0.00	0.11	-	0.01	0.000	-	-	-
	Gülandere	200996	0.48	0.01	0.21	0.33	452	0.22	0.050	43	68	0.47
Upper Cretaceous	Anikdağ	220993	0.00	0.01	0.00	0.20	-	0.01	0.00	-	-	-

Table 2 - Rock-Eval Analyses (Çayırlı-Erzincan)

FORMATION	Sample Pyrolysis No	TOC %	S1	S2	S3	Genetic Potential (S1+S2) mgHK/g rock	Tmax	Hydrogene Index (Iıı)	Oxygene Index (Io)	Transformation Rate S1/(S1+S2)	RC
Balıklı Fm. Miocene	200992	0,49	0,25	0,64	2,10	0,89	374	130	428	0,280	0,42
Balıklı Fm. Miocene	200998	1,43	0,03	1,07	0,41	1,10	434	74	28	0,030	1,34
Neftlik Fm. Miocene	200994	0,00	0,03	0,00	0,89	0,03	-	0	0	1,000	-
Neftlik Fm. Miocene	200995	0,02	0,02	0,02	0,77	0,04	-	100	3850	0,500	0,02
Söğütlü Village Gülandere Fm. Eocene	200996	0,48	0,01	0,21	0,33	0,22	452	43	68	0,050	0,47
Kemah Fm. Kömür Mem. Miocene	200997	0,33	0,02	0,27	0,16	0,29	436	81	48	0,070	0,31
Kemah Fm. Kömür Mem.	200999	0,01	0,02	0,05	0,25	0,01	466	50	2500	0,333	0,01
Anikdağı Fm. Upper Cretac.	200993	0,00	0,01	0,00	0,20	0,01	-	0	0	0,000	-
Gülandere Fm. Eocene	201000	0,00	0,01	0,00	0,11	0,01	-	0	0	0,000	-
Kismisor Fm. Miocene	201001	0,00	0,01	0,00	0,22	0,01	-	0	0	0,000	-

source rock characteristics. The TOC values of the selected samples of four Miocene formations were measured. Accordingly, the TOC value of the Kismisor formation iz zero, it can not be considered as a source rock. The TOC values of the two samples collected from the Balıklı formation are 1.43 and 0.49, the average value is calculated as 0.96. These data indicate that the Balıklı formation has source rock features at medium level. The samples collected from Neftlik formation either does not include organic carbon or include very few; therefore this formation can not be accounted for as a source rock. The TOC values of the samples from the Kemah formation are measured as 0.01 and 0.33, the average value is calculated as 0.17. Accordingly, the Kemah formation is a weak source rock.

Type of Organic Matter

In order to determine the kerosene types of the samples from the Kemah, Gülandere and Balıklı formations, HI-Tmax kerosene type diagram (Mukhopadhyay et al., 1995) was used. According to this diagram, the samples from the Kemah, Gülandere and Balıklı formations fall into the Type III kerosene area (Figure 12). Only one single sample from the Kemah formation was observed to fall on Type II - Type III boundary. The Type III kerosene indicate that these formations include terrestrial organic matters that have the capability to produce gas only.

Maturity of Organic Matter

Maturity of the organic matter is defined as the process of formation of hydrocarbon com-

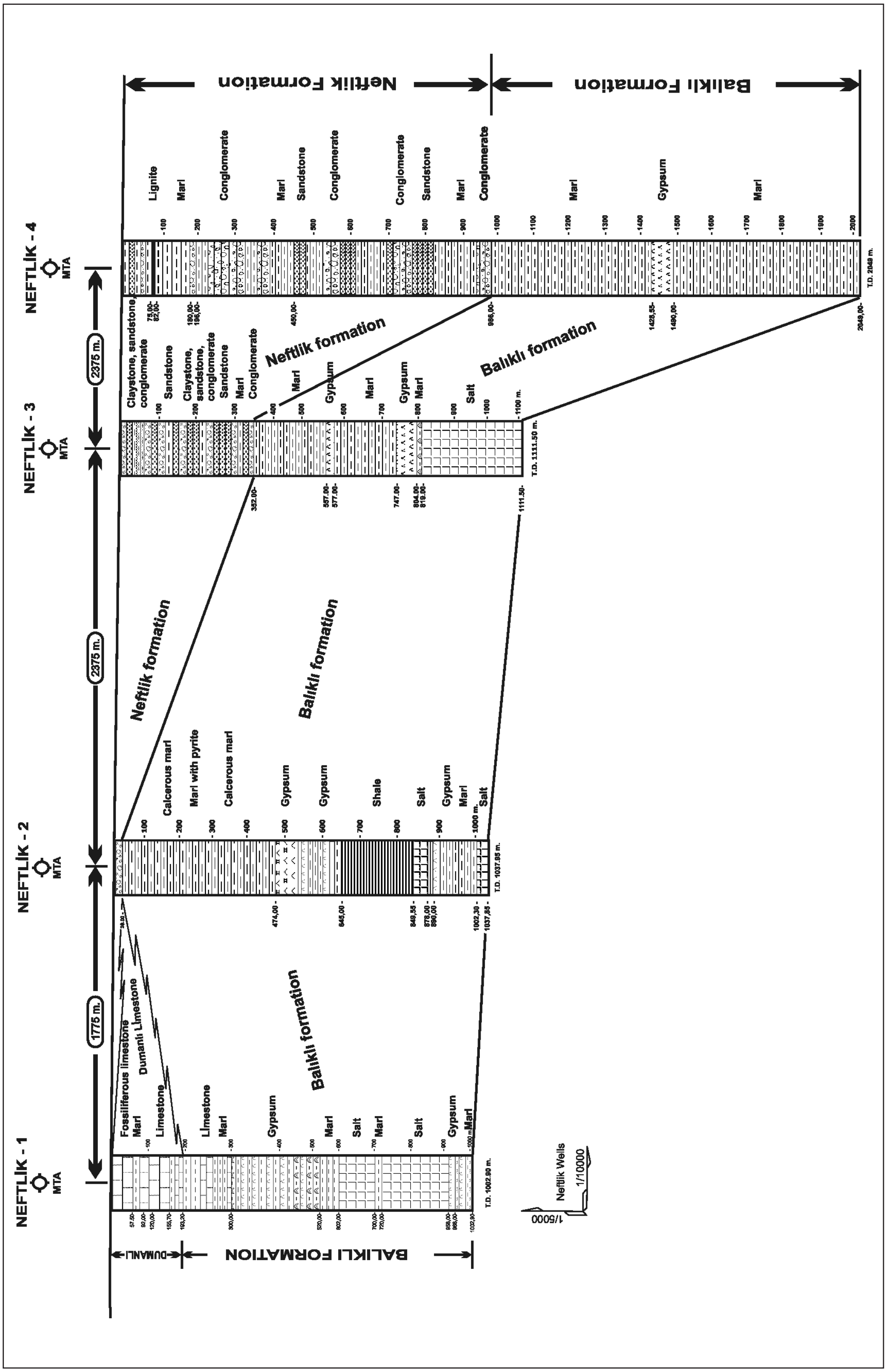

Figure-11 Correlation of the Neftlik-1, Neftlik-2, Neftlik-3, Neftlik-4 wells

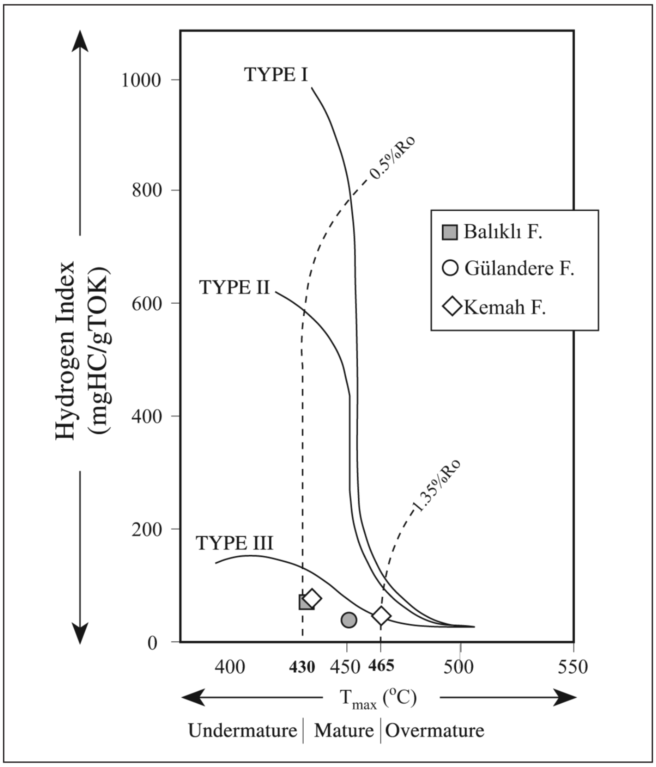

Figure-12 HI-Tmax diagram of the Gülandere, Balıklı, Kemah Formation Kömür member

pounds by physicochemical changes under factors such as temperature, pressure, burial and time. Thermal development of the organic matter changes many physical and chemical feature of the matter and by determining these features maturity of the organic matter can be measured (Tissot and Welte, 1984, Hunt, 1995).

As a consequence of the pyrolysis (Rock-Eval) analysis, the Tmax values of the samples from the Kemah, Gülandere and Balıklı formations were determined as 404 °C which indicates non-mature source rock (Figure 13, 14; Table 2) The average Tmax values of the samples from the Miocene Kemah formation were measured as 451 °C which indicates a mature source rock. The Tmax values of a sample from the Eocene Gülandere formation were measured as 452 °C, this value indicates a mature source rock, too.

Biomarker

The organic compounds of which carbon structures are directly related to the organic molecules of the live organism from which they were formed and are indicators for the live organisms they were derived are called biomarkers (Tissot and Welte; 1984; Waples and Machihara, 1991, Peters and Moldowan, 1993; Hunt, 1995). Because of these features, biomarkers are known as geochemical fossils. In this study, steran and terpan biomarkers of Neftlik oil seep in turn were determined and interpreted in m/z 217 and 191 mass chromatograms.

The biomarker distributions vary depending on the organic facies and depositional environments. By determining these variations type of organic facies, depositional environment and

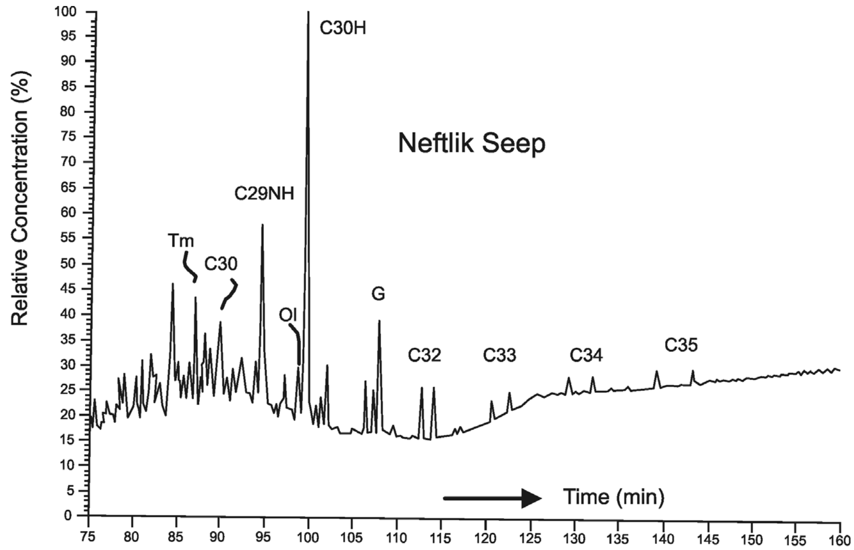

Neftlik Seep	$C_{29}NH/C_{30}H$	Tm/Ts	C_{35}/C_{34}	Gam/C_{30}	C_{32} 22S/22 S+R	NOTE
	0.37	2.4	1.00	0.26	0.50	Oleanane +(Ol)

Figure-13 GC-MS m/z 191 terpan fragmentogramme of the Neftlik oil seep and its parameters

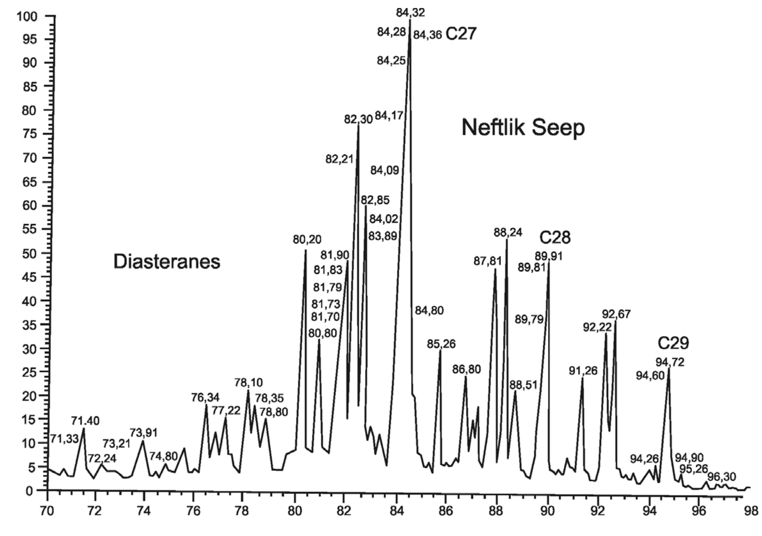

Seep	% C 27	% C 28	% C 29	C 29 20S / 20S+R	% Iso steran	% Normal steran	% Diasteran	NOTE
Neftlik	55	29	16	0.44	43	40	43	4- met. Steran+

Figure -14 GC-MS m/z 217 steran fragmentogramme of Neftlik oil seep and its parameters some features of the depositional environments can be known. Besides, some biomarker transformations are controlled by the underground temperature and the exposure time to this temperature. By determining these transformation ratios, it is possible to make interpretations on the maturity.

In m/z 191 mass chromatogram of the Neftlik oil seep, the C_{27}, C_{28} and C_{29} steran ratios were determined as 55, 29 and 16%, respectively. Huang and Meinschein (1979) stated that the relative ratios of the C_{27}-C_{29} regular sterols are related to specific environments and sterans can provide significant paleo-environmental information. Almost all of the high plants include C_{29} as dominant sterols and the cases where the C_{29} sterans are dominant indicate terrestrial organic matters (Huang and Meinschein,1979; Robinson, 1987). Dominant C_{27} sterans indicate dominance of marine phytoplanctons (Huang ve Meinschein, 1979). The C_{28} steran is the rarest of these three steran groups and when they are rather abundant, presence of intensive lacustrine algae is indicated (Waples and Machihara, 1991). According to the steran distribution of the Neftlik oil seep the most dominant steran is C_{29} and the lowest steran is C_{27}. This distribution indicates that the input of the terrestrial organic matter is less and the organic matter determined is of marine origin. No C_{30} sterans which indicate marine contribution were recorded in m/z 217 mass chromatogram. Although the presence of C_{30} sterans indicate marine origin, it is not the reverse case when they are not present. Besides in m/z 217 mass chromatograms widespread diasterans were recorded. It was observed that the diasterans are widespread in clay rich clastic sediments and the diasteran/steran ratio is used widely for differentiang the carbonaceous - clastic rocks. Abundance of diasterans in Neftlik oil seep indicate that the source rock is a clastic rock. Besides, it was pointed out that the C_{29} hopan recorded in m/z 191 mass chromatogram has an atypical value in carbonates and evaporites (Waples and Machihara, 1991) and C_{29}/C_{30} ratio can be used as a criteron for carbonate content (Riva et al., 1989). Any value larger than 1 correspond to carbonates. The C_{29}/C_{30} of Neftlik seep in m/z 191 mass chromatogram was determined as 0.37, which indicate a clastic source rock. Besides, Ts is more dominant with respect to Tm in m/z 191 mass chromatogram. It was found that the Ts/Tm ratio is low in carbonate rocks and contrarily high in shales (McKirdy et al., 1983; Rullkötter et al., 1985). Therefore, the Ts and Tm values indicate that the source rock is not a carbonate rock. In m/z 191 mass chromatograms high gamaseran amount was recorded and the Gamaseran/C_{30} hopan ratio was calculated as 0.26. Gamaseran is characteristic for lacustrine and marine sediments with high salinity (Waples and Machihara, 1991; Connan, 1993; Peters and Moldowan, 1993). Significant amount of gamaseran indicate that the source rock was deposited in a saline environment. Oleanan is a biomarker which was assumed to be derived from terrestrial sources especially from the angiosperms of the plants and is an indicator for terrestrial organic matter input (Peters and Moldowan, 1993; Hunt, 1995). This biomarker has not been observed in a source rock younger than Cretaceous and its presence indicates Cretaceous or younger times (Waples and Machihara, 1991; Peters and Moldowan, 1993; Hunt, 1995). Oleanan was recorded in less amounts in m/z 191 mass chromatograms. This indicates that the Neftlik seep comes from a source rock of Cretaceous or younger and has very little terrestrial organic matter input.

Some biomarker transformations change with maturity and is used for the interpretation of the maturity. In this study, 20S/(20S+20R) (McKenzie et al., 1980; Spiro, 1984; Seifert and Moldowan, 1981, 1986; Waples and Machihara, 1991; Peters and Moldowan, 1993) and $\beta\beta/(\beta\beta+\alpha\alpha)$ (Peters and Moldowan, 1993; Hunt, 1995), steran (C_{29}), 22S/(22S+22R) homohopan (C_{32}) (Waples and Machihara, 1991; Hunt, 1995; Seifert and Moldowan, 1986) ratios which increase with maturity were calculated. The

20S/(20S+20R) and $\beta\beta/(\beta\beta+\alpha\alpha)$ C_{29} steran ratios of the Neftlik seep were calculated as 0.44 and 0.55, in turn. Besides, the 22S/(22S+22R) C_{32} homohopan ratio is determined as 0.50. According to these values an early maturity feature is observed.

CONCLUSIONS

In Kemah-Erzincan-Çayırlı region, rather thick Tertiary sedimentary sequences comprised of carbonaceous sediments crop out on the pre-Late Cretaceous basement. In this study lithological features, extensions, contact relations and ages of these sequences were described and the depositional environments were interpreted. Oil seeps and the levels including bitumen and asphalt in Tertiary sequences were also studied and the hydrocarbon potential was investigated.

The Late Cretaceous Anikdağ formation does not include any organic matters and therefore is not a source rock. According to its TOC content, the Eocene Gülandere formation is a weak source rock. The Miocene Kismisor and Neftlik formations do not have the characteristic features of a source rock. The Miocene Balıklı formation is a medium level source rock while the Kemah formation is a weak source rock.

The organic matter types of the Kemah, Gülandere and Balıklı formations are determined as Type III according to the results of pyrolysis analyses. The Balıklı formation is not a mature formation based on its Tmax value. On the other hand, the Kemah and Gülandere formations are mature formations.

Widespread diasteran content of the sample from the Neftlik oil seep and its C_{29}/C_{30} hopan ratio calculated to be less than 1 and high Ts/Tm ratio indicates that it seeped from a clastic source rock. Gamaseran indicates that the source rock from which the oil seep was derived was deposited in an environment with high salinity. Presence of the oleanan point out a source rock of Cretaceous age or younger and also the input of terrestrial organic matters. According to the maturity data calculated from the steran and terpan distributions in the oil seep, an early maturity was assigned.

When evaluated with all these geochemical data, it was concluded that there was no good source rock in the basin and consequently the basin does not have oil potential.

ACKNOWLEDGEMENTS

I would like to extend my sincere thanks to Dr. Şükrü Acar who studied the Tertiary foraminifera, to Kemal Erdoğan who studied the Mesozoic foraminifera, to Dr. Tansel Tekin and Haluk İztan who conducted the geochemical analyses and to Prof. Dr. Sadettin Korkmaz for his invaluable contributions during this work.

Manuseript receive June 26,2007

REFERENCES

Akkuş, M., 1964, Erzincan-Tercan bölgesi detay petrol istikşaf etüdü raporu. MTA Report No: 4041 (unpublished) Ankara.

Aktimur, H. T., 1986. Erzincan, Refahiye ve Kemah dolayının jeolojisi. MTA Report No: 7932 (unpublished) Ankara.

_____, Sarıarslan, M., Keçer, M., Turşucu, A., Örçen, S., Yurdakul, M. E., Mutlu, G., Aktimur, S. and Yıldırım, T., 1995. Erzincan dolayının jeolojisi. MTA Report No: 9792 (unpublished) Ankara.

Arpat, E., 1964 Erzincan'ın Çayırlı ilçesinin civarının ve uzakkuzeyinin genel jeolojisi ve petrol imkanları. MTA Report No: 4046 (unpublished) Ankara.

Akyol, Z. and Birgili, Ş., 1966, Neftlik-2 kuyu bitirme raporu. MTA Report No: 4387 (unpublished) Ankara.

_____, Neftlik-3 kuyu bitirme raporu. MTA Report No: 4388 (unpublished) Ankara.

Barker, C. 1986. Organic geochemistry in petroleum exploration. AAPG Bulletin, 10, 39-41.

Birgili, Ş., Yurdakul, M., 1971, Çayırlı Neftlik-4 kuyu bitirme raporu. MTA Report No: 4822 (unpublished) Ankara.

Bulut, C., 1965, Erzincan İ43 b3, İ44d1, 143 c2 paftalarını kapsayan bölgenin detay petrol etüdü raporu. MTA Report No: 4140 (unpublished) Ankara.

_____ and Akyol, Z., 1966, Çayırlı Neftlik-1 kuyu bitirme raporu. MTA Report No: 4386 (unpublished) Ankara.

Connan, J. 1993. Molecular Geochemistry in Oil Exploration. In: M.L., Bordenave (Editor), Applied Petroleum Geochemistry. Paris, pp. 175-204.

Demirmen, F. , 1965, Çayırlı ilçesi (Erzincan civarı) genel jeolojisi ve petrol olanakları. MTA Report No: 4845 (unpublished) Ankara.

Deveciler, E., Canpolat, M. , Küçükefe, Ş. , Karabıyık, N., Kar, H., Ayaz, E., Ünay, E., Tuzcu, S., Karabıyıkoğlu, M., Örçen, S., Genç, S. and Erdoğan, K., 1994, Çayırlı dolayının (Erzincan ili) jeolojisi. MTA Report No: 9672 (unpublished) Ankara.

Gedik, A. 1976. Doğu Anadolu'da açılan stratigrafik istikşaf (açınsama) sondajları, Yeryuvarı ve İnsan, 3, 3, 31-35s.

Huang, W.-Y. and Meinschein W. G. 1979. Sterols as Ecological Indicators. Geochimica et Comochimica Acta, V.43, p. 739-745.

Hunt, J.M. 1995. Petroleum Geochemistry and Geology. W.H. Freeman and Company, New York, 743 pp.

Jarvie, D.M. 1991. Total organic carbon (TOC) analysis. In: Merrill, R.K., (ed.): Source and Migration Processes and Evaluation Techniques. AAPG, Oklahoma, 213pp.

Ketin, İ., 1950, Erzincan ile Aşkale arasındaki sahanın (1/100.000)'lik 46/4 ve 47/3 paftalarının jeolojisine ait memuar. MTA Report No: 1950 (unpublished) Ankara.

Kurtman, F., 1962, Kemah Kömür Tuzlası bölgesinin petrol istikşaf etüdüne ait rapor. MTA Report No: 4849 (unpublished) Ankara.

Lucius, M., 1926, Pülk petrol mıntıkası. MTA Report No : 205 Ankara (unpublished)

Mackenzie, A.S., Patience, R.L., Maxwell, J.R., Vandenbroucke, M. and Durand, B., 1980. Molecular Parameters of Maturation in the Toarcian Shales, Paris Basin-1. Changes in the Configurations of Cyclic Isoprenoid Alkanes and Triterpanes. Geochimica Cosmochimica Acta, 44, 1709-1721.

Mckirdy, D.M., Alridge, A.K., and Ypma, P.J.M., 1983. A Geochemical Comparisan of some Crude Oils from Pre-Ordovician Carbonate Rocks. In: Advances in Organic Geochemistry 1981 (M. Bjor y et. al, eds.), Wiley and Sons, New York, p. 99-107.

Mukhopadhyay, P.K., Wade, J.A. and Kruge, M.A., 1995. Organic facies and maturation of Jurassic/Cretaceous rocks, and possible oil-source rock corelation based on pyrolysis of asphaltenes, Scotion Basin, Canada. Organic Geochemistry 22, 85-104.

Nalifkin, D.V., 1919. Van Gölünden Trabzon'a kadar petrol yataklarının incelenmesi. Jeoloji Komitesinin Haberleri, t.37 (1918) No.1.334-337 Moskova

Paige, S., 1933, The geology of the region near Pülk in the vilayet of (Erzurum). MTA Report No: 203 (unpublished) Ankara.

Peters, K.E., and Moldowan, J.M., 1993. The Biomarker Guide: Interpreting Molecular Fossils in Petroleum and Ancient Sediments. Englewood Cliffs, N.J., Prentice-Hall, 363 pp.

Petukinoff, Cr. , 1932, Pülk petrol arazisi. MTA Report No: 208 (unpublished) Ankara.

Pisoni, C., 1965, Tercan bölgesinin jeolojisi ve petrol olanakları. MTA Report No: 4446 (unpublished) Ankara.

Riva, A., Riolo, J., Mycke, B., Ocampo, R., Callot, H.J., Albrecht, P. and Nali, M., 1989. Molecular Parameters in Italian Carbonate Oils: Reconstruction of Past Depositional Environments, 14th International Meeting on Organic Geochemistry. Paris, September 18-22, Abstracts, Number 335.

Robinson, K. M., 1987. An Overview of Source Rocks and Oils in Indonesia: Proceedings of the Indonesian Petroleum Association Sixteenth Annual Convention, Indonesian Petroleum Association, V., 48, p. 151-157.

Roothan, Ph, J., 1940, Erzurum ve Erzincan vilayetlerindeki petrol jeolojisi araştırma raporu. MTA Report No : 1248 (unpublished) Ankara.

Rullkötter, J., Spiro, B., and Nissenbaum, A., 1985. Biological Marker Characteristics of Oils and Asphalts from Carbonate Source Rocks in a rapidly Subsiding Graben, Dead Sea, Israel. Geochimica Cosmochimica Acta, V. 49, p. 1357-1370.

Seifert W.K. and Moldowan J.M., 1981. Paleoconstruction by Biological Markers. Geochimica Cosmochimica Acta, 45, 783-794.

_____ and _____ 1986. Use of Biological Markers in Petroleum Exploration. In: P.B. Johns (Editor), Methods in Geochemistry and Geophysics, 24, 261-290.

Spiro, B., 1984. Effects of the Mineral Matrix on the Distribution of Geochimical Markers in Thermally Affected Sedimentary Sequences. Organic Geochemistry, 6, 543-559.

Stchepinsky, V., 1940, Erzincan mıntıkası linyitleri ve idrokarbürleri hakkında rapor. MTA Report No: 1004 (unpublished) Ankara.

Tekin, T., 2002, Source rock potential and organic facies properties of the Oligo-Miocene deposits in the Pasinler-Horasan, Tercan-Aşkale basins (East-Anatolia) METU Ph.D Thesis.

Tissot, B.P. and Welte, D.H., 1984. Petroleum Formation and Occurence. Springer Verlag, Berlin Heidelberg, New York, Tokyo, 694 p.

Tur-Kan Petrol Ltd. Şti., 2001, AR/TUR/VII/3617, 3618, 3622, 3623, 3624 ruhsat sahalarının terk raporu. Petrol İşleri Genel Müdürlüğü Arşivi. Ankara

_____, 2002, AR/TUR/VII/3619,3621 ruhsat sahalarının terk raporu.Petrol İşleri Genel Müdürlüğü Arşivi. Ankara

Waples, D.W. and Machihara, T., 1991. Biomarkers for Geologists-A pratical Guide to the Application of Steranes and Triterpanes in Petroleum Geology. American Association of Petroleum Geologists, Methods in Exploration Series, No: 9, 85 pp.

bos

Mineral Res. Expl. Bull., 137, 29-48, 2008

THE MINERALOGIC, PETROGRAPHIC AND ION EXCHANGE CAPACITY FEATURES OF TUFFS CONTAINING CHABAZITE AND PHILLIPSITE MINERALS IN SANDIKLI (AFYON) REGION AND THEIR USAGE IN AGRICULTURE (SOUTHWEST ANATOLIA, TURKEY)

Yahya ÖZPINAR*

ABSTRACT.- The study area is located at southern part of Sandıklı town (Afyon-southwest Anatolia). The volcanics of Sandıklı region in the investigated area are represented by lavas and pyroclastic rocks of Middle-Late Miocene age. The Lavas occur as trachyandesitic, phonolitic tephritic, basaltic andesitic, basaltic trachy-nephelinitic, andesitic and dacitic in compositions. Pyroclastic rocks are composed of lapillistone, tuffaceous conglomerate, tuffaceous sandstone, tuffacous siltstone and tuffaceous mudstone, and also have vitric and crystal vitric tuffs in thrachyandesitic, phonolitic and tephritic compositons. In the tuffs located at the northern part of the investigated area the chabazite occurences, and in the tuffs located at the southern part the phillipsite occurences are found widespreadly. In phillipsitic tuffs, three-phillipsite forms were defined namely potassium-sodium-aluminum-silicate hydrate, sodium-aluminum-silicate hydrate and potassium-calcium-aluminum-silicate hydrate froms. In tuff samples purified with tetrabrom ethane the zeolite contents by weight mostly between 29.00 wt.% and 63.00 wt.%. After the activition of the tuff samples with 0.1N HCl and 0.1N H_2SO_4, their cation exchange features were investigated. In the tuffs activated with both acids, Ca^{+2} content with respect to other cation contents has been passed too much to the solutions depending on time. But those activated with 0.1N HCl, as depending on time, Ca^{+2} content has been passed as more linear to the solutions. When we consider of ion exchange capacity and selection of the radioactive cations such as ^{137}Cs and ^{90}Sr and ^{40}K of chabazite and phillipsite, zeolitic tuffs may be used for improvement of soil, stabilization of pH of acidic soils and to prevent to passing of the radioactive elements from nature to the environment and biological systems. Because of activated natural zeolites tend to the increasing of the resorption and adsorption of moisture which contributes to the plant development, activated natural zeolitic tuffs may be used as desiccants. For the adsorption of the ammonium smells arised from urine and fecal matter, it is thought that zeolitic tuffs may be used to separate methane from other gasses. Besides, it is believed that it is possible to use them as building stone for heating and air conditioner for small houses and animal shelters.

Keywords: Chabazitic and phillipsitic tuffs, Sandıklı, Southwest Anatolia.

INTRODUCTION

The investigated area is located at southern part of Sandıklı town. The Sandıklı is the town of Afyon city and situated at the western part of Central Anatolia in Turkey (Figure 1). This study comprises part of investigations supported by TUBITAK "YDABÇAĞ-198Y102". In this project, geological, petrographical and mineralogical features of Sandıklı volcanics were investigated and experiments were made to determine technologic usage of tuff and tuffites. However the purpose of this paper is to report the results of detailed

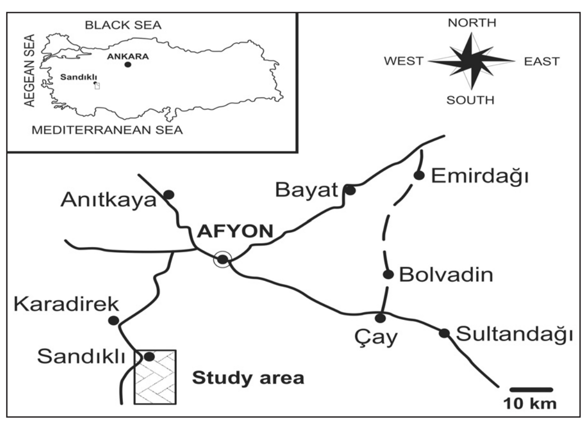

Figure 1- Location map of the study area.

*Pamukkale Üniversitesi, Mühendislik Fakültesi, Jeoloji Müh. Bölümü, Kınıklı Kampüsü, 20017, Denizli.

study of mineralogic, petrographic and ion exchange capacity features of tuffs containing of chabazite and phillipsite minerals at southern part of Sandıklı town and their evaluation for healthing.

The investigated area and its surrounding districts have been studied by many investigators based on investigation topics. Some of these studies can be grouped as following. The Afyon and Sandıklı Neogene basins and hydrogeological feature of Hüdai geothermal area in Sandıklı region have been studied by Ronner (1962), Bulutcu (1975) and Afşin (1991) and they pointed out that the Hüdai geothermal water have high radioactive features. The geological and petrological features of Afyon and Sandıklı volcanics of Middle and Late Miocene age, namely trachyte, thrachyandesite, rhyolite, latite and basalt having alkaline and calk-alkaline character have been studied by Villari and Keller (1972), Keller (1983), Öngür (1973), Başarır and Kun (1982) and Ercan(1986). Using the K-Ar age method, of the Sandıklı volcanics have been dated by Besang et al. (1977) and obtained the ages 14±0.3- to 8.0±0.6 Ma. Çoban and Flower (2007) asserted that the magmatism in the Kırka-Afyon-Isparta region shows a temporal progression from calk-alcaline to ultrapotassic affinity which is associated with the geodynamic evolution of the "Isparta Angle". The petrological evolution and lamprophyres of Afyon stratovolcano have been investigated by Aydar et al. (1996, 2003). Tectonic and metamorphic evolutions of Sandıklı-Afyon region have been studied by Öngür (1973) and Tolluoğlu et al. (1997). Zeolitization in Sandıklı tuffs, firstly has been discovered by author (Özpınar, 1998; Özpınar et al. 1998). In addition, Özpınar et al. (2002) studied petrographic and petrochemical features of zeolitic tuffs at southern part of Sandıklı region.

METHOD OF STUDY

In this study, for determining the distribution of Sandıklı volcanics, detailed mapping of an area about 180 km^2 was firstly done at 1/25 000 scale and microscopic studies of 98 samples were carried out. Later, for all study 101 samples of lavas, tuffs and tuffites were qualitatively determined by XRD and zeolites specimens purified with heavy liquid (tetrabrom ethane) qualitatively determined by DTA (10 sample) and electron microscope (8 sample) and chemical analyses of the altered lavas, tuffs and tuffits (58 sample) were carried out by XRF in R&D laboratories of Turkish Cement Manufacturer's Association. In addition the chemical analyses of the lavas (8 sample) and tuffs (2 samples) were carried out by ICP-MS in Acme Analytical Laboratories Ltd., Canada. Beside, cation exchange capacity tests were carried out by flame photometry (JENWAY mark) apparatus in laboratory geological engineering department of Pamukkale University.

STRATIGRAPHY AND PETROGRAPHY

In the study area the Karatepe formation represented by violet colored conglomerate and siltstone of Late Triassic-Early Jurassic age is exposed at the bottom of the sequence and well observed southwest of Yeniçay located at the western part of the area (Figure 2). The Karatepe formation is transitionaly overlain by Derealanı formation of Jurasssic age which is also transitionaly overlain by Akdağ formation of Late Jurassic- Early Cretaceous age exposed at the mountainous areas of the southern and southeastern part of Sandıklı region. From lower to upper parts, the Akdag formation is represented by gray and dark gray colored micritic and cherty limestones, respectively.

The Akdağ Formation is unconformably overlain by Neogene age units. Lacustrine detritic rocks of Middle(?)-Late Miocene age is located at the lower part of lithologic units and composed of conglomerate, sandstone, marl and limestone. This unite is unconformably overlain by the detritic rocks of Quaternary represented by gravel, sand and clay (Figure 2 and 3).

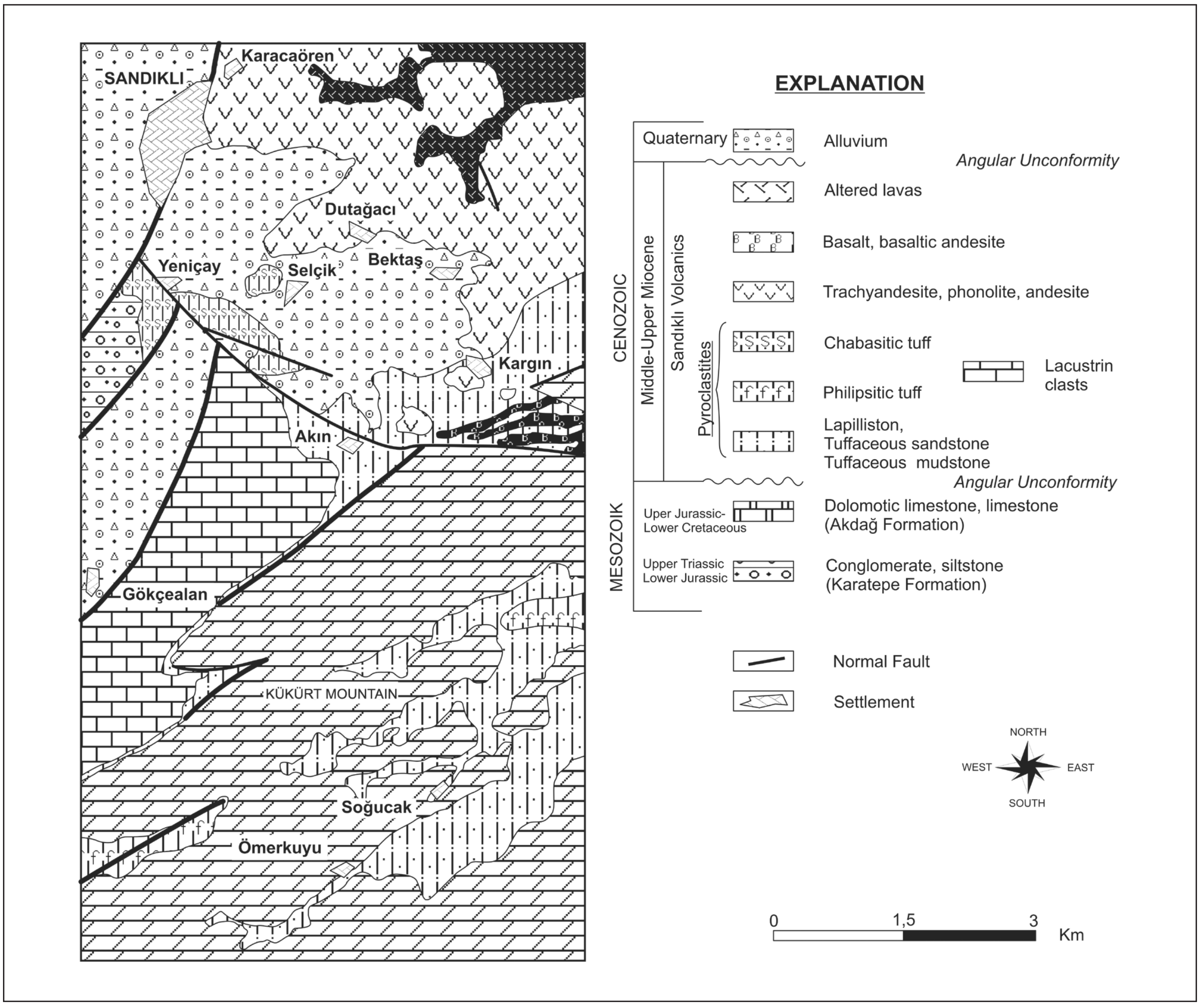

Figure 2- Geological map of the study area.

In the study area, the Middle-Late Miocene volcanics and volcano-sedimentary units have been named as Sandıklı volcanics. By using the radiometric age method, the age of Sandıklı Lavas have been dated by Besang et al. (1977) and the ages obtained range between 14±0.3 - 8.0±0.6 Ma (Ercan, 1986). The Sandıklı volcanics are mainly composed of red, gray and light brown colored lavas and pyroclastic rocks (Figure 2 and 3).

The pyroclastic rocks have various ratio of pyroclastites, epiclastites (Schmidt, 1981), pyrogenetic and secondary minerals. The pyroclastic rocks are named as lapillistone, tuffaceous conglomerate, tuffaceous sandstone, tuffaceous siltstone and tuffaceous mudstone. The coarse grained pyroclastic rocks are found at lower part of the sequence. At bottom, lapilli could become thrachyandesitic rock pieces and also could become white and gray colored pumice pieces (Figure 4). The matrix generally comprises fine and coarse grained volcanic ash. Above these rocks the tuffaceous sandstone overlies which contains few sand sized epiclasts and at the upper leves of sequence the tuffaceous mudstone is present (Schmidt, 1981; Fisher and Schmincke, 1984).

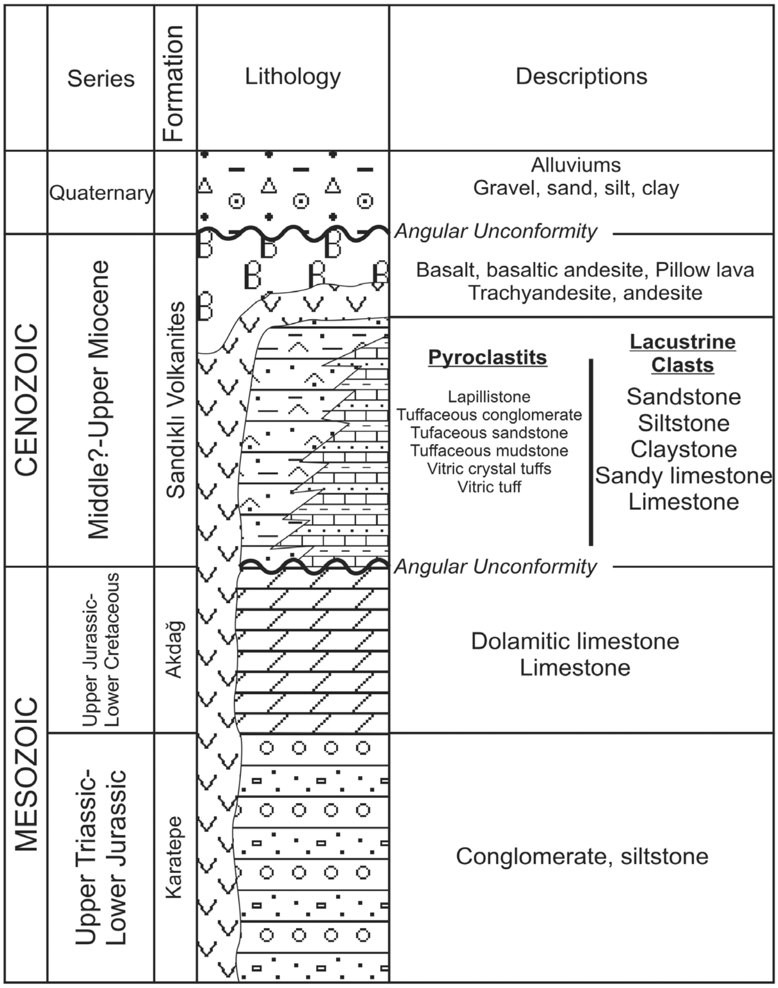

Figure 3- The simplified schematic columnar section of the study area, (not to scale).

Tuffs are exposed at southern and northern parts of investigated area. They have thrachyandesitic, phonolitic and tephritic compositons (Özpınar, 2001; Özpınar et al., 2002) named as vitric tuff and crystal vitric tuff. As depending on zeolite type (chabazite and phillipsite), zeolitic tuffs indicate different textural and structural features.

Chabazitic tuffs have cream colored, consolidated components and contain high porosity which are exposed at northern part of investigated area (south and west of Selçik village). According to identification by optical microscope, they have pyroclasts and epiclast in various ratio and sizes. In the tuffs, pyroclasts have microlitic and micro-porphyric texture. In the pyroclasts, plagioclase and augite are found as microlite and phenocrystalls. As a result, cream colored tuffs contain sanidine, albite, augite, biotite, clay minerals (illite), zeolite (chabazite) chlorite, opaque minerals and iron oxide. These minerals have also been determined by X-ray diffractometer.

Phillipsitic tuffs are gray, dark gray and brownish in color and have extremely consolidated components and high specific density than cha-

Figure 4- Field views from pyroclastic rocks. A, B and C) Tuffaceous conglomerate, tuffaceous sandstone, tuffaceous siltstone and tuffaceous mudstone. D) Tuffaceous lapillistone with rhyodacitic pumice E) Cream colored tuffs located at northern part of study area and F) Dark gray and brownrish colored tuffs located at southern part of study area.

bazitic tuffs. These are exposed at southern part of study area and located at Ballık, Ömerkuyu and Soğucak village, Sütlüce Küfeke tepe and its surrounding area. In the gray, dark gray and brownish tuffs, pyroclasts have microlitic and porphyritic texture. In addition, they have fine gravel and coarse sand sized and reworked and partly rounded. Beside, the tuffs contain a few radiolarite fragments which are partly rounded. The Soğucak tuffs have fine gravel and coarse sand sized particles of basaltic and trachy-basaltic compositions and Fe-oxide alteration is commonly seen. In Sütlüce Kufeke hill area, tuffs present columnar structure and they have lesser pyrogenic minerals and contain partly microcrystalline limestone "micrite" (Folk, 1962). The pumice contents are too much. According to the identification by optical microscope, the phillipsitic tuffs contain plagioclase (albite), augite, zeolite (phillipsite), biotite, clorite, calcite and iron oxide (Figure 5 and 6). These minerals have also been determined by X-ray difractograms. In gray, dark gray and brownish tuffs, three phillipsite form were determined. These are potassium-sodium-aluminum-silicate hydrate, potasium-aluminum-silicate hydrate and potassium-calcium-aluminum-silicate hydrate.

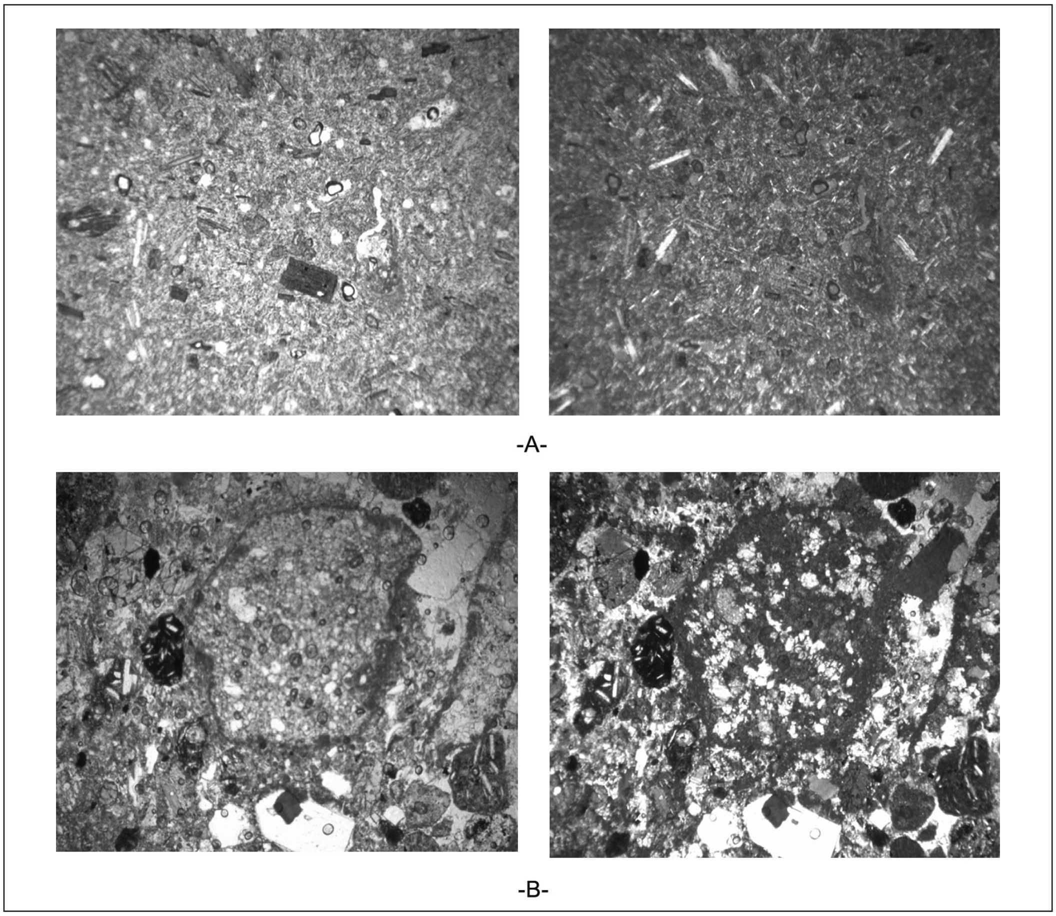

Figure 5- Microscopic views of vitric and crystal tuff (A), zeolitization of in pyroclasts and glassy matrix (B). Microscopic views at single (on the left) and double nicol (on the right) prism (A: 40X. B: 100X)

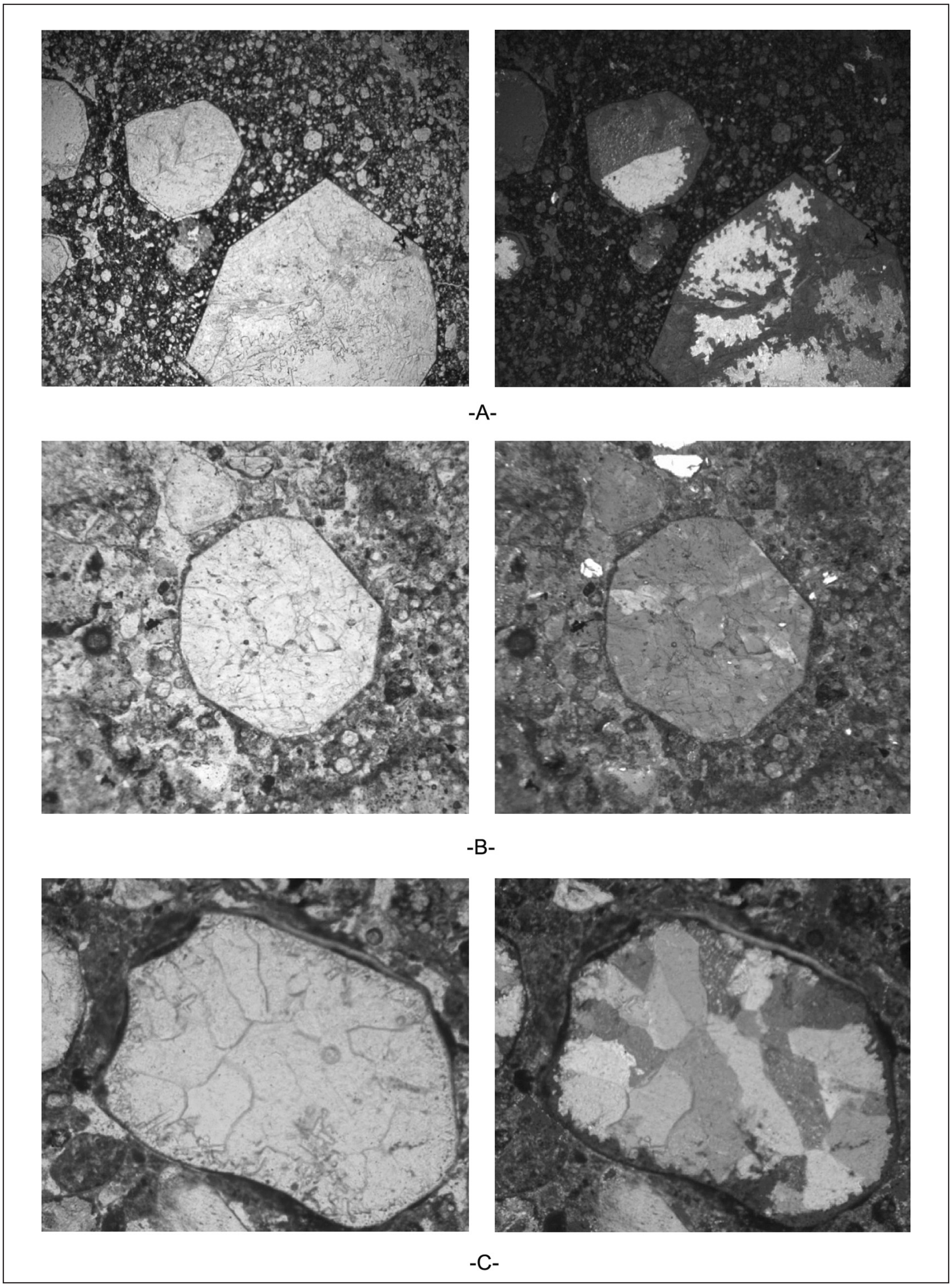

Figure 6- Thin section views of zeolitic tuffs. Zeolites have been seen with pseudo-hexagonal and isometric dodecahedron forms, under the microscope (A and B), large grain zeolite minerals (C) microscopic views from single (on the left) and double nicol (on the right) prism (100X)

In these area, phillipsites genarally have K, Na- form and K-form and besides K, Ca-form is lesser than the other form. In these tuffs, zeolitization of Soğucak location is too much and at some locations, ratio of zeolitization approach to 80% and 85%.

Sandıklı lavas have trachyandesitic, phonolitic tephritic, basaltic andesitic, basaltic trachynephelinitic, andesitic and dacitic compositions (Özpınar , 2001., Özpınar et al., 2002), mineralogic composition and textural features of andesite and trachyandesite specimens is essentially pilotaxitic, hyalopilitic, hyalo-porphyritic and micro-porphyritic. Groundmass essentially consists of fine and medium sized plagioclase microlites in a glassy matrix. Sanidine, plagioclase (oligoclase), biotite, basaltic hornblende occur as phenocrysts. The sanidine phenocrysts determined in the samples have very large sizes (from 3 to 5 cm). Apatite, sphene and zircon can be observed as accessory minerals. The chlorite and calcites have been found as secondary minerals. The results of microscopic and X-ray diffractograms are similar. Quartz, albite, sanidine, orthoclase, augite, biotite and illite from the mineralogic compositon of the samples in general.

In some locations located at the northern part of the investigated area, the lavas of andesitic and trachyandesitic compositions have been extensively altered by hydrothermal solutions (Figure 7) and changed to the clay (illite) and zeolite (chabazite) minerals. The zeolite formation of altered lavas is small in amount. In lavas where alteration is less, the zeolite mineral is not found. In altered lavas, the following minerals were identified by optical microscope and X-ray diffractograms; sanidine, plagioclase (albite), basaltic hornblende, biotite, chlorite, illite, montmorillonite (in some specimens), zeolite (chabazite), calcite, opaque minerals and iron oxide.

SEPERATION OF ZEOLITE MINERALS FROM TUFFS BY USING HEAVY LIQUID

Firstly, mineralogic composition and textural features of the zeolitic tuff specimens were defined under the polarized microscope. Later the specimens were investigated by X-ray diffraction method. Secondly, by using heavy liquid (tetrabrom ethane), the zeolite minerals were purified from zeolitic tuffs (Minato, 1992). The separation process used by heavy liquid is as following; sample is crushed to fine powder in agate mortar. The fine powder (clay minerals) is dispersed in a

-A- -B-

Figure 7- A) Field views of trachyandesitic and altered trachyandesitic lavas (A) and basalts (B).

distilled water by ultrasonic vibrator in beaker and are filtered by filter paper and dry up at about 60°C. Heavy liquid separation processes are carried out by using tetrabrom ethane. Purifed zeolite grains are filtered by filter paper and washed by acetone and dried up. The purifed zeolite grains are analyzed by X-ray diffraction method. At this method, if zeolite minerals have large grains, it can be obtained higher rate of success. According to the results which have been arranged, the amount of chabazite as weight % are 55.86 %, 29.00 %, 58.93 % and 42.4 % (Sample numbers: Z-2, Z-3, Z-6, Z-8) respectivelly. The amount of phillipsite as weight % are 62.40 %, 63.0 %, 51.53 % and 61.86 % (sample numbers: Z-1, Z-4, Z-5, Z-7) respectivelly.

Investigation of Zeolite Minerals by Electron Microscope and X-Ray Diffraction Method

The purified zeolite specimens were tested by means of X-ray diffraction method. According to X-ray diffractograms, determined minerals are given at table 1, figure 9 and 10. As mentioned above, while the tuffs located at Selçik village and its surrounding area contain only chabazite, the tuffs located at Ballık village (Table 1) and its surrounding area contain chabazite and phillipsite, and tuffs located at Alılı, Soğucak, Ömerkuyu and Sütlüce Küfeke and their surrounding area contain only phillipsite. In addition, three-phillipsite forms were determined. These are potassium-sodium-aluminum-silicate hydrate, pota-

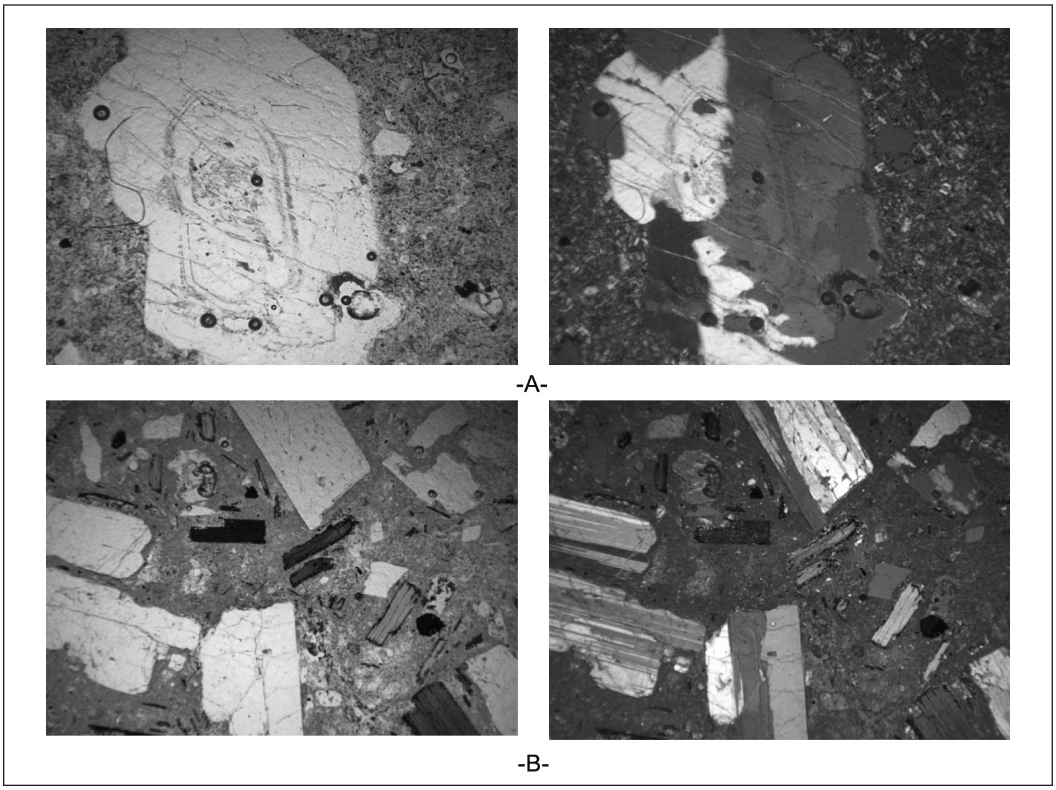

Figure 8- Microscopic views from trachyandesitic (A) and andesite (B) Large sanidine crystal from trachyandesite specimen (A) and biotite and plagioclase crystals from andesite specimens (B). Microscopic views from single (on the left) and double nicol (on the right) prism, 40 X.

sium-aluminum-silicate hydrate and potassium-calcium-aluminum-silicate hydrate. While in tuffs of southern part of investigated area three form of phillipsite have been determined, in tuffs of Sütlüce Küfeke tepe and its surrounding area two phillipsite form have been observed. These are potassium-sodium-aluminum-silicate hydrate and potassium-calcium-aluminum-silicate hydrate.

As mentioned above, if zeolite minerals have large grains, it can be obtained higher rate of success. In southern part of study area tuffs, zeolite minerals are large grains than zeolite minerals of northern part of study area. Because of this, at purified processes of phillipistic tuffs became with a few errors, these results can be seen in table 1. Appearances under the electron microscope (SEM) and their EDS spectrums of phillipsite (Z-1) and chabazite (Z-8) are given in figure 10.

Thermal Features of the Zeolite Minerals

The different data were obtained from thermograms of zeolite minerals purified by heavy liquid (Figure 11), In thermograms of chabazite specimens, the first endothermic peaks at temperature of 178 °C, 186 °C and 234 °C show maximum water loss. Second endothermic

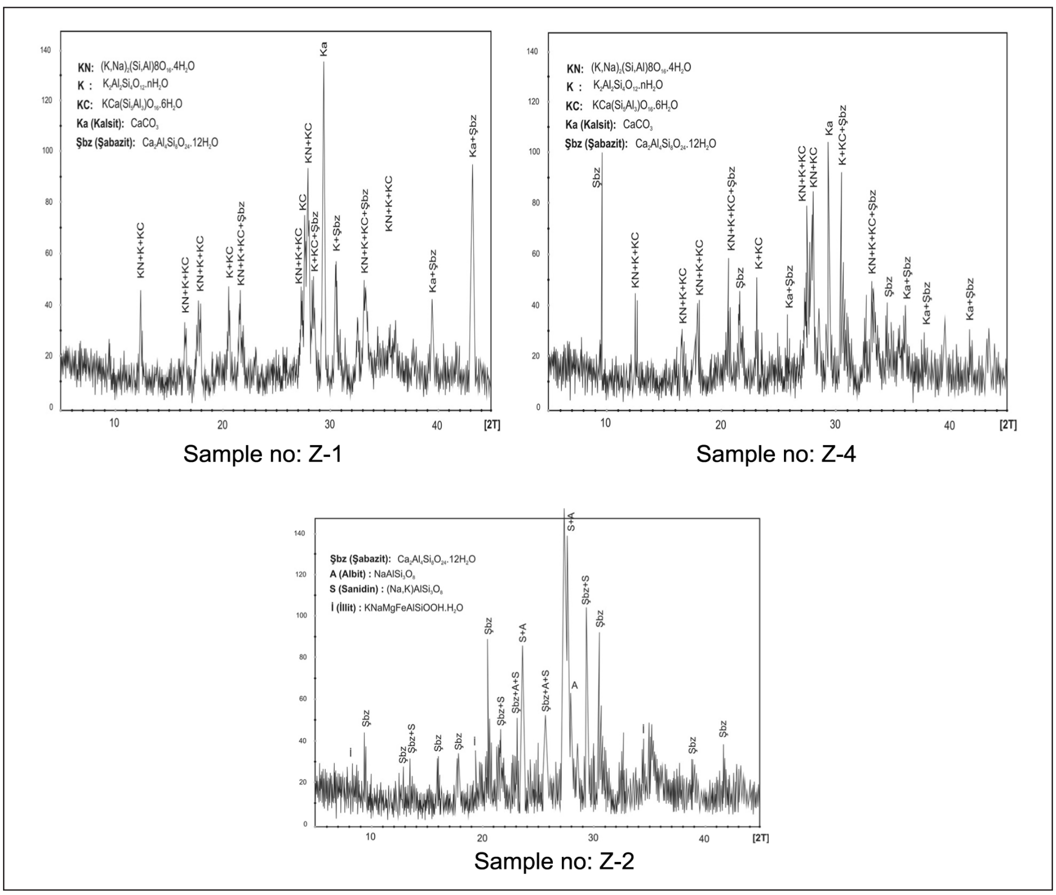

Figure 9- After separation processes with heavy liquite, mineralogic composition of determined by means X-ray diffractogram (A: albite; S: sanidine, Ca: calcite, Ch: chabazite, phillipsite (KN: K, Na form, K: K form, KC: K, Ca form).

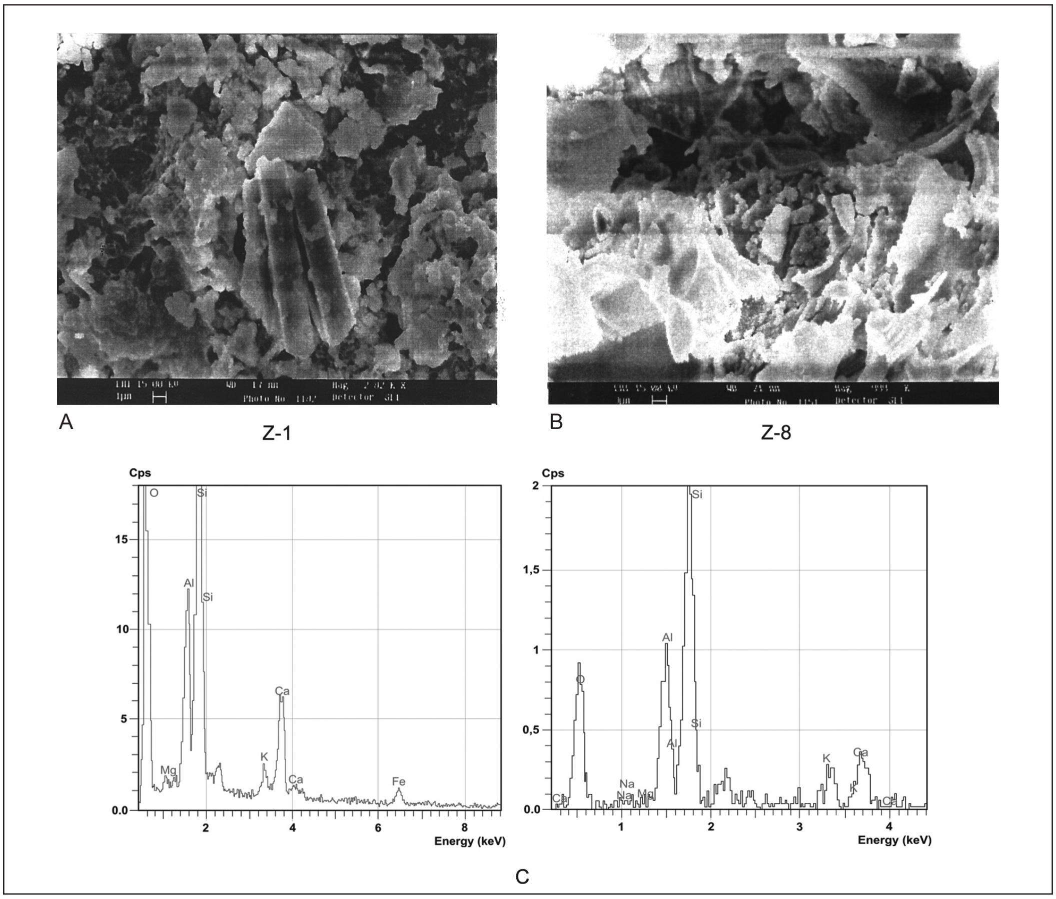

Figure 10- A: Phillipsite (Z-1) B: chabazite (Z-8) SEM and C: Their EDS spectrumes.

peaks show that the dehydration ends at temperature of 446 °C and 552 °C. Third endothermic peaks occurred at temperatures of 717 °C and 742 °C. These peaks indicate that due to narrowing of channels and breakdown of connected with the loss of huge free surface of dehydrated channels. Exothermic peaks at temperature of 846 °C ile 879 °C are associated with breakdown of sample mass change considerably. In all chabazite samples approximately at 1000 °C mass loss by weight occurred 12.5 % (Figure 11).

According to phillipsite forms, loss of water in phillipsite samples occurs at 70 °C, 120 °C, 140°C, 180 °C and 320 °C. In addition, It is concluded that endothermic peaks at 205 °C and 280 °C are not sharper peaks. The endothermic peaks due to loss of water in philipsite samples of study area occurred at temperature of 155 °C and 272 °C. According to chemical forms of phillipsites, endothermic peaks make clear that dehydration ends in intervals of temperature at 415 °C and 536 °C. After these temperatures having been determinated, metaphilipsite forms are protected and also exothermic peaks in intervals of temperature at 839 °C ve 879 °C and in all phillipsite samples mass loss of 12.7 % by weight were become approximately at 1000 °C (Figure 11).

Table 1- After separation processes with heavy liquite, mineralogic composition determined by means of X-ray diffractogram (Alb: albite; San: sanidine, Ort: orthoclase, Q: quarts, Cal: calcite, il:illite, He. hematite, Cha: chabazite, Phillipsite (K, Na form, K form, K, Ca form).

Sample. No	MINERALOGICAL COMPOSITION											Locations and Sample numbers
	Feldspars			Q	Kal.	İl.	He.	ZeolitE Minerals.				
	Alb.	San	Ort.					Cha.	KN	K	KC	
Z-1					+			+	+	+	+	Ballık tuffs, Sample Num:ST-11,12
Z-2	+	+		+	+			+				Selçik tuffs, sample num.: ST-25,26,27
Z-3	+	+		+				+				Selçik tuffs, Sample num.: :ST-1,2,3,4
Z-4					+			+	+	+	+	Ballık tuffs, Sample num.: : ST-13,14
Z-5			+						+	+	+	Soğucak tuffs, sample num.: ST-16,17
Z-6	+	+		+	+			+				Southern part of Selçik , tuffs.Sample num.: : ST-24,25,26
Z-7					+		+		+		+	Sütlüce küfeki tepe tuffs . SAmple num.: ST:19,20
Z-8	+	+				+		+				Selcik tuffs Smple num.: S-109

ION EXCHANGE FEATURES OF ZEOLITES

Depending on Si/Al ratios of chabazite structure, cations exchanged forms can be changed by temperatures and environmental conditions. According to Tsitsishvili et.al (1992), investigation of exchange reactions Na↔K, Na↔Cs and Cs↔K at 250 °C showed that exchange for large cations causes the structure to become stable. Chabazite is known to be selective towards Cs (cesium). The stability of ion exchanged forms decreases in the series Cs>K>Rb>Na. Apart from Cs, other cations substitute up to 84% of Na ions in chabazite structure. K^{+1} ions are easily concentrated on chabazite from solutions containing high concentrations of Na^{+1} ions. The following selectivity series are known (Tsitsishvili et al. 1992).

Cs>K>Rb>Na>Li
Ti>Cs>K>Ag>Rb>NH_4
Na=Ba>Sr>Ca>Li
Cd>Cu>Zn>Co>Ni

In terms of ion exchange features, phillipsite behaves more selective towards K^{+1} and Na^{+1}. Na- form of phillipsite is selective for large cations. In addition, phillipsite is selective for ^{90}Sr and ^{137}Cs. At high concentrations, the metals can be concentrated on NH_{4-} phillipsite. The selections towards potasium ions in presence of Na^{+1}, and towards sodium ion in presence of Ca^{+2} are greater in lower temperatures. Phillipsite rich in silicon is more selective to cation K^{+1} in Na-K system and less so to in Na-Ca system. On different samples of phillipsite, in 0.1M solutions, selective series of K^{+1}>N^{+1}>Ca^{+2} are similar for all samples which do not depend on temperature (in range 35-70 °C), Tsitsishvili et al (1992). The following

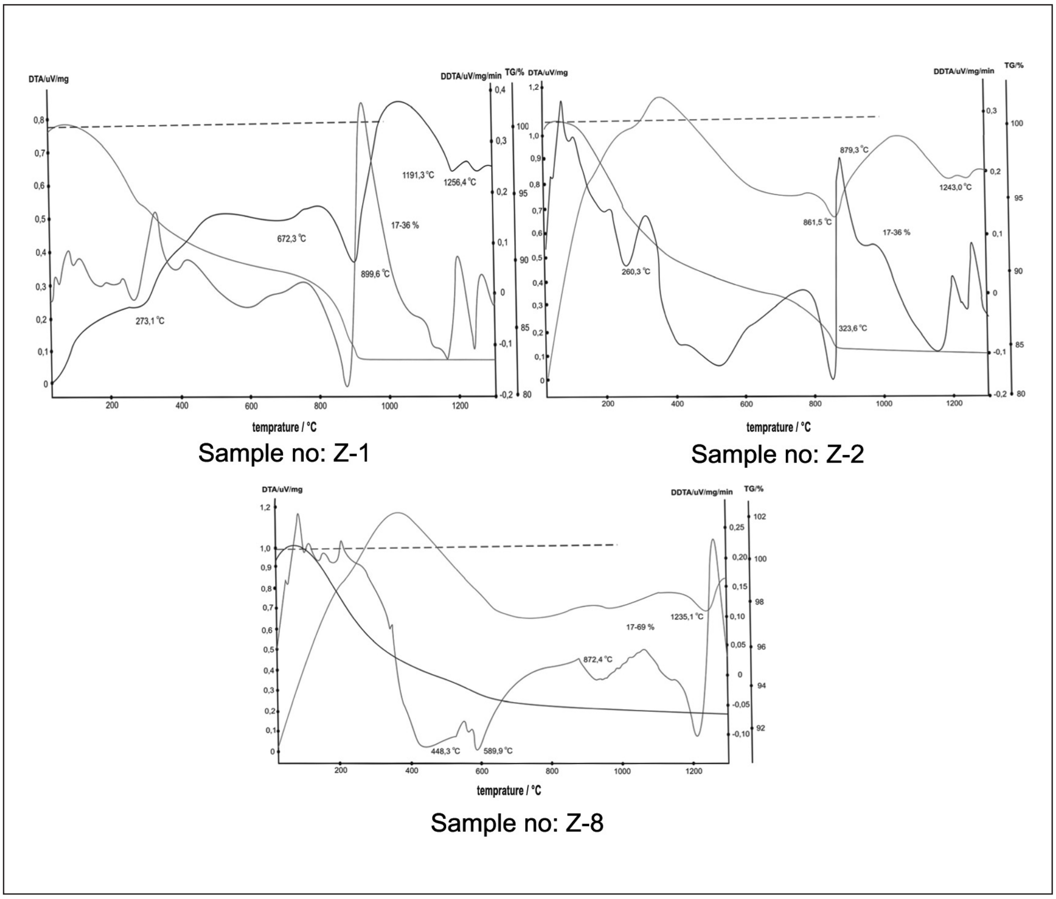

Figure 11- Thermograms of phillipsite chabazite (Sample num: Z-1) and chabazite (Sample num: Z-2, Z-8).

selectivity series are known (Tsitsishvili et al. 1992).

Cs>K>Rb>Na>Li
Ba>Rb>Cs>K>Na>Li
Ca>Na>Sr=Ca

INVESTIGATION OF CATION EXCHANGE FEATURES OF CHABAZITIC AND PHILLIPSITIC TUFFS IN THE STUDY AREA

The 0.1N HCl and 0.1N H_2SO_4 solutions of 2.5 liters were prepared from each of the samples of cream coloured tuffs at Selçik and surrounding area and dark gray, brownish coloured tuffs at Ballık-Soğucak-Ömerkuyu and Sütlüce Küfeke tepe. After this, 50 gram samples were taken from both chabazitic and phillipsitic tuffs and settled in 0.1N HCl and 0.1N H_2SO_4 solutions and shaked for two hours. Aftyer filtering the samples were washed by deionized water and dried up in an oven at 105 °C temperature.

For determining cation exchange capasity, 10 gr activated zeolitic tuff samples were taken and put in plastic bottles with NaCl, KCl, $CaCl_2$, $MgCl_2$ and $FeCl_3$ solutions (500 ppm), and after this they were shaked 10 hours by hands. As using paper filter, solutions were filtered with interval two hours and analyses caried out by using flame photometry. From activated chabazitic tuffs with 0.1N H_2SO_4, depending on time, Ca^{+2} content has been passed increasingly to the NaCl and KCl solutions and descreasingly to the $MgCl_2$, $FeCl_3$ solutions and also from activated chabazitic tuffs with 0.1N HCl, depending on time, Ca^{+2} has been passed decreasingly to the KCl, NaCl, $MgCl_2$ and $FeCl_3$ solutions (Table 2 and Figure 12)

From phillipsitic tuffs activated (with 0.1N H_2SO_4, and 0.1N HCl) Ca^{+2}, as depending on time Na^{+1} ve K^{+1} contents passing to the $MgCl_2$ and $FeCl_3$ solutions were obtained as quantitatively (mg/l), respectively. (Table 5 and Figure 13)

From phillipsitic tuffs activated with 0.1N H_2SO_4 Ca^{+2}, K^{+1}, as depending on time, Ca^{+2}, K^{+1} content passing to the 500 ppm $FeCl_3$ solution have became too much than passing in 500 ppm $MgCl_2$ solution. In spite of this, Na^{+1} content passing to the $MgCl_2$ solution have become too much than passing to the $FeCl_3$ solution (Table 4 and Figure 13).

On the other hand, Ca^{+2}, K^{+1} and Na^{+} cations, from activated phillipsitic tuffs with 0.1N HCl, Ca^{+2}, K^{+1} and Na^{+1} contents passing to the $MgCl_2$ solutions have become a decrease as depending

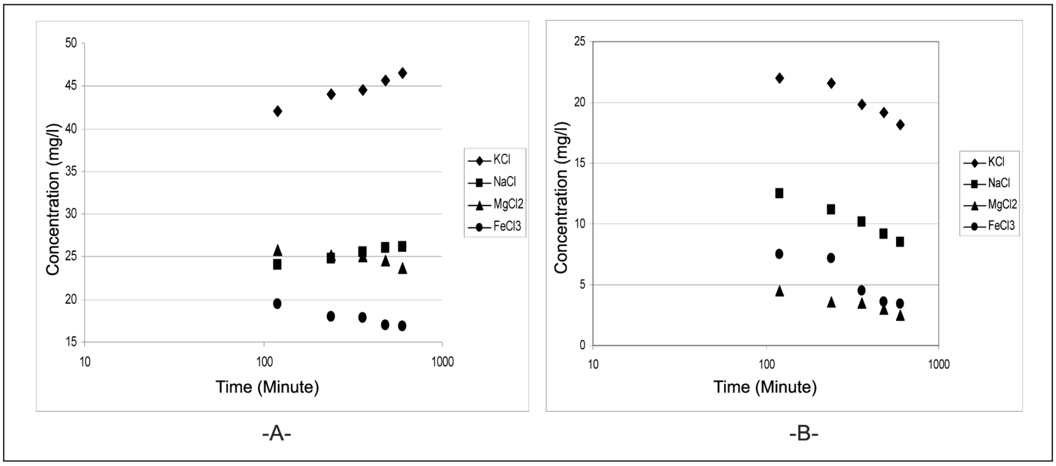

Figure 12- From activated chabazitic tuffs with 0.1 N H_2SO_4 (A) and with 0.1 N HCl (B) as depend ing on time, Ca^{+2} content passing to the solutions.

Table 2- From activated chabazitic tuffs with 0.1N H_2SO_4, as depending on time, Ca^{+2} content passing to the solutions

Time Minute	The cation from chabazitc tuffs passing to the solutions	Solutions (500 ppm)			
		In KCl solution	In NaCl Solution	In $MgCl_2$ solution	In $FeCl_3$ Solution
120	Ca^{+2} (mgr/l)	42.0	24.0	25.8	19.5
240	Ca^{+2} (mgr/l)	44.0	24.8	25.2	18.0
360	Ca^{+2} (mgr/l)	44.5	25.5	25.0	17.8
480	Ca^{+2} (mgr/l)	45.6	26.0	24.5	17.0
600	Ca^{+2} (mgr/l)	46.5	26.2	237.0	16.8

Table 3- From activated chabazitic tuffs with 0.1N HCl , as depending on time, Ca $^{+2}$ content passing to the solutions

Time Minute	The cations, from chabazitic tuffs passing to the solutions	Prepared Solutions (500 ppm)			
		In KCl solution	In NaCl solution	In $MgCl_2$ solution	In $FeCl_3$ Solution
120	Ca^{+2} (mgr/l)	22.0	12.5	4.5	7.5
240	Ca^{+2} (mgr/l)	216.0	11.2	3.6	7.2
360	Ca^{+2} (mgr/l)	19.8	10.2	3.5	4.5
480	Ca^{+2} (mgr/l)	19.2	9.2	3.0	3.6
600	Ca^{+2} (mgr/l)	18.2	8.5	2.5	3.4

on time. In spite of having became a decreasing of Ca^{+2} ,K^{+1} contents from phillipsitic tuffs activeted with 0.1N HCl passing to the $FeCl_3$ solution, having became a increase of Na^{+1} content pasing to the $FeCl_3$ solution were determined (Table 5 and Figure 14).

DISCUSSIONS

In the light of the experimental results of ion exchange capacity of Sandıklı chabasitic and phillipsitic tuffs, the zeolitic tuffs of the region will be evaluated for healthing and soil improvement in this part. According to existing data, obtained results are debated below.

The agricultural areas of the region are settled on the pyroclastic rocks and/or lacustrine sediments with volcanic ash intercalations. In the investigated area, the volcanic rocks have high concentrations of Cs (11. 10 - 88.30 ppm) and Sr (1208.20 - 3246.70 ppm) (Özpinar, 2001). In addition, in the region, cold water contains of Sr about 2.65 mgr and hot water contain of Sr between (4.15-4.75 mgr) (Afşin, 1991). Besides, while the ^{90}Sr is between 1.22 pCi/l and 2.5 pCi/l in the hot water of the region, it is 0.44 pCi/l in the cold water. After this, Cs and Sr passing from phosphatic organic dungs to the soil and to the vegetables are about 80 mgr/kg and between 25-500 mgr/kg respectivelly and Sr passing from organic dungs to the soil and vegatables are about 20 mgr/kg (Mikayilov and Acar, 1998). As a result in soils and vegetables the contents of Cs and Sr increase. After Chernobyl nuclear accident, no any region except east Black Sea, have been investigated in terms of ^{137}Cs consantration in soils. According to Gür and Yaprak (2003) Gediz Region (western Anatolia) has been contaminated by radioactive elements (^{137}Cs and ^{90}Sr) distributed from the Chernobyl nuclear accident. Like Gediz region, all western Anatolia have been affected by ^{137}Cs and ^{90}Sr isotops distributed with air circulations, and ^{137}Cs and ^{90}Sr concentration have been increased too much in the environment. In this situation, chabazite and phillipsite may be used to prevent passing of radioactive elements from nature to the environment and biological systems.

Radioactive elements cause important differences on the biological systems. According to the study of Epik and Yaprak (2003) on the leafed forests of the İzmir -Kozaklı region, the ^{40}K contamination is in excess concentrations. In the investigated area, volcanics are potasic and ultrapotasic in character (Özpınar, 2001). In studied area, it is estimated that ^{40}K contamination may be too much. As known, the human's body of weight about 70 kg contains about 140 gr K and only the part of 0.03 gr of this content is ^{40}K. As a result, it is understood that these minerals may be used for improvement of soil.

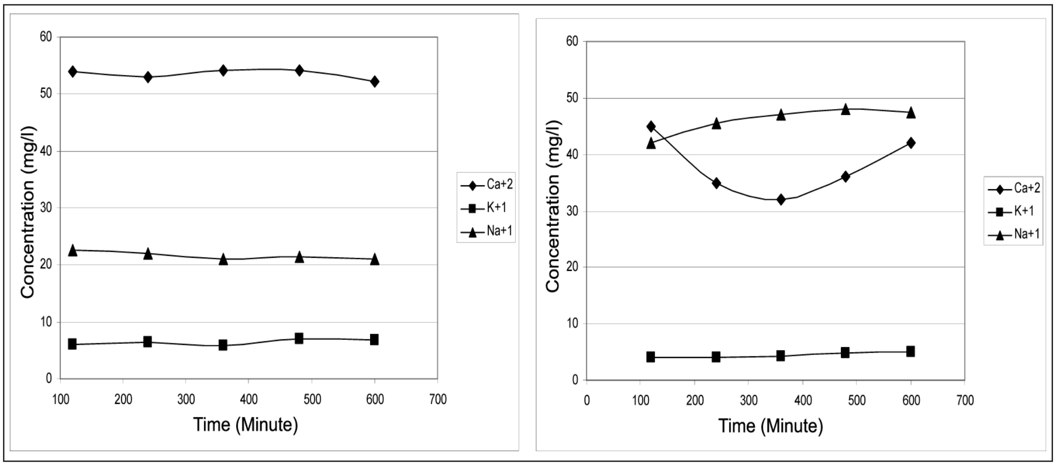

Figure 13- From activated phillipsitic tuffs with 0.1N H_2SO_4, as depending on time, Ca^{+2}, K^{+1} and Na^{+1} content passing to the $FeCl_3$ and $MgCl_2$ solutions.

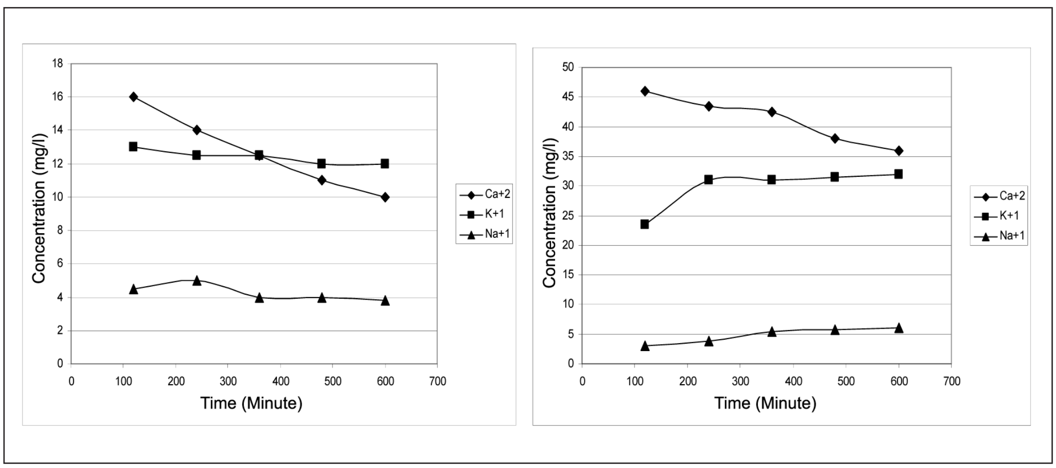

Figure 14- From activated phillipsitic tuffs with 0.1N HCl, as depending on time, (Ca^{+2}, K^{+1} and Na^{+1} contents passing to the $FeCl_3$ and $MgCl_2$ solutions.

In Gördes zeolitic rocks, ammonium-exchange capacity were studied by Esenli (2006). According to author, the zeolite contents increased from 0 (non-zeolitic) to about 30-40 wt, % in the rock samples. It is not seen a significant increase on the ammonium-exchange capacity for the group of samples containing 40-80 wt, % of zeolite. But the ammonium-exchange capacity is higher for the samples containing more than 70-80 wt, % of zeolite. Using of nitrogenous manure cause to inrease amount of nitrate (NO_3) and ammonium (NH_4) in soil and groundwater. Related to this, the amount of ammonium is too high in the agricultural areas of this region. Because of ammonium exists in the selective series of chabazite, ammonium ions are easily concentrated on chabazite from solutions. As a result by using of the zeolites in agricultural areas, the excess ammonium is removed from soil and prevent ammonium poisoning.

It is important that activated natural zeolites become excessively tendency to the resorption and adsorption of moisture. Because of this fea-

Table 4- From activated phillipsitic tuffs with 0.1N H_2SO_4, as depending on time, Ca^{+2}, K^{+1} and Na^{+1} contents passing to the $FeCl_3$ and $MgCl_2$ solutions

	$MgCl_2$ solution(500 ppm)			$FeCl_3$ solution (500 ppm)		
Time Minute	Ca^{+2} content, from phillipsite passing to the solution (mgr/l)	K^{+1} content from phillipsite passing to the solution (mgr/l)	Na^{+1} content from phillipsite passing to the solution (mgr/l)	Ca^{+2} content from phillipsite passing to the solution (mgr/l)	K^{+1} content from phillipsite passing to the solution (mgr/l)	Na^{+1} content from phillipsite passing to the solution (mgr/l)
120	54,0	6,0	22,5	45,0	4,0	42,0
240	53,0	6,5	22,0	35,0	4,0	45,5
360	54.2	5,9	21,0	32,0	4,3	47,0
480	54.1	7,0	21,5	36,0	4,8	48,0
600	52.3	6,8	21,0	42,0	5,0	47,5

Table 5- 0.1N HCl ile aktifleştirilmiş doğal zeolitten zamana bağlı olarak $FeCl_3$ ve $MgCl_2$ çözeltilerine geçen Ca^{+2}, K^{+1} ve Na^{+1} iyonlarının miktarı

	Solution; $MgCl_2$(500 ppm)			Solution; $FeCl_3$(500 ppm)		
Time Minute	Ca^{+2} content , from phillipsite passing to the solution (mgr/l)	K^{+1} content from phillipsite passing to the solution (mgr/l)	Na^{+1} content from phillipsite passing to the solution (mgr/l)	Ca^{+2} content from phillipsite passing to the solution (mgr/l)	K^{+1} content from phillipsite passing to the solution (mgr/l)	Na^{+1} content from phillipsite passing to the solution (mgr/l
120	16,0	13,0	4,5	46,0	23,5	3,0
240	14,0	12,5	5,0	43,5	31,0	3,8
360	12,5	12,5	4,0	42,5	31,0	5,5
480	11,0	12,0	4,0	38,0	31,5	5,7
600	10,0	12,0	3,8	36,0	32,0	6,0

ture, activated natural zeolites may be used as decicant as well. This quality of zeolites makes contribution to the plants development by preserving of the moisture of the soil. In this context, the tuffs of the study area have value of absobtion wt % between 13.40% -24.45 % and vol.% between 24.8% -33.17 % (Özpınar, 1998; Özpınar et al., 2002). As resut, for plant development, it is thought that zeolitic tuff of this region will do important contribution.

As it is known that phillipsite contains sodium and potasium ions. Using for soil improvement may cause increasing of the amount of alkali in soil, so in the acidic soils it plays a role of stabilization of pH, and because of this feature they may be used in soil improvements.

In the last years, using of zeolite instead of clay for garbage dumps has increased. It is shown that they may be used to prevent leaking of harmful ions into the groundwater from the surface. Beside, if they use, they reduce the dirty smells and decrease to cost of making dump.

At Sandıklı and its surrounding area, there are many shelters of cattle and goats. Because of this situation, they disperse dirty smells to the environment. Zeolites can absorp the dirty smells deriving from urine, fecal matter and ammonium. So, zeolitic tuffs may be used for shelter of cattles and goats.

Chabazitic tuffs use in different localities of world for heating and air conditioner of small houses. Compressive strength of zeolitic tuffs are 108 kgf/cm² as average (Özpınar, 1998; Özpınar et al., 2002). It may be used for this purpose in the Sandıklı and surroundings settlements.

In study area, because of tuffits are consolidated, it may be used to store fruits and vegetables too. and finally it is satisfacted that for this situation can be encouraged by local authority.

CONCLUSIONS AND SUGGESTIONS

By this study, the results obtained are given below, Sandıklı volcanics are widespreadly exposed at the southern part of Sandıklı and they are represented by lavas of trachyandesitic, phonolitic tephritic, basaltic andesitic, basaltic trachy-nephelinitic, andesitic and dacitic in compositions and thick pyroclastics rocks. Pyroclastic rocks from bottom to top are represented by lapillistone, tuffaceous conglomerate, tuffaceous sandstone, tuffaceous siltstone and tuffaceous mudstone.

The tuffs and altered lavas contain chabazite and phillipsite minerals firstly determined by Özpınar (1998). However, in this paper, investigations on the zeolite occurences in tuffs have been focused much more. At Selcik village and its surrounding area which is located in the northern part of the investigated area the chabazite occurences are found widespreadly in cream coloured tuffs and in the southern part the phillipsite occurences are found widespreadly in gray, dark gray and brownish coloured tuffs. The tuffs outcropped at Ballık village and its surrounding area, contain chabazite and phillipsite occurences. Three phillipsite forms were defined. These are potassium-sodium-aluminum-silicate hydrate, potasium-aluminium-silicate hidrate, potasium-calsium-alüminum silicate hidrate.

In tuff specimens purifed with heavy liquid, in cream colored tuffs, the amount of chabazite as wt. % are between 29.00 % -58.93 % and in gray, dark gray and brownish colored tuff, the amount of phillipsite as weight % are between 51.53 % - 63.00 %. However, tuffs located at eastern of Soğucak village are found extensively zeolitization which the amount of phillipsite are about 80- 85 %.

From chabazitic tuffs (Selçik tuffs) activated with 0.1 N H_2SO_4, as depending on time, Ca^{+2} content (mgr/l) has been passed increasingly to the NaCl and KCl solutions and decreasingly to the $MgCl_2$, $FeCl_3$ solutions and also from activated chabazitic tuffs with 0.1 N HCl, depending on time, Ca^{+2} (mgr/l) content has been passed decreasingly to the KCl, NaCl, $FeCl_3$ and $MgCl_2$ solutions (Table 5 and figure 12).

From phillipsitic tuffs activated with 0.1N H_2SO_4 Ca^{+2}, K^{+1}, as depending on time, Ca^{+2}, K^{+1} contents passing to the $FeCl_3$ solution (500 ppm) have become too much than passing to the $MgCl_2$ solution (500 ppm). In spite of this, Na^{+1} content passing to the $MgCl_2$ solution have become too much than passing to the $FeCl_3$ solution. On the other hand, Ca^{+2}, K^{+1} and Na^{+1} contents, from activated phillipsitic tuffs with 0.1N HCl, Ca^{+2}, K^{+1} and Na^{+} contents passing to the $MgCl_2$ solutions have become a decrease as depending on time. In spite of having became a decreasing of Ca^{+2}, K^{+1} content from phillipstic tuffs activeted with 0.1N HCl passing to the $FeCl_3$ solution, having became a increase of Na^{+1} content pasing to the $FeCl_3$ solution were determined.

When we keep in view of ion exchange capacity and selection of the radioactive cations such as ^{137}Cs, ^{90}Sr and ^{40}K of chabazite and phillipsite tuffs may be used for improvement of soil, stabilization of pH of acidic soil and for prevent to pass by radioactive element from nature to environment and biological systems. Because of activated natural zeolites become excessively tendency to the resorption and adsorption of moisture and for the plants development will do contribution, activated naturel zeolitic tuffs may be used as decicant. Because of adsorption of ammonium smells arised from urine and fecal matter, it is thought that zeolitic tuffs may be used to separation of the methane gas, from the other gases. Besides, it is believed that they are possible to use as building stone for heating and air conditioner of small houses and shelter of cattles and goats.

In order to prevent the leaking harmful ions into the groundwater from surface and to reduce dirty smells, it could be possible to make low cost garbage dumps by using the zeolitic tuffs of the region .

ACKNOWLEDGEMENTS

I would like to express my great acknowledgements to the authorities of TUBITAK (The Scientific and Tecnical Research Council of Turkey) for their contributions to this study.

Manuscript received December 17, 2007

REFERENCES

Afşin, M.,1991. Afyon-Sandıklı Kuruçay Ovası ve Hüdai Kaplıcasının Hidrojeolojik İncelemesi (Hydrogeological investigation of the Afyon-Sandıklı Kuruçay plain and Hüdai hot-spring). Ankara Üniversitesi, Fen Bilimleri Enstitüsü, Doktora Tezi, Ankara. 329p (unpublished).

Aydar, E., Bayhan, H., and Zimitoğlu, O., 1996. Investigation of volcanological and petrological evolution of Afyon stratovolcano, Hacettepe University, Bulletin of Earth Sciene Applied and Research Center 18, 87-107.

_____, _____, and Gougaud, A., 2003. Lamprophyres of Afyon Stratovolcano, Western Anatolia, Turkey, desription and genesis. Comptes Rendusde I'Academie des Sciences 335, 279-288.

Başarır, E., and Kun, N., 1982. Afyon Kalesi çevresindeki volkanitlerin petrografik incelemesi (Petrographic investigation of the volcanics around the Afyon castle). KTÜ Yerbilimleri Derg., Trabzon, 26, 27-36.

Besang, C., Eckahtrdt, F.J., Harre, W., Kreuzer, H., and Müller, P., 1977, Radiometricshe Altersbesttimmungen der Türkei, Geol. Jb. B., 25, 3-5.

Bulutçu, C., 1975. Afyon-Sandıklı, Hüdai kaplıcası hidrojeolojik etüdü (Hydrogeological investigation of the Hudai hot-spring of Afyon-Sandıklı). Ankara, MTA Report No: 3321, (unpublished).

Çoban, H., and Flower M.F.J, 2007. Late Pliocene Lambroites from Bucak, Isparta (Soutwesthern Turkey): Implications for mantle"Wedge" evolu tion during Africa-Anatolian plate convergence, Journal of Asian Earth Sciences, 29, 160-176.

Epik, Ö., and Yaprak., G., 2003. Kozaklı Çam Ormanlarında ^{7}Be, ^{40}K ve ^{137}Cs Aktivite Dağılımları (The distribution of the ^{7}Be, ^{40}K ve ^{137}Cs activities in the pine forests of Kozaklı), VIII. Ulusal Nükleer Bilimleri ve Teknoloji Kongresi, Bildiri Metni, 15-17 Ekim, Kayseri.

Ercan, T., 1986. Orta Anadolu'daki Senozoyik Volkanizması (Cenozoic volcanism of the Central Anatolia). MTA Bulletin. 107,119-141.

Esenli, F., 2006. Piroklastik kayalarda zeolit içeriği ile amonyum değişim kapasitesi arasındaki ilişki: Türkiye'den örnekler (The relation between the zeolite contents of pyroclastic rocks and ammonium-exchange capacity: examples from Turkey), Kibited, Kil Bilimleri ve Teknoloji Dergisi, 1(2), 9-19.

Fisher, R.V., and Schminke, H.U.,1984. Pyroclastic Rocks, Springer Verlag, 472 p, Berlin.

Folk, R., 1962. Classification of carbonate rocks; Assoc. Petroleum Geologist, Mem.,1, 62-82.

Gür, F., and Yaprak, G., 2003. Gediz havzasında radyosezyum dağılımı (The radiocaesium distribution of the Gediz basin), VIII. Ulusal Nükleer Bilimleri ve Teknoloji Kongresi, Bildiri Metni, Kayseri, 15-17 Ekim, 2003.

Keller, J., 1983. Potasic lavas in Orogenic Volcanisim of Mediterranean Area, J. Volcanol. Geothermal Res. 18(36), 321-335.

Mikayilov, D.F., and Acar, B., 1998. Toprak ekosistemlerinde kirleticilerin tanım mekanizmasının incelenmesi ve modellenmesi (The investigation and modeling of the pollutants in the soil ecosystems), Ekoloji, 7(28), 20-23.

Minato, H., 1992. Methods for measurement of zeolite amount. Naturel Zeolite and its utilization, International Symposium, Japan, 401 p.

Öngür, T., 1973. Sandıklı (Afyon) jeotermal araştırma bölgesine ilişkin jeolojik durum ve jeotermal enerji olanakları (The geology and the geothermal energy possibilities of the Sandıklı geothermal region), MTA Report No:5520, Ankara (unpublised).

Özpınar, Y., 1998. Sandıklı (Afyon) volkanitlerinin jeolojik, petrografik ve petrokimyasal incelemesi ve tras olarak değerlendirilmesi (The investigation of the petrographic, petrochemical properties of the Sandıklı volcanic and their evaluation as trass material), (AR-GE Proje No:97 MHF.006.Jeo.002-3, Denizli 38 p.

_____, 2001. Petrographical and petrochemical investigation of Sandıklı volcanic and usabilty of this rocks as trass, in Afyon region (Western Anatolia), Turkey, 9Th International Congress of The Geologıcal Society of Greece, Atina, Volume, 3, 959-967.

Özpınar, Y., Bozkurt, R., Çobanoğlu, İ., and Küçük, B., 1998. Sandıklı Zeolitik Tüflerinin petrografik, petrokimyasal incelemesi ve bunların teknolojik açıdan değerlendirilmesi (The investigation of the petrographic, petrochemical properties of the Sandıklı zeolitic tuffs and their technological evaluation), I. Batı Anadolu Hammadde Kaynakları Sempozyumu BAKSEM'99 Bildiriler Kitabı, İzmir, 277-289.

_____, Çobanoğlu, İ., and Bozkurt R., 2002. Sandıklı Zeolitik tüflerin petrografik ve petrokimyasal ve teknolojik özelliklerinin incelenmesi (The investigation of the petrographic, petrochemical and technologic properties of Sandıklı zeolitic tuffs), TÜBİTAK -YDABÇAĞ-198Y102, Ankara, 268p.

Ronner, F., 1962. Sandıklı ovası çöküntüsü, genç tektonik ve volkanik durumlar (The Sandıklı depression and, tectonics and volcanism), 59, 69-88.

Schmidt, R., 1981. Descriptive nomenclature and classification of pyroclastic deposits and fragments: Recommendations of the IUGS Subcomission on the Systematics of Igneous Rocks. Geology 9, 41-44.

Tsitsishvili, G.V., Andronikashvili, T.G., Kırov G.N., Filizova, L.G., Potashnikov I.B., and Williams P.A., 1992. Natural Zeolite, Ellis Horwood, Singapore, 293p.

Tolluoğlu, Ü. A., Erkan, Y., Sümer., Ö.E., Boyacı, N.M., and Yavaş (Bektaş), F., 1997. Afyon metasedimenter grubunun Mesozoyik öncesi metamorfik evrimi (The pre-Mesozoic metamorphic evolution of the Afyon Metasedimentary Group), Türkiye Jeoloji Bülteni, 40(2), 1-17.

Villari, L. and Keller, J., 1972. Rhyolitic ignimbrites in region of Afyon (Central Anatolia): Bull. Volcan., 36(4), 342-358.

THE TAXONOMIC DISTRIBUTION OF BENTHIC FORAMINIFERA AROUND OF ALİBEY AND MADEN ISLANDS (AYVALIK-BALIKESİR)

Engin MERİÇ*, Niyazi AVŞAR**, Baki YOKEŞ*** and Feyza DİNÇER**

Four cores were collected from different localities and depths around the Alibey and Maden Islands (north-western Ayvalık). 91 young sediment samples obtained from these cores were analysed for their foraminiferal content. 42 genera and 77 species of foraminifers, belonging to 22 families and 19 subfamilies were identified. Agglutinated species were found to be rare, however species with calcareous test were represented with 18 families and 74 species. Observation of large benthic foraminifer species in abundance suggests the presence of submarine springs with high $CaCO_3$ content, which might be the results of broken faultlines. Accordingly, plenty of large sized (>0.5mm) Peneroplis, Lobatula, Ammonia, Challengerella and Elphidium individuals were observed. Besides, gypsum crystals observed in one of the core samples were suggested to be caused by the high temperature characteristics of these submarine springs. The aim of this study is to figure out the recent and near past foraminiferal assemblages, the distribution patterns of the species related to ecological conditions and compare the study area with nearby localities.

Key words: Alibey and Maden islands, Ayvalık/Balıkesir, Benthic foraminifera, Taxonomy.

Mineral Res. Expl. Bull., 137,49-59, 2008

BIOSTRATIGRAPHY OF THANETIAN-ILERDIAN BENTHIC FORAMINIFERA IN THE AKÇATAŞ - CEBECİ (NW TOSYA - SE KASTAMONU) REGION

Nazire ÖZGEN - ERDEM*

ABSTRACT.- In this study, the benthic foraminiferal biostratigraphy and paleoecological features of Thanetian-Ilerdian unit were investigated in the northwest of Tosya (SE Kastamonu). The range of the unit, which had been determined as Paleocene-Eocene by former studies, was established as Thanetian-Ilerdian after conducting detailed paleontological research works on this unit. The unit begins with conglomerates from the base and continues with sandstones, sandy limestones and limestones upwards. *Haymanella paleocenica* Sirel, *Idalina sinjarica* Grimsdale, *Mississippina binkhorsti* (Reuss) and *Pseudocuvillierina*? sp. were described in the Thanetian levels of the unit. The Ilerdian levels are characterized by the following benthic foraminifera assemblages: *Glomalveolina lepidula* Schwager, *G. subtilis* Hottinger, *G. pilula* Hottinger, *G. karsica* Sirel, *Alveolina ellipsoidalis* Schwager, *A. moussoulensis* Hottinger, *A. corbarica* Hottinger, *A. laxa* Hottinger, *A. ilerdensis* Hottinger, *A. minervensis* Hottinger, *A. subpyrenaica* Leymerie, *A. decipiensis* Schwager, *A.* aff. *pisella* Drobne, *A. erki* Acar, *A. trempina* Hottinger, *A. aragonensis* Hottinger, *Orbitolites complanatus* Lamarck, *O. megasphericus* Zhang, *Opertorbitolites lehmanni* Montanari. The fossil content and sedimentological features indicate deposition in a shallow restricted platform (10-30 m depth) with low energy at the beginning and subsequently in a deeper carbonate shelf environment (40-80 m) conditions.

Key words: Benthic Foraminifera, Ilerdian, Thanetian, Tosya

INTRODUCTION

This study was carried out in the vicinity of Akçataş and Cebeci villages, which are located to the northwest of Tosya town (SE Kastamonu). The study area is located in the western part of Kastamonu F32-d1 quadrangle of 1:25000 scale (Figure 1).

Geological studies carried out in the Tosya region have mainly focused on economical geology and tectonics. There are also a number of geological studies and geological research reports of the General Directorate of the Mineral Research and Exploration (MTA) carried out in the region. Early studies in the region belong to Coulant (1894) and Pilz (1937), which were concentrated on nickel deposits. Blumenthal (1939, 1948 and 1950) carried out geological research in the area and prepared a 1/100 000 scale geological map. Ayaroğlu (1980), concentrated on the economical possibilities of the region in his

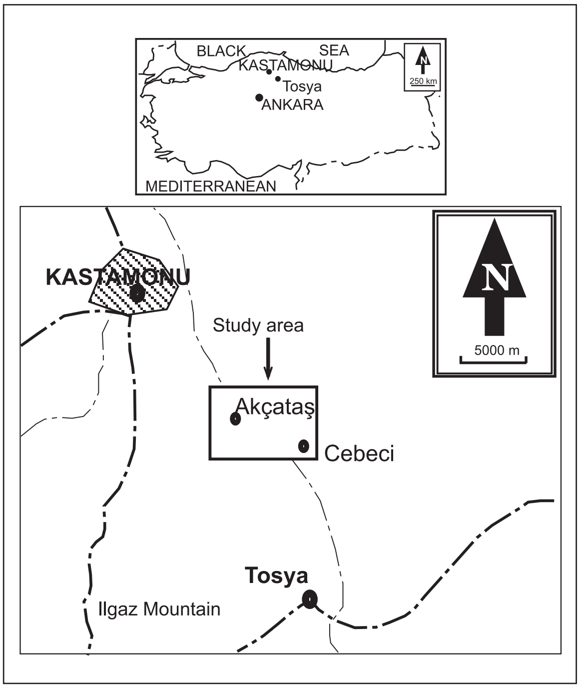

Figure 1- Location map of the investigated area.

* Cumhuriyet Üniversitesi, Mühendislik Fakültesi, Jeoloji Mühendisliği Bölümü, 58140, Sivas
E-posta: nozgen@cumhuriyet.edu.tr

study. Later, Yılmaz and Tüysüz (1984) investigated the regional geology of the area. While some detailed paleontological researches have been carried out in the north and northeast parts of Kastamonu (Tunoğlu, 1992*a*, 1992*b*, 1993 and 1994), no detailed paleontological studies were done on the Tertiary units with fossils in the southeast of Kastamonu, yet. These units were aged as Paleocene-Eocene based on a number of genus determined in the previous studies (Ayaroğlu, 1980; Yılmaz and Tüysüz, 1984). First comprehensive paleontological research in the Akçataş-Cebeci region is reported by Özgen (1998) and Özgen-Erdem et al., (2005), which focused on merely Lower-Middle Ilerdian levels of the unit.

This study aimed at putting forward the benthic foraminiferal biostratigraphy, determining the stratigraphic range and interpreting paleoecological features of this unit. The stratigraphic distributions of the benthic foraminifera, which are described in this study, have also been correlated with Tethyan Belt shallow benthic Foraminifera biozones (Serra-Kiel et al., 1998). Towards realizing these objectives, three stratigraphic sections, which are named as Akçataş, Karapınar and Kirenler, have been measured and some 86 systematic samples were collected from the unit (Figure 2,4 -6). Systematic descriptions are based on oriented and random thin sections. All thin sections containing the benthic foraminifera described and shown in this paper are stored in

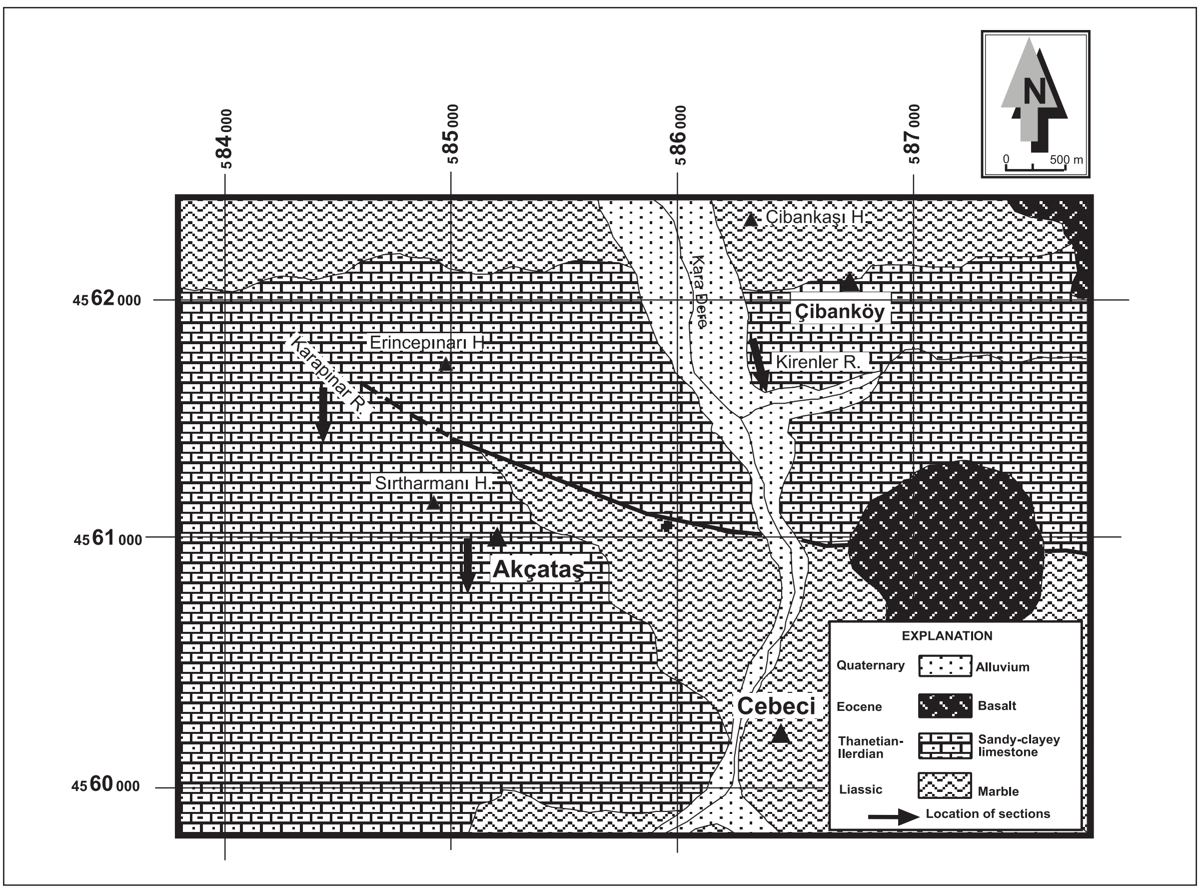

Figure 2- Geological map of Akçataş-Cebeci region (Yılmaz and Tüysüz, 1984).

the palepntological collection of Cumhuriyet University, Department of Geological Engineering, Sivas (Turkey).

STRATIGRAPHY

The Liassic aged Bekirli Metamorphics constitute the basement of the study area (Tüysüz, 1986) and consist of schist, marble, diabase and metadiabase. The limestones, which are dated as Upper Cretaceous in previous studies, were observed as a small outcrop in the vicinity of Cebeci village. *Hellenocyclina beotica* Reichel, *Siderolites* sp. and *Orbitoides* sp. are described in the samples obtained from the unit, which was then assigned to the Late Maastrichtian age (Figure 3). The unit, whose age is determined as Thanetian-Ilerdian in this study, starts with a thin conglomerate level in the base, which overlies Bekirli Metamorphics unconformably. The conglomerates are followed by sandstones, sandy limestones and limestones toward the upper levels. The sandstones are yellowish-brown coloured, well-compacted and carbonated. The sandy limestones are yellowish sometimes gray

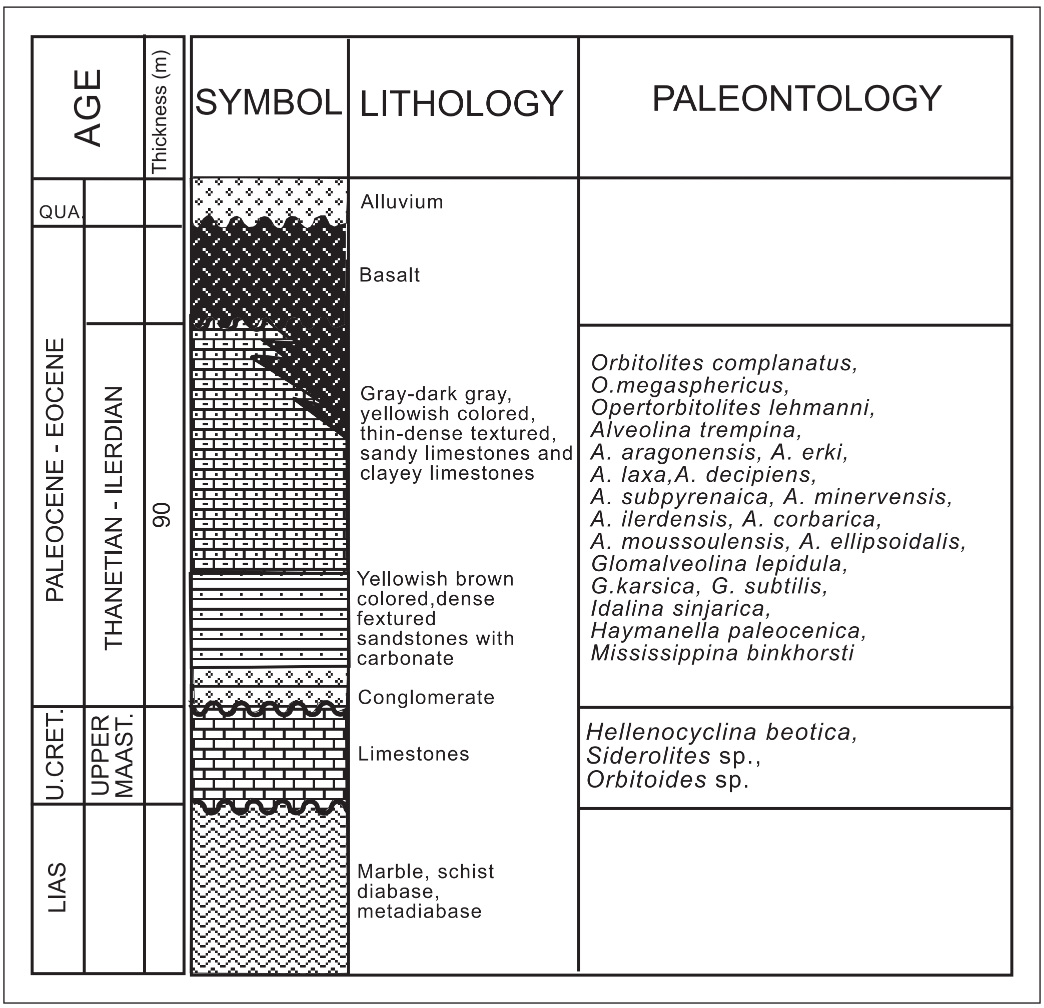

Figure 3- Generalized columnar section of the investigated area (nonscale).

coloured, well-compacted and fossiliferous. The limestones, which outcropped most, are gray-white sometimes yellowish coloured, thin-dense textured, fossilliferous and contain small amount of clays. Sedimentary petrography analyses show that the unit is presented with boundstones and wakestones, which contain benthic foraminiferal fragments within a micritic cement.

Haymanella paleocenica Sirel, *Idalina sinjarica* Grimsdale, *Mississippina binkhorsti* (Reuss), *Pseudocuvillierina*? sp., *Rotalia* sp., *Miscellanea* sp. and *Discocyclina* sp. are found in the lower levels of the unit. These levels are aged Thanetian. *Idalina sinjarica* Grimsdale, *G. lepidula* Schwager, *G. subtilis* Hottinger, *G. karsica* Sirel, *A. ellipsoidalis* Schwager, *Orbitolites complanatus* Lamarck, *O. megasphericus* Zhang, *Opertorbitolites lehmanni* Montanari, *Glomalveolina* sp., *Triloculina* sp., *Alveolina* sp., *Orbitolites* sp., *Opertorbitolites* sp., *Cribrobulumina* sp., *Lockhartia* sp., *Asterigerina* sp., *Miscellanea* sp., *Nummulites* sp., *Operculina* sp., *Discocyclina* sp. and *Haddonia* sp. have been determined in the Lower Ilerdian levels. *G. lepidula* Schwager, *G. pilula* Hottinger, *A. ellipsoidalis* Schwager, *A. moussoulensis* Hottinger, *A. corbarica* Hottinger, *A. laxa* Hottinger, *A. ilerdensis* Hottinger, *A. minervensis* Hottinger, *A. subpyrenaica* Leymerie, *A. decipiens* Schwager, *A.* aff. *pisella* Drobne, *A. erki* Acar, *O. complanatus* Lamarck, *O. megasphericus* Zhang, *Opertorbitolites lehmanni* Montanari, *Glomalveolina* sp., *Alveolina* sp., *Orbitolites* sp., *Opertorbitolites* sp., *Cribrobulumina* sp., *Lockhartia* sp., *Asterigerina* sp., *Miscellanea* sp., *Rotalia* sp., *Gypsina* sp., *Nummulites* sp., *Assilina* sp., *Operculina* sp. and *Discocyclina* sp. have been defined in the Middle Ilerdian levels. *G. lepidula* Schwager, *A. trempina* Hottinger, *A. aragonensis* Hottinger, *O. complanatus* Lamarck, *Op. lehmanni* Montanari, *Alveolina* sp., *Orbitolites* sp., *Opertorbitolites* sp., *Cribrobulumina* sp., *Lockhartia* sp., *Miscellanea* sp., *Asterigerina* sp., *Rotalia* sp., *Gypsina* sp., *Nummulites* sp., *Assilina* sp., *Operculina* sp. and *Discocyclina* sp., have been described in the Upper Ilerdian levels (Plate I, II). However this formation has not been named in the previous studies, to avoid a confusion, the formation has not been named in this study either. But instead, the unit is stated as Thanetian-Ilerdian aged. Eocene basalts are observed in places in the investigated area (Yılmaz and Tüysüz, 1984). The youngest deposits are Quaternary alluviums.

MEASURED STRATIGRAPHIC SECTIONS

Akçataş measured stratigraphic section

The section was measured within Akçataş village, which is located 10 km northwest to the Tosya town (Figure 2). The section is situated in the Kastamonu F32d1 quadrangle (start point: 4 561 000 - 585 100; end point: 4 560 900 - 585 100). Some 27 samples were collected along the section, which advanced from north to south for a total of 90 m in thickness (28 m Lower Ilerdian and 62 m Middle Ilerdian) (Figure 4). The unit is represented by gray, varigated coloured, thin-dense textured limestones in this section. *Idalina sinjarica* Grimsdale, *Glomalveolina subtilis* Hottinger, *G. lepidula* Schwager, *G. karsica* Sirel, *Alveolina ellipsoidalis* Schwager, *Orbitolites complanatus* Lamarck, *Opertorbitolites lehmanni* Montanari, *Glomalveolina* sp., *Alveolina* sp., *Opertorbitolites* sp., *Cribrobulumina* sp., *Lockhartia* sp., *Asterigerina* sp., *Miscellanea* sp., *Nummulites* sp., *Operculina* sp., *Discocyclina* sp. and *Haddonia* sp. were described in the Early Ilerdian levels. The benthic foraminifera such as *G. lepidula* Schwager, *G. pilula* Hottinger, *Alveolina ellipsoidalis* Schwager, *A. moussoulensis* Hottinger, *A. laxa* Hottinger, *A. minervensis* Hottinger, *A. subpyrenaica* Leymerie, *A. decipiensis* Schwager, *A.* aff. *pisella* Drobne, *Orbitolites complanatus* Lamarck, *O. megasphericus* Zhang, *Opertorbitolites lehmanni* Montanari, *Glomalveolina* sp., *Alveolina* sp., *Opertorbitolites* sp., *Cribrobulumina* sp., *Lockhartia* sp., *Asterigerina* sp., *Miscellanea* sp., *Nummulites* sp. and *Discocyclina* sp. were determined in the Middle Ilerdian levels (Figure 4).

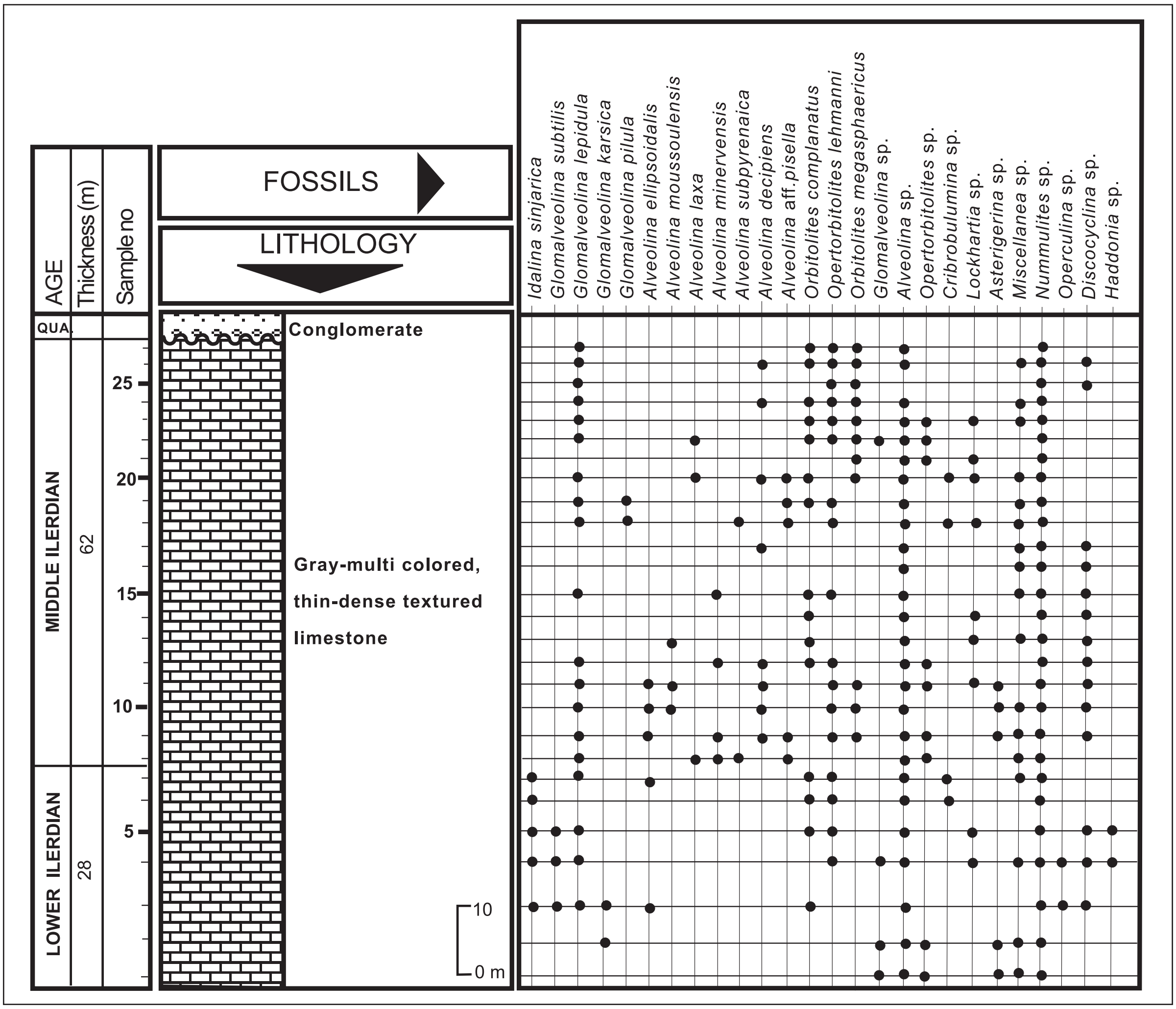

Figure 4- Akçataş section, Akçataş, NW Tosya, SE Kastamonu.

Karapınar measured stratigraphic section

This section was measured from the Karapınar ridge, which is 1 km northwest of the Akçataş village (Figure 2). The section is located in the Kastamonu F32d1 quadrangle (start point: 4 561 600 - 584 500; end point: 4 561 500 - 584 500) and has been measured from north to south. Middle-Upper Ilerdian levels of unit are ob-served in this section. A total of 65 m thickness (27 m Middle Ilerdian and 38 m Upper Ilerdian) was measured and some 24 samples collected (Figure 5). Middle Ilerdian levels are formed from sandy limestones in the base; gray, white coloured, dense textured limestones in the top and are characterized by *Glomalveolina lepidula* Schwager, *Alveolina moussoulensis* Hottinger, *A. ilerdensis* Hottinger, *A. minervensis* Hottinger, *A. subpyrenaica* Leymerie, *A. decipiensis* Schwager, *Orbitolites complanatus* Lamarck, *O. megasphericus* Zhang, *Opertorbitolites lehmanni* Montanari, *Glomalveolina* sp., *Alveolina* sp., *Orbitolites* sp., *Opertorbitolites* sp., *Cribrobulumina* sp., *Lockhartia* sp., *Miscellanea*

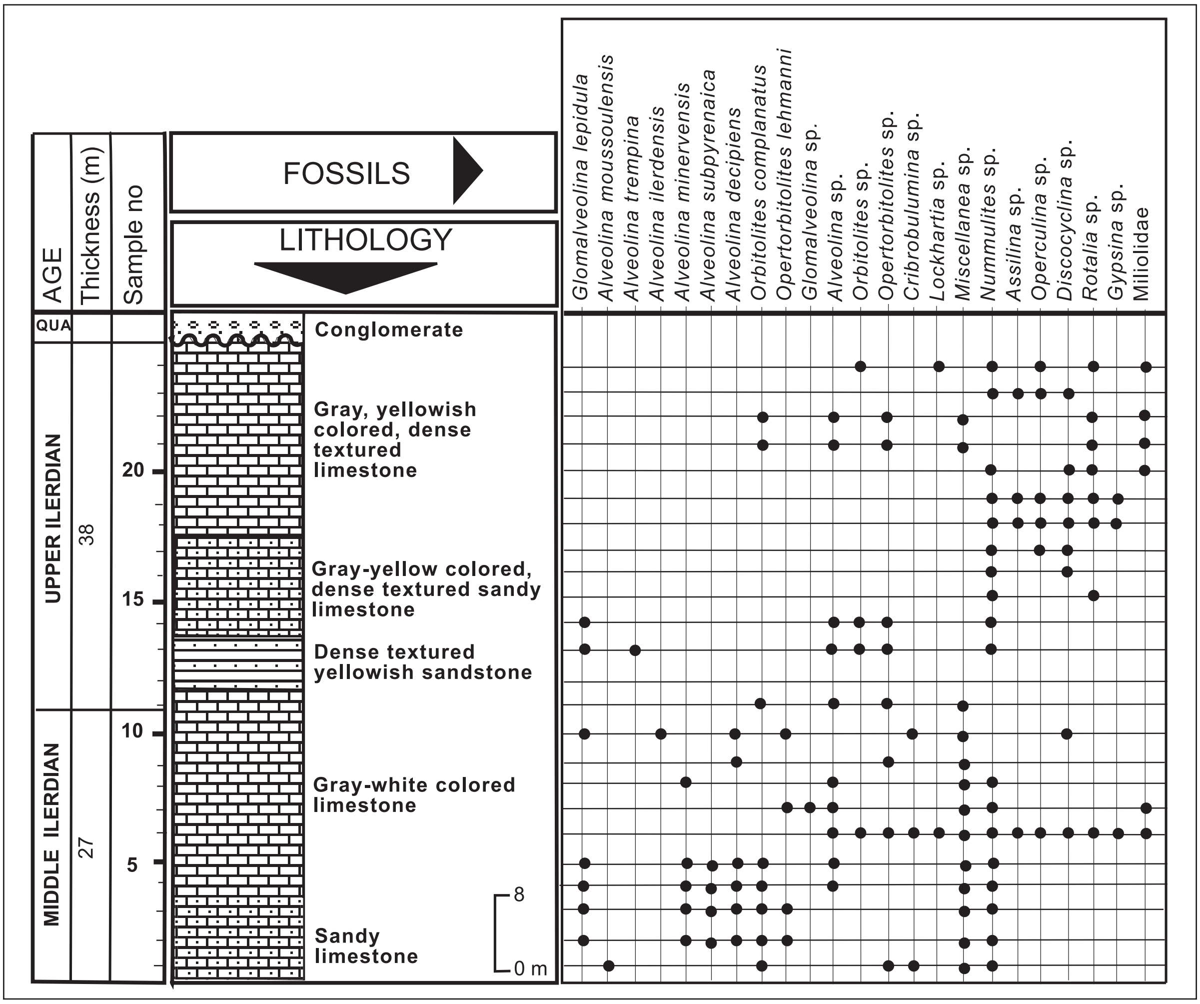

Figure 5- Karapınar section, NW Akçataş, NW Tosya, SE Kastamonu.

sp., *Nummulites* sp., *Assilina* sp., *Operculina* sp., *Discocyclina* sp., *Rotalia* sp. and *Gypsina* sp. Upper Ilerdian levels are represented by yellowish coloured, well-compacted sandstones, gray-yellowish coloured, dense textured sandy limestones and gray sometimes yellowish coloured, dense textured limestones from base to top. *G. lepidula* Schwager, *A. trempina* Hottinger, *Orbitolites complanatus* Lamarck, *Alveolina* sp., *Orbitolites* sp., *Opertorbitolites* sp., *Lockhartia* sp., *Miscellanea* sp., *Nummulites* sp., *Assilina* sp., *Operculina* sp., *Discocyclina* sp., *Rotalia* sp. and *Gypsina* sp. were observed in these levels (Figure 5).

Kirenler measured stratigraphic section

This section was measured from Kirenler ridge, which is 500 m southwest of Çibanköy (Figure 2). It is situated in the Kastamonu F32 d1 quadrangle (start point: 4 561 750 - 586 200; end point: 4 561 650 - 586 250). Previously Lower-Middle Ilerdian levels were studied by Özgen (1998). In this subsequent study, basal and top levels of this section are worked. A total thickness of 59 m (7 m Thanetian, 18 m Lower Ilerdian, 26 m Middle Ilerdian and 8 m Upper Ilerdian) was measured and 35 samples collected (Figure 6). The section starts with conglomerates in the base and continues with sandstones with carbonate, gray sometimes yellowish colored, thin-dense textured clayey limestones toward top levels. *Haymanella paleocenica* Sirel, *Idalina sinjarica* Grimsdale, *Mississippina binkhorsti* Reuss, *Pseudocuvillierina*? sp., *Rotalia* sp., *Miscellanea* sp. and *Discocyclina* sp. were described in the levels containing sandstones with carbonate. These levels are given Thanetian age. The Lower Ilerdian levels are characterized by *Idalina sinjarica* Grimsdale, *G. lepidula* Schwager, *G. karsica* Sirel, *A. ellipsoidalis* Schwager, *Orbitolites complanatus* Lamarck, *O. megasphericus* Zhang, *Opertorbitolites lehmanni* Montanari,

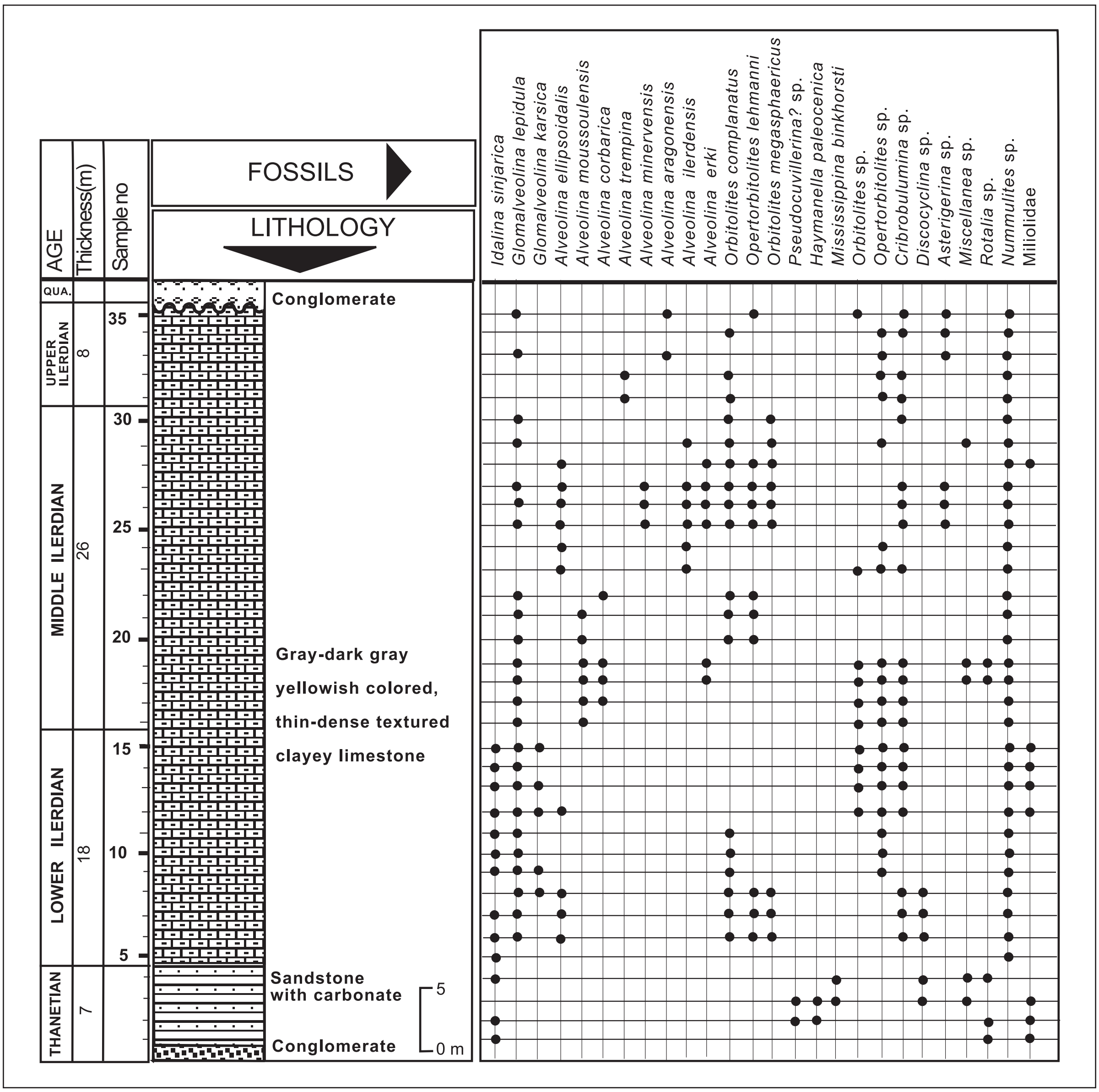

Figure 6- Kirenler section, SW Çibanköy, NW Tosya, SE Kastamonu.

Triloculina sp., *Alveolina* sp., *Orbitolites* sp., *Opertorbitolites* sp., *Cribrobulumina* sp. and *Nummulites* sp.

In the Middle Ilerdian aged levels, *G. lepidula* Schwager, *A. ellipsoidalis* Schwager, *A. moussoulensis* Hottinger, *A. corbarica* Hottinger, *A. ilerdensis* Hottinger, *A. minervensis* Hottinger, *A. erki* Acar, *Orbitolites complanatus* Lamarck, *O. megasphericus* Zhang, *Opertorbitolites lehmanni* Montanari, *Alveolina* sp., *Orbitolites* sp., *Opertorbitolites* sp., *Cribrobulumina* sp., *Asterigerina* sp., *Miscellanea* sp., *Rotalia* sp. and *Nummulites* sp. were found. Late Ilerdian aged levels are represented by *G. lepidula* Schwager, *A. trempina* Hottinger, *A. aragonensis* Hottinger, *Orbitolites complanatus* Lamarck, *Opertorbitolites lehmanni* Montanari, *Alveolina* sp., *Orbitolites* sp., *Opertorbitolites* sp., *Cribrobulumina* sp., *Nummulites* sp. and *Asterigerina* sp. (Figure 6).

BIOSTRATIGRAPHY AND DISCUSSION

In this section stratigraphic ranges of benthic foraminifera defined in the studied area are correlated with Shallow Benthic Foraminifera Biozones (SBZ) of the Tethyan Belt (Serra-Kiel et al., 1998).

Similar to Serra-Kiel et al., (1998), *Idalina sinjarica* Grimsdale is observed in the Thanetian-Lower Ilerdian levels of the unit (SBZ 3-6).

As in the Tethyan Belt Shallow Benthic Foraminifera Biozones (Serra-Kiel et al., 1998), *Glomalveolina lepidula* Schwager is found in the Ilerdian (SBZ 5-9) levels of the study area. In the Tethyan Belt Biozones, while *Alveolina moussoulensis* Hottinger, *A. subpyrenaica* Leymerie and *A. laxa* Hottinger are shown in the lower levels of Middle Ilerdian (SBZ 7), *A. corbarica* Hottinger is shown in the upper levels of Middle Ilerdian (SBZ 8) and *A. decipiens* Schwager is shown in Middle Ilerdian (SBZ 7-8) by Serra-Kiel et al., (1998). However, these species are observed in the Middle Ilerdian levels of the northwestern Tosya region. According to Serra-Kiel et al. (1998) *A. trempina* Hottinger characterizes Upper Ilerdian levels (SBZ 9) in the Tethyan biozones. The same stratigraphic range has been determined for *A. trempina* Hottinger in the studied area. *A. ellipsoidalis* Schwager indicate Early Ilerdian (SBZ 6) in the Tethyan biozones (Serra-Kiel et al., 1998) and Early-Middle Ilerdian in this study. *A. aragonensis* Hottinger and *A. ilerdensis* Hottinger are shown in the Middle-Late Ilerdian (SBZ 7-9) of the Tethyan biozones (Serra-Kiel et al., 1998). The former species is found in the Upper Ilerdian levels while the latter is observed in the Middle Ilerdian levels of the studied area.

PALEOENVIRONMENTAL INTERPRETATION

Paleoenvironmental interpretations of the Thanetian-Ilerdian unit are mainly based on *Alveolina* species, other described benthic foraminifera and sedimantological data. As in most benthic foraminifera the test shape of Alveolina genus is an important criterion in the paleoecological studies (Hottinger, 1960, 1977, 1997; Lutherbacher, 1970; Hottinger and Dreher, 1974; Larsen, 1976; Hallock and Glenn, 1986). Hottinger (1960) stated that species of *Alveolina ellipsoidalis, Alveolina subpyrenaica* and *Alveolina decipiens* groups live in restricted platform environments with normal salinity. Similarly Luterbacher (1970), in his study on environmental distribution of Tertiary benthic foraminifera of Tremp basin, expressed that spheric alveolinids were found in lagoonal deposits while elongated alveolinids restricted in platform deposits. Both studies revealed that *Orbitolites* and *Opertorbitolites* inhabit together with these *Alveolina* species in identical environmental conditions. These types of environments, where low energy conditions are dominant, are characteristic for *Alveolina, Orbitolites* and *Opertorbitolites* assemblages (Hottinger, 1960).

The presence of Upper Cretaceous limestones with larger benthic foraminifera in the studied area indicates the activity of shallow water conditions during this period. The units in the region were affected from the Laramian phase of Alpin orogenesis in the end of Late Cretaceous (Ayaroğlu, 1980). Following this period sea advanced forward and covered the region in the Thanetian. The beginning of Thanetian-Ilerdian unit with a basal conglomerate, and continuning with sandstones and sandy limestone lithologies are the evidences of this transgression. Poor fossil content of Thanetian levels which is mostly characterized by small rotaliid foraminifera (*Cuvillierina, Mississippina, Miscellanea, Rotalia*) indicate restricted platform environment with abnormal salinity (Hottinger, 1960).

However, Lower-Middle Ilerdian levels of the unit contain abundantly *Alveolina, Opertorbitolites* and *Orbitolites* species. These fossil assemblages with porcellaneous shell walls (Grenier, 1969; Murray, 1973; Reiss and Hottinger, 1984) and boundstones and wakestones with micritic cement indicate low energy conditions. Presence of these fossil assemblages and sedimentological data show that these levels of the unit were deposited in a shallow (about 10-30 m depth) restricted platform environment with normal salinity. Starting from upper levels of Middle Ilerdian and to the Upper Ilerdian, genera *Nummulites* and *Assilina* become more dominant. These fossil assemblages indicate the development of a deep (40-80 m depth) carbonate shelf environment in this period (Henson, 1950; Hottinger, 1960; Örçen et al., 1994).

CONCLUSION

In this study paleontological investigations are carried out on Thanetian-Ilerdian unit, which outcrops in the southeast (NW Tosya) of Kastamonu. In the study area a unit, which was aged Paleocene-Eocene by previous studies conducted in the region, unconformably overlies the Bekirli Metamorphics. However this study determined that the unit is Thanetian-Ilerdian aged.

The unit begins with basal conglomerate and continues upward with sandstones, sandy limestones and limestones. The following benthic foraminifera are described: *Haymanella paleocenica* Sirel, *Idalina sinjarica* Grimsdale, *Mississippina binkhorsti* (Reuss) in the Thanetian levels; *İdalina sinjarica* Grimsdale, *G. lepidula* Schwager, *G. subtilis* Hottinger, *G. karsica* Sirel, *A. ellipsoidalis* Schwager, *Orbitolites complanatus* Lamarck, *O. megasphericus* Zhang, *Opertorbitolites lehmanni* Montanari in the Lower Ilerdian levels; *G. lepidula* Schwager, *G. pilula* Hottinger, *A. ellipsoidalis* Schwager, *A. moussoulensis* Hottinger, *A. corbarica* Hottinger, *A. laxa* Hottinger, *A. ilerdensis* Hottinger, *A. minervensis* Hottinger, *A. subpyrenaica* Leymerie, *A. decipiens* Schwager, *A.* aff. *pisella* Drobne, *A. erki* Acar, *O. complanatus* Lamarck, *O. megaspherocus* Zhang, *Op. lehmanni* Montanari in the Middle Ilerdian levels and *G. lepidula* Schwager, *A. trempina* Hottinger, *A. aragonensis* Hottinger, *O. complanatus* Lamarck, *Op. lehmanni* Montanari in the Upper Ilerdian levels. The stratigraphic range of these species presents close similarities with Tethyan Belt Shallow Benthic Foraminifer Biozones (Serra-Kiel et al., 1998) except for a few differences. The fossil assemblage and sedimentological data indicate the deposition of the Thanetian levels in restricted platform environment with abnormal salinity, the deposition of the Lower-Middle Ilerdian levels in a shallow and restricted platform environment with normal salinity, and finally the deposition of the Upper Ilerdian levels in a deep carbonate shelf environments in the region.

ACKNOWLEDGEMENT

The support of the Council of Scientific Research Projects of Cumhuriyet University is acknowledged.

Manuscript received June 30, 2008

REFERENCES

Ayaroğlu, H. 1980. Tosya kuzeybatısının (Karadere) jeolojisi ve ekonomik olanakları. Jeoloji Mühendisliği, 10, 65-73 (In Turkish).

Blumental, M. 1939. Über den stand der geologischen aufnahmen im Ilgaz Dağ.). Maden Tetkik Arama Genel Müdürlüğü Report No: 842, 35s. Ankara (unpublished).

_____, 1948. Bolu civarı ile Aşağı Kızılırmak arasındaki Kuzey Anadolu Silsilelerinin jeolojisi.). Maden Tetkik Arama Genel Müdürlüğü yayınları seri B, no, 13, 71-119) (In Turkish).

_____, 1950. Orta ve aşağı Yeşilırmak bölgelerinin jeolojisi. Maden Tetkik Arama Genel Müdürlüğü Yayınları seri D, no, 4, 153s (In Turkish).

Coulant, E. 1894. Kastamonu vilayeti Çiban Köyü Nikel Yatakları. Maden Tetkik Arama Genel Müdürlüğü Report No: 1398, 12s. Ankara (in Turkish) (unpublished).

Grenier, G.O.G. 1969. Recent benthic foraminifera, environmental factors controlling their deposition. Nature, 223, 168-170.

Hallock, P. and Glenn, E.C. 1986. Larger Foraminifera: A Tool for Paleoenvironmental Analysis of Cenozoic Carbonate Depositional Facies. Palaios, 1, 55-64.

Henson, F.R.S. 1950. Middle Eastern Tertiary Peneroplidae (Foraminifera) with remarks on the phylogeny and taxonomy of the family. West Yorkshire Printing Co., 70p.

Hottinger, L. 1960. Recherches sur les alveolines du Paléogene et de l'Eocene. Mémoires Suisses de Paléontologie, 75-76, 1-236.

_____, 1977. Foraminiféres Operculiniformes. Mémoirs du Museum d'Histoire Naturelle, 40, 1-159.

_____, 1997. Shallow benthic foraminiferal assemblages as signals for depth of their limitations. Bulletin de la Société Géologique France, 168/4, 491-505.

_____, and Dreher, D. 1974. Differentiation of protoplasm in Nummulitidae (Foraminifera) from Elat, Red Sea. Marine Biology, 25, 41-61.

Larsen, A.R. 1976. Studies of Recent Amphistegina: taxonomy and some ecological aspects. Israel Journal Earth Science, 25, 1-26.

Lutherbacher, H.P. 1970. Environmental distribution of early Tertiary microfossils, Tremp Basin, North-eastern Spain. ESSO Production Research-European Laboratories, 46p.

Murray, J.M. 1973. Distribution and ecology of living benthic foraminiferids. New York, Crane, Russak and Co., 274 p.

Örçen, S., Yıldız, A. and Toker, V. 1994. Yukarısazcağız yöresi (Gürün KB, Sivas) Lütesiyen'inin biyostratigrafik olayları ve paleoekolojisi. Türkiye Jeoloji Bülteni, 9, 97-108 (in Turkish).

Özgen, N. 1998. Batı Pontid'lerin Paleosen-Eosen bentik foraminifer toplulukları. Türkiye Jeoloji Bülteni, 41 /2, 63-78 (in Turkish).

Özgen Erdem, N., İnan, N., Akyazı, M. and Tunoğlu C. 2005. Benthonic foraminiferal assemblages and microfacies analysis of Paleocene-Eocene carbonate rocks in the Kastamonu region, Northern Turkey. Journal of Asian Earth Sciences, 25/3, 403-417.

Pilz R. 1937. Kastamonu ve Sinop vilayetlerindeki çeşitli mineral yataklarının tetkiki. Maden Tetkik Arama Genel Müdürlüğü Report No: 644. Ankara (in Turkish) (unpublished).

Reis, Z. and Hottinger, L. 1984. The Gulf of Aqaba, Ecological Micropaleontology. Springer-Verlag, 354 p.

Serra-Kiel, J. Hottinger, L., Caus, E., Drobne, K., Ferrandez, C., Jauhri, A.K., Less, G., Pavlovec, R., Pignatti, J., Samso, J.M., Schaub, H., Sirel, E., Strougo, A., Tambareau, Y., Tosquella, J. and Zakrevskaya, E. 1998. Larger foraminiferal biostratigraphy of the Tethyan Paleocene and Eocene. Bulletin Société Géologique France, 169, 2, 281-299.

Tunoğlu, C. 1992*a*. Devrekani havzası (Kastamonu kuzeyi) Üst Jura-Alt Kretase yaşlı karbonat istifinde mikrofasiyes analizleri. Türkiye Petrol Jeologları Derneği Bülteni, 3/1, 75-86 (in Turkish).

Tunoğlu, C. 1992*b*. Devrekani havzası (Kastamonu kuzeyi) Maastrihtiyen yaşlı pelajik karbonat istifinde mikrofasiyes analizleri. Türkiye 9. Petrol Kongresi, 17-21 Şubat 1992, 112-113 (in Turkish).

_____, 1993. Devrekani Havzasının (Kastamonu kuzeyi orta Pontidler) litostratigrafi birimleri. A.Suat Erk Simpozyumu, 2-5 Eylül 1991, Ankara, 183-191 (in Turkish).

_____, 1994. Devrekani Havzası (Kastamonu Kuzeyi) Üst Paleosen-Alt-Orta Eosen yaşlı karbonat istifinde mikrofasiyes analizleri. Türkiye Jeoloji Bülteni, 37/2, 43-51 (in Turkish).

Tüysüz, O. 1986. Kargı masifi ve dolayındaki tektonik birliklerin ayrımı ve araştırılması (petrolojik inceleme). Doktora Tezi, İstanbul Üniversitesi, 431s. İstanbul.

Yılmaz, Y. and Tüysüz, O. 1984. Kastamonu-Boyabat-Vezirköprü-Tosya arasındaki bölgenin jeolojisi (Ilgaz-Kargı masiflerinin etüdü). Maden Tetkik Arama Genel Müdürlüğü Report No:7838, 275s. Ankara (in Turkish) (unpublished).

bos

PLATES

PLATE I

Haymanella paleocenica Sirel, Thanetian

Figure 1-2- Vertical sections, megalospheric form (Kirenler section, Nçb. 2), 1-X50, 2-X40.

Idalina sinjarica Grimsdale, Thanetian

Figure 3- Axial section, megalospheric form (Kirenler section, Nçb.2), X20.

Mississippina binkhorsti (Reuss), Thanetian

Figure 4- Subaxial section (Kirenler section, Nçb.3), X30

Pseudocuvillierina? sp., Thanetian

Figure 5- Axial section, megalospheric form (Kirenler section, Nçb.3), X30

Figure 6- Equatorial section, megalospheric form (Kirenler section, Nçb. 3), X30

Glomalveolina lepidula Schwager, Ilerdian

Figure 7- Axial section, megalospheric form (Kirenler section, Nçb.7), X30.

Glomalveolina karsica Sirel, Early Ilerdian

Figure 8- Axial section, megalospheric form (Kirenler section, Nçb.9), X30.

Alveolina erki Acar, Middle Ilerdian

Figure 9- Axial section, megalospheric form (Kirenler section, Nçb.18), X20.

Alveolina ellipsoidalis Schwager, Early Ilerdian

Figure 10- Axial section, megalospheric form (Kirenler section, Nçb. 12), X20.

Alveolina corbarica Hottinger, Middle Ilerdian

Figure 11- Axial section, megalospheric form (Kirenler section, Nçb. 17), X20.

Alveolina ilerdensis Hottinger, Middle Ilerdian

Figure 12- Axial section, megalospheric form (Kirenler section, Nçb. 27), X20.

Alveolina decipiens Schwager, Middle Ilerdian

Figure 13- Axial section, megalospheric form (Akçataş section, Ak.26), X20.

PLATE - I

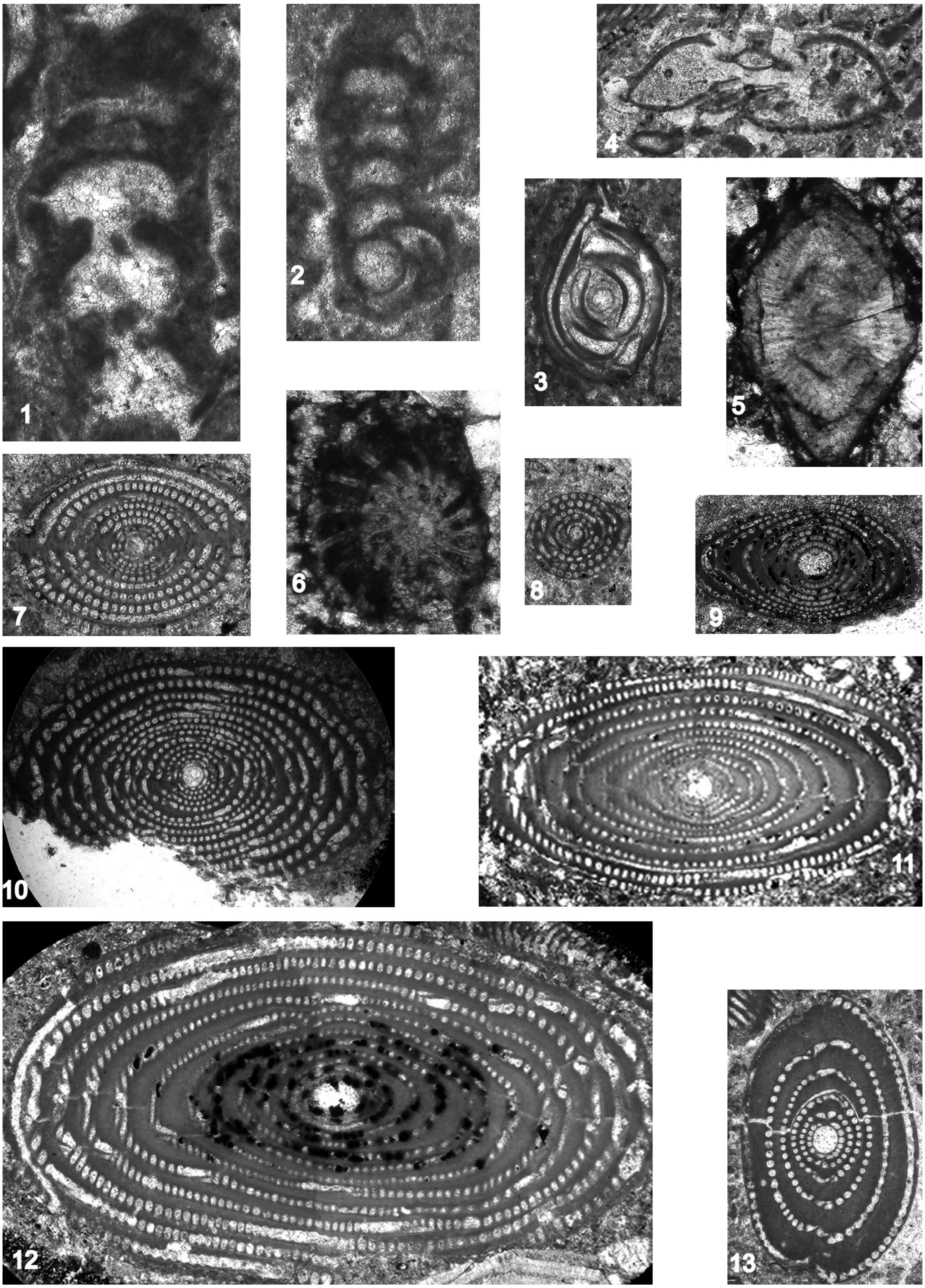

PLATE II

Alveolina subpyrenaica Leymerie, Middle Ilerdian

Figure 1- Axial section, megalospheric form (Akçataş section, Ak.8) X20.

Alveolina aragonensis Hottinger, Late Ilerdian

Figure 2- Axial section, megalospheric form (Kirenler section, Nçb.33) X20.

Alveolina trempina Hottinger, Late Ilerdian

Figure 3- Axial section, megalospheric form (Kirenler section, Nçb.32), X20.

Alveolina aff. *pisella* Drobne, Middle Ilerdian

Figure 4- Axial section, megalospheric form (Akçataş section, Ak.18), X20.

Alveolina minervensis Hottinger, Middle Ilerdian

Figure 5- Axial section, megalospheric form (Akçataş section, Ak.8), X20.

Opertorbitolites lehmanni Montanarii, Middle Ilerdian

Figure 6- Axial section, megalospheric form (Akçataş section, Ak.11), X20.

Orbitolites megasphericus Zhang, Early- Middle Ilerdian

Figure 7- Axial section, megalospheric form (Akçataş section, Ak. 22), X20

Figure 8- Axial section, megalospheric form (Kirenler section, Nçb.6), X20.

Orbitolites complanatus Lamarck, Ilerdian

Figure 9- Axial section, megalospheric form (Kirenler section, Nçb.7), X20.

Discocyclina sp., Middle Ilerdian

Figure 10- Axial section, megalospheric form (Akçataş section, Ak.25), X20.

PLATE - II

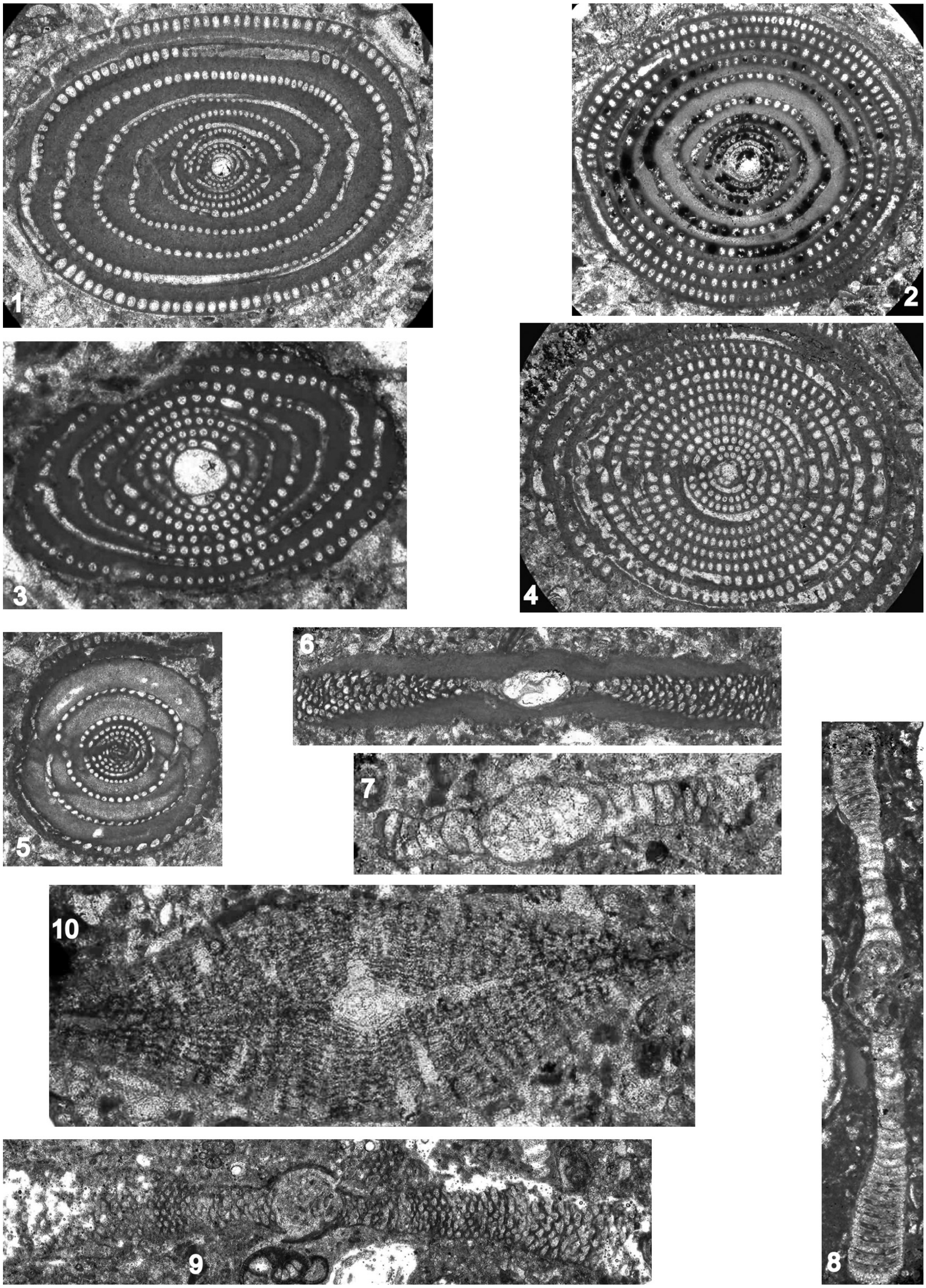

bos

Mineral Res. Expl. Bull., 137, 61-72, 2008

SOME GEOMORPHOLOGICAL FEATURES OF THE ORHANELİ PLUTON: IMPLICATIONS FOR DENUDATION HISTORY

Ahmet Evren ERGİNAL* and Ahmet ERTEK**

ABSTRACT.- The granitic intrusions of variable age of cooling, size and mineral composition are widely exposed in the northwest Anatolia, Turkey. The nearly circular Orhaneli Pluton emplaced during the Early Eocene with some 15 km in diameter, is one of such plutonic bodies. Geomorphological features of the pluton is discussed here with special emphasis given on the denudation history. To this end, evidences from two isolated Inselberg-like hills as remnants of roof rocks in the centre of the pluton and episodically emergence of granite landforms of etch origin after unroofing process were investigated. Field data reveal the absence of granodiorite clasts within Early to Middle Miocene lacustrine deposits in the north of the pluton, implying that the pluton might has not been exposured prior to Upper Miocene as a whole. After the first exposure, the granite landforms, such as boulders, corestones and tors constituting sound evidence of an etch origin, became exposured by continual removing of regolith cover by surficial runoff. These forms of various scale were formed at first by subsurface weathering and shaped by surficial weathering processes after any stages of removal of the regolith cover. Drainage segments accounted for removal of regolith is mostly structurally controlled defined by NW-SE, NE-SW and N-S-aligned fracture systems.

Key words: Differential weathering, Weathering front, Regolith, Orhaneli Pluton, NW Turkey.

INTRODUCTION

Granite masses and associated terrains cover wide areas in the northwestern part of Anatolia, Turkey (Figure 1). One of them is the Orhaneli Granodiorite Pluton that lies within latitudes 39°52'02'' N to 39°42'21'' N and longitudes 28°51'38'' E to 29°02'48'' E, located in approximately 28 km south of the Mt. Uludağ in the northwestern part of Turkey. It has a diameter of about 15 km and a surface area of almost 200 km². As a clear example to nearly circular-shaped plutons emplaced at shallow crustal levels, the Orhaneli Granodiorite Pluton has some significant geomorphological and petrographical implications for explaining the denudation chronology of such well-exposured intrusive bodies. The two huge resistant blocks at its central part, quitely sharp contact relations with the host rocks and granite landforms provide clear evidences for denudation chronology and geomorphological evolution of the pluton.

In this study, the geomorphological development of the Orhaneli Pluton is discussed petrological, remote sensing and based on geomorphological data. The denudational history of the pluton was revealed by etching processes, which imply preferential weathering of the granodiorite and continual stripping of resultant regolith cover by the Sadagi River and its tributaries.

GEOLOGICAL AND GEOMORPHOLOGICAL SETTING

The geology of the pluton has been previously discussed by several authors (Okay, 1948; Kaaden, 1959; Altınlı, 1966; Bürküt, 1966; Özkoçak, 1969; Ataman, 1972; Bingöl et al., 1982; Emre, 1986; Harris et al., 1994; Okay et al., 1998; Delaloye and Bingöl, 2000). A general geological map, generalized stratigraphic section and cross-section of the pluton is shown in figure 2, where it can be seen that the outcrop of granodioritic rocks of Lower Eocene is bordered

* Çanakkale Onsekiz Mart Üniversitesi, Fen-Edebiyat Fakültesi, Coğrafya Bölümü, Terzioğlu Kampüsü, Çanakkale. aerginal@comu.edu.tr
** İstanbul Üniversitesi, Edebiyat Fakültesi, Coğrafya Bölümü, Laleli, İstanbul. taertek@istanbul.edu.tr

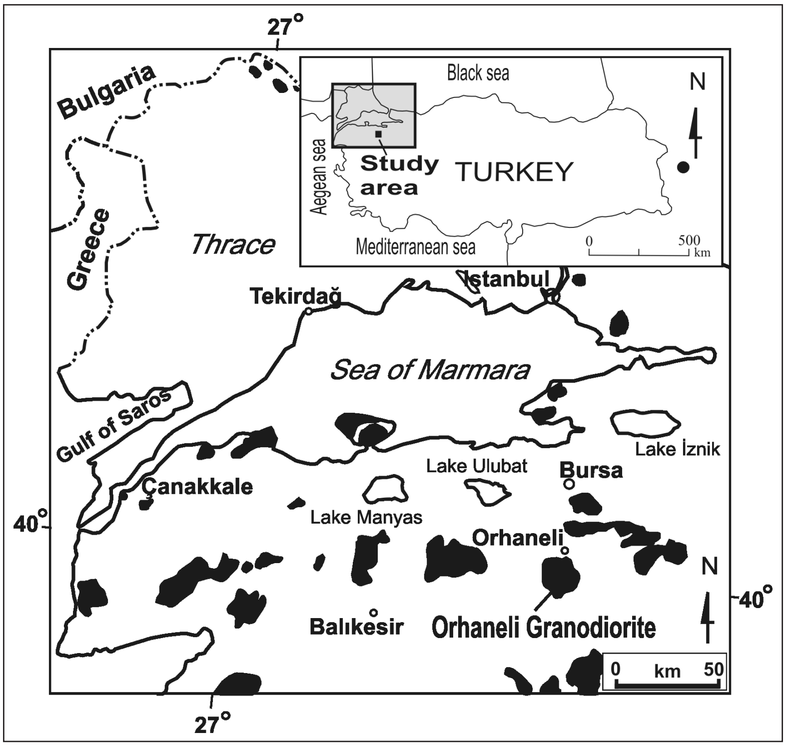

Figure 1- Location map and spatial distribution of granitic terrains in the northwest Anatolian region of Turkey.

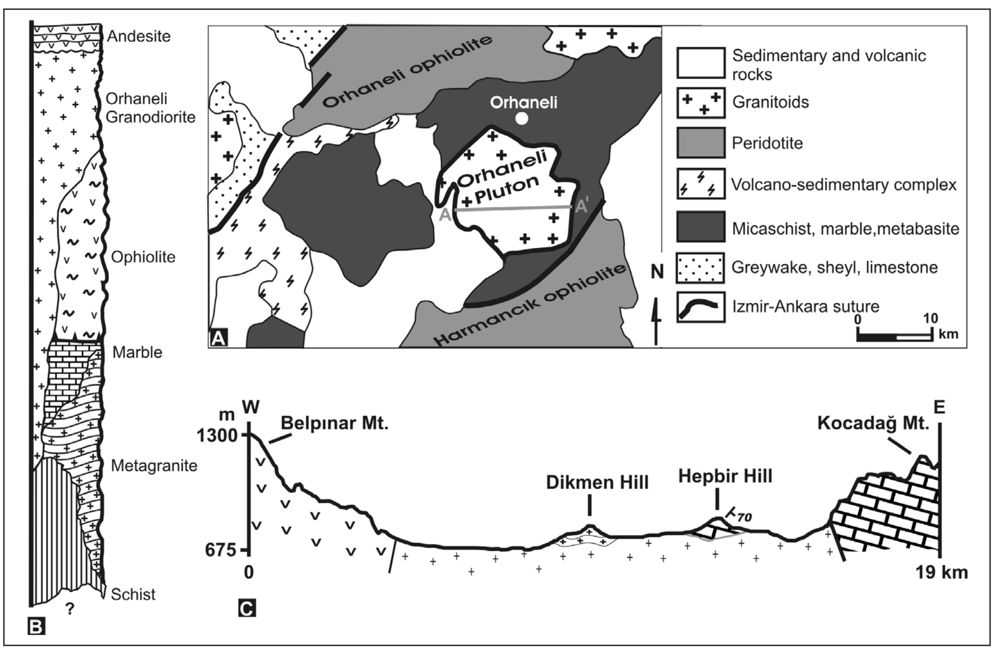

Figure 2- Generalized geological map (A) modified from Emre (1986), stratigraphic columnar section (B) and cross-section (C) of the study area.

to the east by Paleozoic schist and marble, roof remnants of which occur near Eskidanişment village.

Based on Ar/Ar laser spot analysis on biotite samples, it was explained that the pluton intruded into a metamorphic sequence at a deph of ~10 km during the Early Eocene (52.4±1.4 Ma) (Harris et al., 1994). It outcrops at an area of approximately 200 km² and consists of medium-grained granodiorite including 50-60% plagioclase, 20-25% quartz, 10-15% biotite, about 10% alkali feldspar, about 5% plus hornblende, sundry minor minerals (Harris et al. 1994), abundant microgranitoid enclaves and zircon, apatite and opaque as accessory minerals. Its texture is commonly holocrystalline granular (Figure 3A).

The host rocks of the Orhaneli Pluton are composed of schists, marbles and metagranites, among which the last two are of wider extension. They occupy a large area to the north, east and south of the pluton. Having a mosaic texture, the marble, which crops out at the eastern and southern borders of the pluton is a grey to white-coloured rock containing calcite and opaque minerals. It includes intense fractures and gives a typical section on Mt. Kocadağ to the east. A north-south trending fault that juxtaposes the marble against the pluton rocks displays a tectonic contact, along which an intense cataclasis was detected on thin sections (Figure 3B).

The metagranite defined as Belenoluk Metagranite by Emre (1986) bounds the pluton to the north and consists mainly of hornblende, quartz, plagioclase, orthoclose, opaque and abundant titanite. Its texture is holocrystalline porphyritic with commonly developed alteration on mineral grains. Metagranite and marble also cap Dikmen and Hepbir Hills, respectively (Figure 4).

To the western border the pluton is also in contact with and is in part overlain by Miocene volcanics forming steep erosional scarps. The lavas resting on the metamorphic associations in

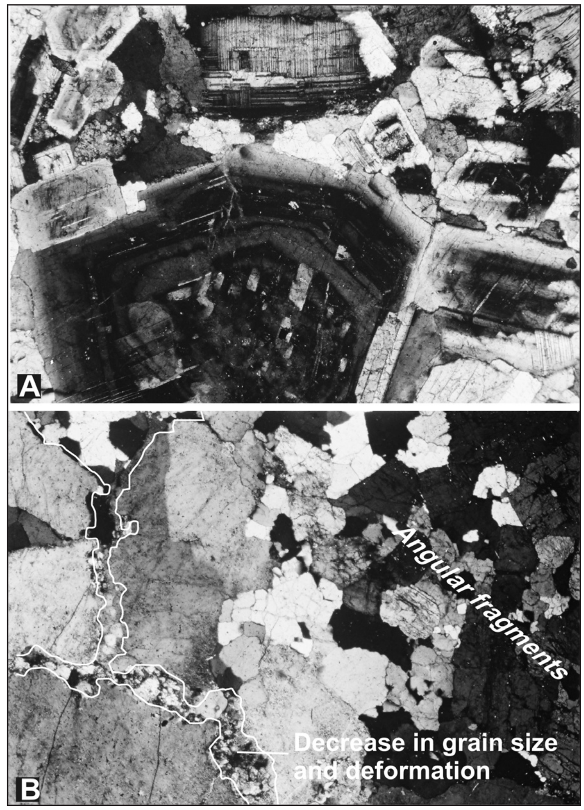

Figure 3- Photomicrographs of samples: a zoned crystal in granodiorite at inner parts of the pluton (A) and intense cataclasis along N-S trending contact zone (B).

the area are commonly characterized by andesite and dacite in composition, and consist of plagioclase, biotite and opaque minerals set in a vitrophric texture. An isotopic age of 17.6±0.2 Ma (Okay et al., 1998) from tuff samples resting on andesitic flows near Büyükorhan dates these volcanic to Early Miocene. They actually constitute an eastern extension of Miocene volcanics defined in western and northwestern Anatolian parts of Turkey (Ercan, 1979; Ercan et al., 1990).

From geomorphological point of view, the Orhaneli Pluton is characterized by a slightly dissected ondulated plateau with an average altitude between 750-950 m above sea level (Figure 4). It is surrounded by higher ridges and ranges

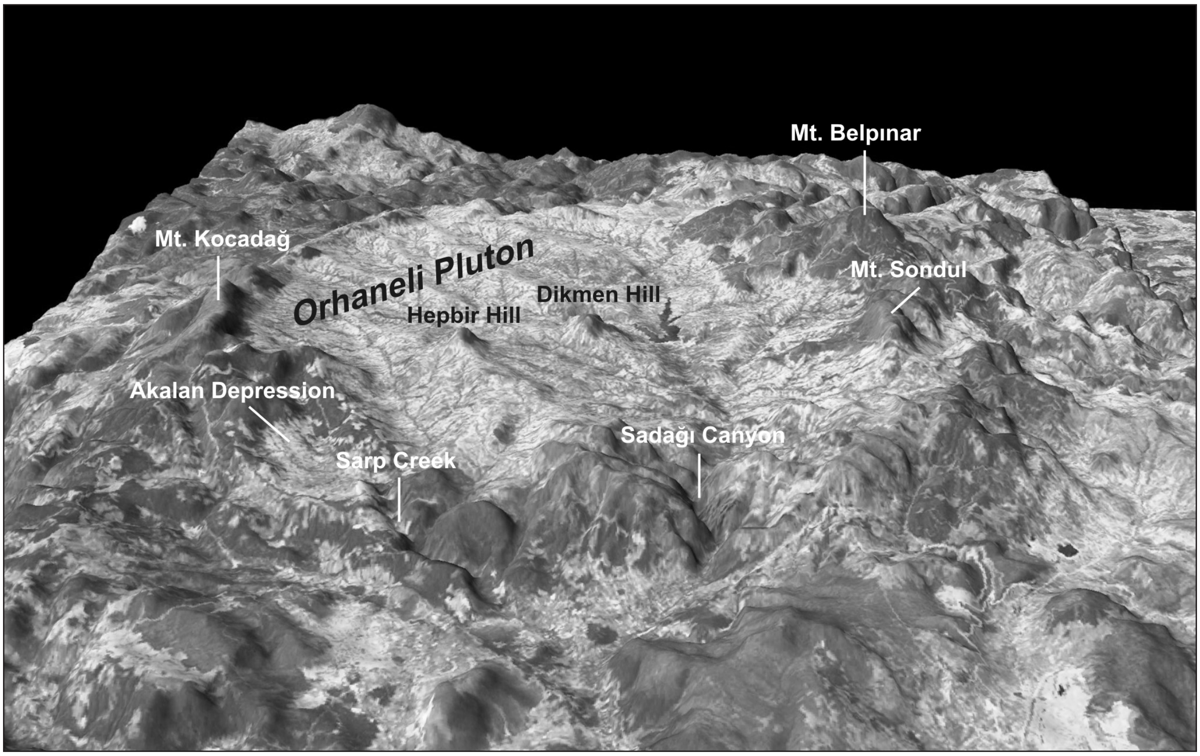

Figure 4- Digital Elevation Model of the Orhaneli Pluton and its surroundings (note the circular dome surface and two inselberg-like hills in the central part). Drainage channels of the to main streams, Sadağı and Sarp Rivers, are severely controlled by NW-SE trending fractures. In addition, a dendritic drainage pattern with high bifurcation ratio is dominant. View direction is southward.

reaching up to 1400 m in altitude, the highest of which are Mt. Belpınar (1391 m) underlained by silicic volcanic rocks to the west and Mt. Kocadağ (1323 m) formed by marbles to the east. They are seperated from the pluton by north-south-trending escarpments with approximately 200 m high. The granodioritic rocks have been eroded to form a rolling plain (or plateau) between these highlands.

The plateau, which is sparsely coated with vegetation, is characterized by low erosional surfaces seperated by slightly incised broad valleys. Two Inselberg-like hills, i.e. Dikmen and Hepbir Hills, in central part of the pluton form conspicious anomalies in morphology of the area, since they are more resistant to weathering and erosion. The lowland is drained by the Sadağı River and its tributaries, which runs northwards through the 300-450 m deep Sadağı Canyon. Most of the stream channel network that drain the pluton area is joint controlled.

METHODS

A digital terrain model (DTM) digitizing 20-meter-interval contours from 1/25.000-scaled topographic maps has been produced to characterize mathematically topographic features. DTM was superimposed with Landsat ETM satellite images (2000) using ERDAS Imagine 8.3 Software. Distribution of the lineaments determined from satellite images were compared with 545 fracture measurements performed on fresh rock exposures to explain relationships between fracture patterns and construction of drainage network.

Standard thin sections of many rock samples were produced to examine mineral fabrics and compositions and traces of shearing deformation of mineral grains.

DISCUSSION

Preferential weathering of the granodioritic rocks and stripping of regolith

The Orhaneli Pluton is situated at a lower elevation than the surrounding metamorphic terrain both because of its composition and because of its closely spaced fractures. It is well known that biotite, plagioclase and hornblende are particularly susceptible to attack by water (e.g. Goldish 1938; Loughnan, 1969). The percentages of plagioclase (50-60%), quartz (20-25%) and biotite (10-15%) are thus of great importance for velocity of weathering and the resulting thickness of regolith. In other words, the weathering-prone mineral content of the granodiorite has determined erosional lowering of the pluton relative to the adjacent metamorphic terrains.

In many parts of the study area, where the regolith is partly stripped, some specific granitic forms, such as corestones, boulders and tors of various size and shape give numerous exposures as clear evidences of epigene weathering processes developed on the weathering front (Mabbutt, 1961). These specific forms are of subsurface initiation in origin (Twidale and Bourne, 1975) and are the result of rapid or episodically stripping of weathering mantles or regoliths as previously imparted by several authors (Twidale and Bourne, 1975; Twidale,1993). During the field study, it was observed that boulders with 50 cm to 2 m high have a circular shape because of spheroidal weathering or exfoliation. The exfoliation slabs on boulders are equal to or thinner than 1-2 cm. Their distribution and geometry is controlled almost everywhere by vertical and sheet fracture patterns. In road cuttings, the visible thickness of the regolith cover under these stripped forms was measured as thick as 3 to 5 m. The regolith with light colour contains abundant quartz and alkaline feldspar grains and some decomposed microdioritic enclaves. The quartz veins are also difficult to observe due to intensive weathering.

The closely spaced fractures typical of the upper part of the pluton have allowed ready penetration of meteoric water, resulting in the differential weathering of the fracture-defined blocks. This circumstance has caused the formation of corestones in a grus (Figures 5A and B), in many instances with "onion skin" texture. After the evacuation of the grusified rock, corestone boulders were exposed (Figure 5C). This process commonly occurs in granite terrains, as previously referred to multistage landform development by Twidale (1993).

In many exposures of corestones and tors, sheet fractures cut by vertical fractures are well developed. The thickness of slabs seperated by sheet fractures reaches up to 1 m (Figure 5D). Although these fractures have been habitually ascribed to pressure release consequent on erosional offloading in the existing literature (Gilbert, 1904; Chapman, 1956), the geometry of the horizontal slabs and sheet fractures in the study area are a little distinct and support some evidences of tectonic impacts discussed by Twidale et al. (1996).

In both sections of regoliths and tor exposures, sheet fractures were observed to have a shape of partly upward arching and frequent diagonal fractures with, somewhere, abundant quartz veins (Figure 5B). Because of scarcity of typical great fresh rock exposures, sheet fractures having more thickness in depth were not possible to observe for a detailed discusion here.

Relations between structure, drainage and geomorphology

Major faults and fractures are shown in figure 6. In addition to their effects on river patterns, the

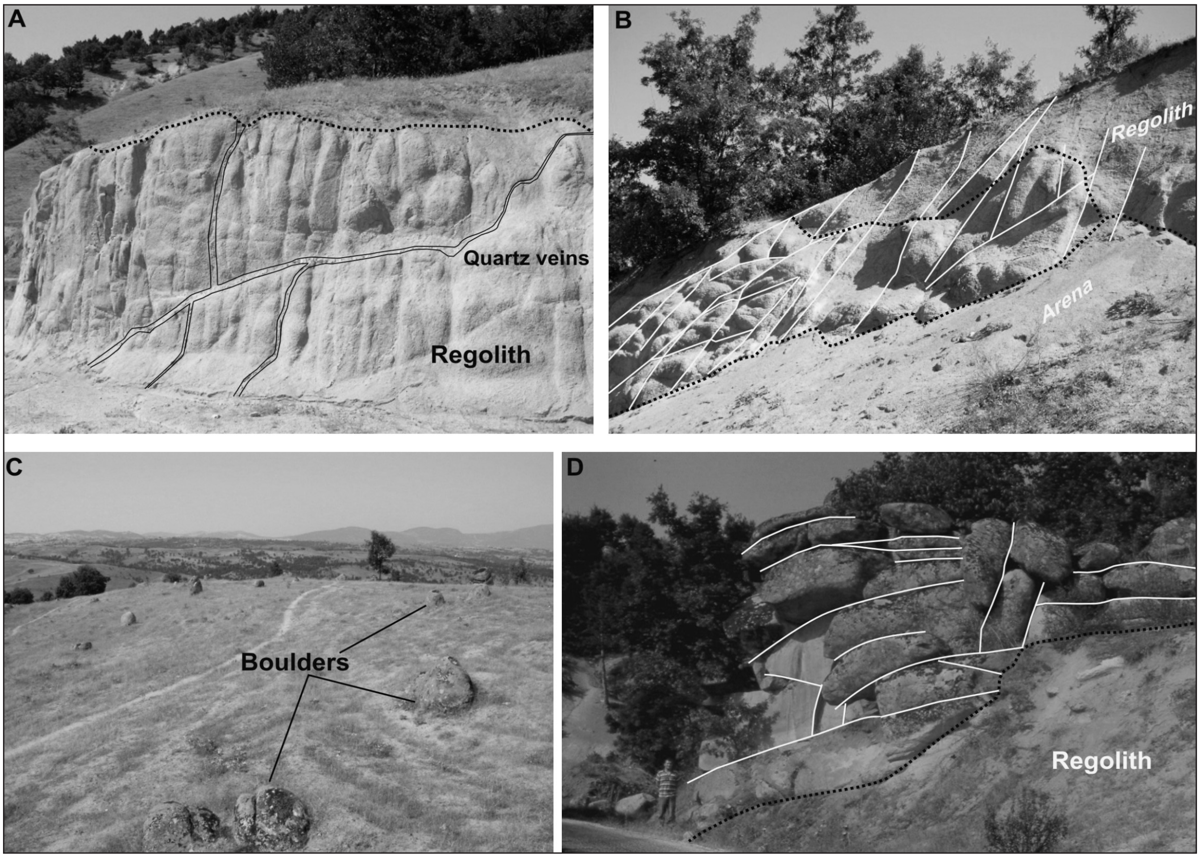

Figure 5- A typical section for regolith cover with some thin quartz veins (A), sheet and cross fractures among newly exposed corestones (B), stripped boulders on a flat erosional surface (C) and an example of boulder formation with dense sheet fractures stripped from regolith cover (D).

pluton is bounded on its eastern side by a fault which juxtaposes the granitic rocks against Paleozoic marble. The topographic expression of this structure corresponds to a linear scarp on marbles. The north-south trending steep slope along this linear scarp corresponds to a fault-line scarp, which has been identified from a thin section with clear evidence of cataclastic deformation (Figure 3B).

In addition to facilitating the weathering of the granodiorite, fractures are also lines of weakness that controlled not only the alignment of streams and rivers but also determined which of them evolved into major waterways. Numerous field measurements of fractures demonstrate that NW-SE, NE-SW and N-S orientations are prevalent (Figure 6). These orientations coincide with the dominant azimuths of the lineaments determined from Landsat ETM satellite images. These partings have determined the development of many angular stream patterns.

The course of Sadağı Stream and its right bank tributary are obvious examples. The 400 m-deep Sadağı Canyon is controlled by a NW-SE trending fault located at the east of Hepbir Hill (Figure 7A). The longitudinal profile of the Sadağı River reflects changes in the physical and chemical properties of the bedrock geology, and shows a graded curve in metagranite rocks because of the effect of the Sadağı Fault with a

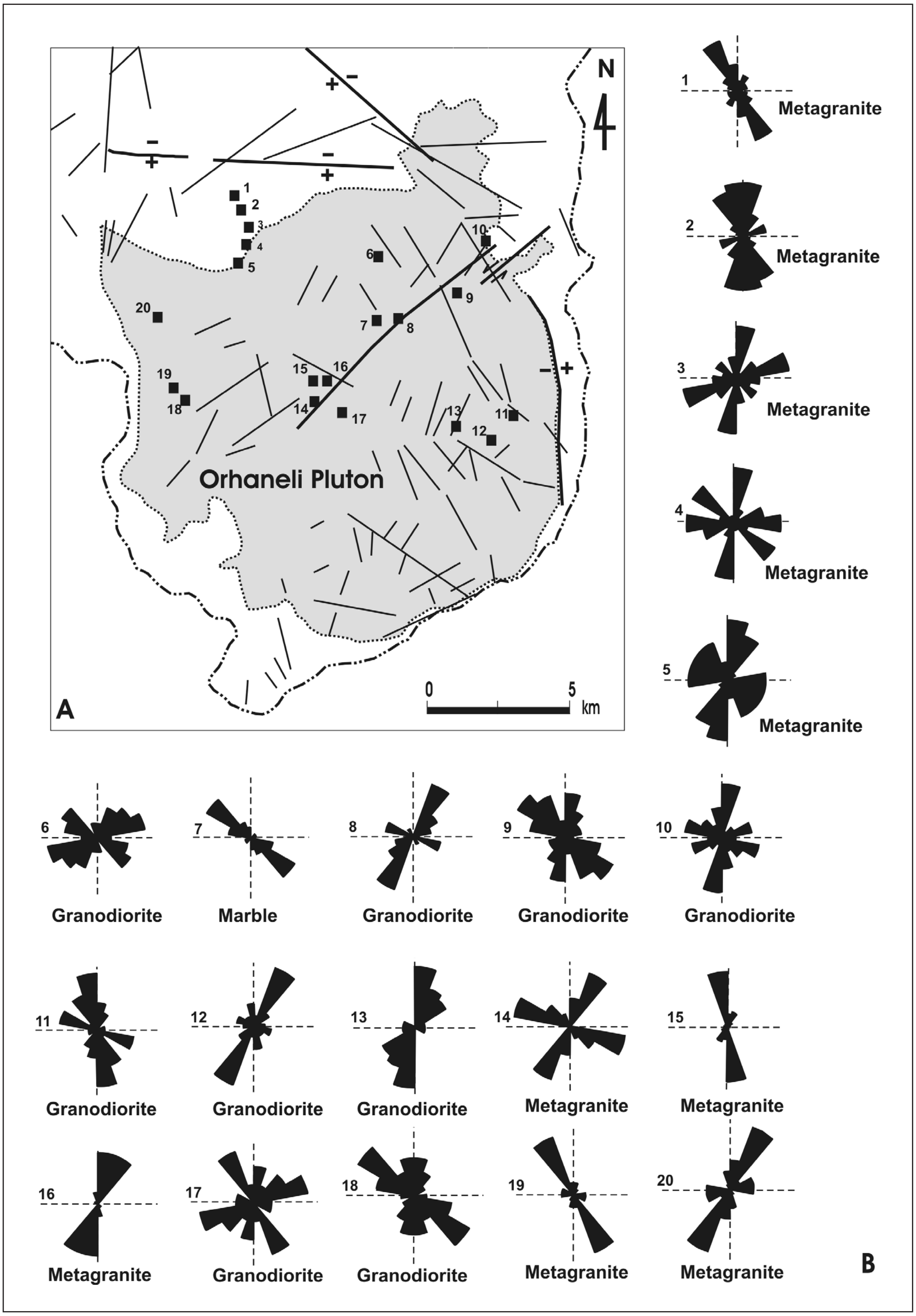

Figure 6- Distribution of main faults and fractures in the study area (A) and rose diagrams representing predominant fracture azimuths in measurement locations (B).

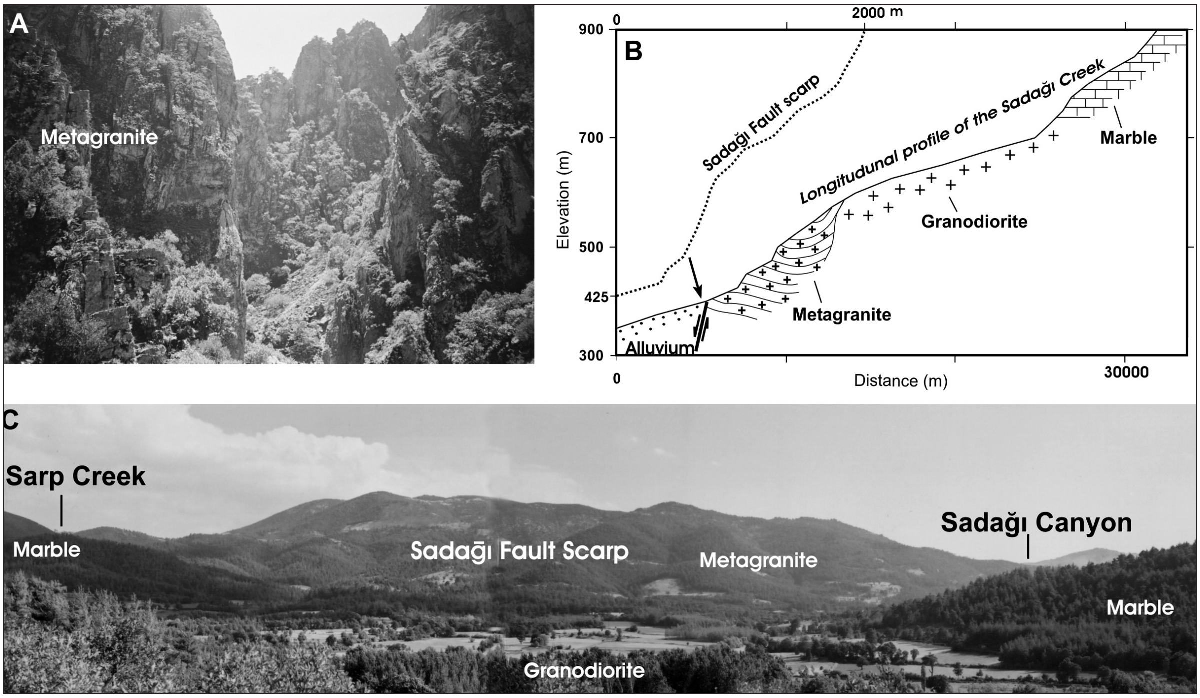

Figure 7- The Sadağı Canyon (A), longitudinal profile of the Sadağı Stream (B) and E-W-oriented Sadağı Fault (C) (the small depression in foreground developed on an apophysis of the Orhaneli Pluton. The Orhaneli Pluton remains behind the Sadağı fault scarp).

visible scarp of 300 m high (Figure 7B). The Sadağı Fault with east-west direction (Figure 7C) has allowed river incision and this in turn has caused the regolith to be stripped by the river and its tributaries.

In addition to the orthogonal subvertical fracture systems, sheeting joint sets define slabs up to one meter thick. Though commonly attributed to pressure release caused by erosional offloading (e.g. Gilbert, 1904), a critical factor for the development of fractures in granitic terrains (e.g. Chapman, 1956), these partings may primarily be due to tectonic compression (Dale, 1923; Twidale et al., 1996). The systematic orientations consistent with remotely sensed lineaments ought to be suggestive of tectonic stress fields, because they were observed not only on granodiorite but also on marble and metagranite exposures. For instance, the point eight measurement location situated in the top of the Hepbir Hill composed of marble, shows an evident NE-SW trending fracture system, which is very similar with those of points 12, 16, and 20 in metagranite exposures (Figure 6A and B). This orientation is also the common trend of many of the granodiorite exposures.

The cross fractures are observed on metagranite exposures, indicating various tectonic stresses. The similar orientations of the fractures in points 14, 15, 16, 19 and 20, measured on the Dikmen Hill are in good aggrement with those of points 1-5 along the Sadağı Canyon in the north.

Original denudation history

The Orhaneli Pluton has an intended shaped roof, a typical polygonal shape and very steeply dipping walls through contact zone with host rocks (Figure 8 A and B). Its eastern margin dis-

Figure 8- The Kocadağ block (A), a thin residual of marble on granodiorite near Eskidanişment village (B), Dikmen and Hepbir Hills (C) and Miocene silicious volcanics (D).

plays a conspicious discordant contact, along which various annular and radial dykes were observed in field surveys. A typical cataclastic deformation was also observed under thin section images taken from rock samples along this sharp contact. This deformation microstructure might be an indicator for a north-south-trending fault that juxtaposes the pluton rocks against the host rock.

From geomorphological point of view, the presence of two erosion-resistant hills at central part of the pluton and linear fault segments on eastern and southern contacts may have some important implications for denudation chronology of the pluton area. These hills, Dikmen and Hepbir Hills, are formed by metagranite and marble, respectively, and have been preserved in central part of the pluton. They are found at almost the same NW- SE alignment (Figure 4 and 8C). The size of the blocks are about 750 m and 1000 m above sea level respectively.

A thin section analysis of metagranite sample taken from the Dikmen Hill showed that it is composed of quartz, orthoclase, pertite, plagioclase, hornblende, titanite and apatite set in a holocrystalline porphyritic texture. Another sample from its contact with granodiorite, however, displayed a well developed cataclasis in primary magmatic minerals, such as quartz, plagioclase, orthoclase and biotite. The Hepbir Hill is, however, located at 500 m northeast of the Dikmen Hill. It is composed of calcite and opaque minerals set in a mosaic texture. In thin section interpretation, a partly developed cataclastic deformation was determined in mineral fabric of a granodiorite sample taken from its eastern margin. Similar microdeformation structure existed in the samples collected from the contact zone of the marble with the granodiorite, implying that both roof rocks and their remnants were affected by tectonic forces prior to the exposure.

The unique approach on the timing of first exposure of the pluton was suggested by Okay et al. (1998), who indicated that a tuff exposure (Figure 8D) with an isotopic date of 17.6±0.2 Ma at the western contact is indicative of Early Miocene. Nevertheless, this idea is not supported due to the absence of granodiorite clasts within Lower to Middle Miocene lacustrine deposits at the north of the pluton. Thus the initial period of denudation chronology of the pluton would be at least the Late Miocene as evidenced by the widespread extension of an planation surface cutting roof rocks with the Miocene deposits at a regular level.

The rolling planation surface preserved on the adjacent metamorphic terrains may have its equivalent in the Orhaneli granitic plain. The height difference may simply reflect differential erosion. The development of the Sadağı Canyon may simply have facilitated removal of the granitic regolith from the lower plain. On the other hand the Sadağı River may have controlled the evacuation of a thick regolith and be responsible for the present rocky plain which would thus be younger than the high paleosurface. There are no traces of younger cover deposits along the valley to infer relative age of the canyon.

The widespread occurrence of boulders, corestones and tors that constitutes clear evidence of an etch origin (Twidale and Vidal Romani, 2004) indicates that subsurface weathering is an important part of the denudation history of the Orhaneli Pluton. These form could be indicative for discontinuous (or episodic) progression of the weathering front. Nevertheles, absence of weathering rinds on corestones and boulders in the study area indicates that any pause might had not occured in the advance of the weathering front. Thus, stripping of the regolith have long been continued, and these residual features had later exposured from a thick cover of regolith. The fact that the weathering front is not exposed anywhere may also suggest that the subsurface weathering is an ongoing process caused by shallow groundwaters. The etching process that might had been operating since the Late Mio-cene, can therefore be supposed for the Orhaneli Pluton.

CONCLUSION

Based on petrological analysis, remote sensing data and field observations the following results were obtained:

Radiometric age of 17.6±0.2 Ma from biotite grains of dacitic tuffs at the western contact as indicative of initial exposure of the pluton would be a minimum age. However, granodiorite clasts are not found within the Early-Middle Miocene aged limnic sequences in the north of the pluton, indicating likely that it might had not been entirely exposured prior to the Late Miocene.

The Inselberg-like hills cut by a slightly inclined erosional surface with similar elevation to those located on the western and eastern country rocks are probably indicative of the remnants of roof rocks. However, their transition with the surrounding granodiorite is everywhere represented by microstructural deformations, suggesting tectonic effects or possible faults. The same deformations occur along the pluton-host rock contact as possible evidences for brittle deformation during or after the pluton emplacement.

Fracture measurements obtained from fresh rock exposures indicate an evident NW-SE fracture orientation. When this medium is evaluated with numerous lineament distributions determined from LANDSAT ETM (2000) satellite images, the principal vector was found to be 24.61°. Thus, it is concluded that NW-SE, NE-SW and N-S lineament patterns are prevailent in the study area. These fractures are of importance as both they controlled the development of the streams and facilitated the weathering of the granodiorite.

Many granitic landforms, such as boulders, corestones and tors formed by subsurface weathering constitute sound evidence of an etch origin in the study area. Thus, subsurface weathering and following stripping of the regolith have played an important role in the rapid denudation of the Orhaneli Pluton. The etching process is suggested to have been operating since the Late Miocene, which is thought to be exposure period for the pluton. The fracture-controlled Sadağı River and its tributaries also might have been responsible for stripping of the regolith, and thus causing the pluton area to have had a well-defined circular depression.

ACKNOWLEDGEMENTS

Drs Yıldırım Güngör and Sabah Yılmaz Şahin are thanked for thin section analyses. Professor C.R. Twidale (University of Adelaide) is thanked for his useful comments on the early draft of the paper. This study was supported by the research fund of the Istanbul University. Project Number T/96 11112002.

Manuscript received February, 22, 2008

REFERENCES

Ataman, G. 1972. Orhaneli granodiyoritik kütlesinin radyometrik Yaşı (L'age radiometrique du massif granodioritique d'Orhaneli). Türkiye Jeoloji Kurumu Bülteni, XV (2), 125-130.

Altınlı, E. 1966. Orhaneli havzasının jeoloji ve hidrojeoloji incelemesi. İstanbul (unpublished report).

Bingöl, E., Delaloye, M. and Ataman, G. 1982. Granitic intrusions in western Anatolia: A contribution to the geodynamic study of this area. Eclogae Geol. Helv., 75/2, 437-446.

Bürküt, Y. 1966. Kuzeybatı Anadolu'da yer alan plütonların mukayeseli jenetik etüdü (İstanbul Teknik Üniversitesi Maden Fak.Yay. No:272, İstanbul.

Chapman, C.A. 1956. The control of jointing by topography. Journal of Geology, 66, 552-558.

Dale, T.N. 1923. The commercial granites of New England. United States Geological Survey Bulletin, 738, 488 p.

Delaloye, M. and Bingöl, E. 2000. Granitoids from western and northwestern Anatolia: geochemistry and modelling of geodynamic evolution. International Geology Review, 42, 241-268.

Emre, H. 1986. Geology and Petrology of the Orhaneli ophiolite. PhD thesis, Istanbul University, Istanbul, Turkey (unpublished).

Ercan, T. 1979. Batı Anadolu, Trakya ve Ege adalarındaki Senozoik volkanizması, Jeoloji Mühendisliği Dergisi, 9, 23-46.

_____, Ergül, E., Akçören, F., Çetin, A., Granit, S. and Asutay, J. 1990. Balıkesir-Bandırma arasının jeolojisi, Tersiyer volkanizmasının petrolojisi ve bölgesel yayılımı, Maden Tetkik ve Arama Dergisi, 110, 113-130.

Gilbert, G.K. 1904. Domes and dome structures of the High Sierra. Geological Society of America Bulletin, 15, 29-36.

Goldish, S.S. 1938. A study in rock-weathering. Journal of Geology, 46, 17-58.

Harris, N.B.W., Kelley, S. and Okay, A.I. 1994. Post-collision magmatism and tectonics in northwest Turkey. Contrib. Mineral Petrol., 117, 241-252.

Kaaden, V. Der. 1959. Anadolu'nun kuzeybatısında yer alan metamorfik olaylarla magmatik faaliyetler arasındaki yaş münasebetleri, Maden Tetkik ve Arama Enstitüsü Dergisi., 52, 15-34.

Loughnan, F.C. 1969. Chemical Weathering of the Silicate Minerals. Elsevier, New York.

Mabbutt, J.A. 1961. A stripped land surface in eastern Australia. Trans. & Papers Inst. Brit. Geogr., 29, 101-114.

Okay, A.C. 1948. Orhaneli bölgesi, Mustafa Kemalpaşa bölgesi, Çataldağ bölgesine ait izahname 54/2, 54/1, 53/2 paftaları, Maden Tetkik ve Arama Genel Müdürlüğü Rapor No: 2215.

Okay, A.I., Harris, N.B.W. and Kelley, S.P. 1998. Exumation of blueschists along a Tethyan suture in northwest Turkey. Tectonophysics, 285, 275-299.

Özkoçak, O. 1969. Etude geologie de massif ultrabazique D'Orhaneli et de sa proche bordure, Bursa-Turquie. Thise, Fac. Sci. Üniv., Paris (unpublished).

Twidale, C.R. 1993. The research frontier and beyond: granitic terrains. Geomorphology, 7, 187-223.

______ and Bourne, J.A. 1975. The subsurface initiation of some minor granite landforms. Journal of the Geological Society of Australia, 22, 477-484.

Twidale, C.R., Vidal Romani, J.R., Campbell, E.M. and Centeno, J.D. 1996. Sheet fractures: response to erosional offloading or tectonic stress? Zeitschrift für Geomorphologie Supplement Band, 106, 1-24.

______ and Vidal Romani, J.R. 2004. Identification of exposed weathering fronts. Geodynamica Acta, 17/2, 107-123.

HISTORY OF MINING IN ANATOLIA: THE MINING ACTIVITIES IN KÜTAHYA - GÜMÜŞKÖY SINCE 3500 YEARS

Ahmet KARTALKANAT****

The C^{14} age of the charcoal collected from the damped material of the silver mine in Kütahya-Gümüşköy which is operated by Eti-Silver Ltd. has been dated as 3534±24 y. This data points that the mining activities has been lasting since 1500 BC in Kütahya-Gümüşköy region. This finding also shows that the silver ore deposits of Gümüşköy had been known and operated by Hitites before Phyrigians who were in power by 12^{th} centuries BC in this region of Anatolia.

Key Words: Mining history, Gümüşköy, Phyrigians, C14 dating